U. S. DEPARTMENT OF COMMERCE
Alexander B. Trowbridge, Acting Secretary
ENVIRONMENTAL SCIENCE SERVICES ADMINISTRATION
Robert M. White, Administrator
INSTITUTES FOR ENVIRONMENTAL RESEARCH
George S. Benton, Director

ESSA TECHNICAL REPORT IER 26-ITSA 26

Interference Predictions For VHF/UHF Air Navigation Aids

G. D. GIERHART

M. E. JOHNSON

INSTITUTE FOR TELECOMMUNICATION SCIENCES AND AERONOMY
BOULDER, COLORADO
March, 1967

FOREWORD

This report has been prepared by the Institute for Telecommunication Sciences and Aeronomy for the Systems Research and Development Service, Federal Aviation Agency, under Contract No. FA-64-WAI-69. It reflects the views of I. T. S. A., which is responsible for the facts and the accuracy of the data contained, and does not necessarily reflect the official views or policy of the FAA. This report does not constitute a standard, specification, or regulation.

For Sale by the Clearinghouse for Federal Scientific and Technical Information
Springfield, Virginia 22151 – Price $3.00

TABLE OF CONTENTS

LIST OF FIGURES

List of Figures (Continued)

List of Figures (Continued)

LIST OF TABLES

LIST OF SYMBOLS

In the following list the English alphabet precedes the Greek alphabet, lower-case letters precede upper-case letters, and alphabetical subscripts precede numerical subscripts.

a	Effective earth's radius, taken as 5280 statute miles (fig. 65).
	Free-space antenna gain for the main lobe of a desired ILS station localizer carrier array with reference to an isotropic radiator in dB (sec. 5.2).
A_U	Similar to A_D, but for an undesired station.
B	Dimensionless ratio of d_D to d_U (sec. 5.5).
C	Distance from midpoint of line between desired and undesired stations to the center of a circular D/U (95) locus in nautical miles (fig. 64).
C_f	Combination factor used in D/U(95) to N{D/U(95)} conversion to account for equipment parameters associated with various types of ILS stations in dB (sec. 5.2).
d	Great circle distance from ground station to aircraft in nautical or statute miles as specified (fig. 65).
d_e	Effective distance used by Rice, et al. [1966] in kilometers (sec. 3 footnote).
d_D	Great circle distance from desired station to aircraft in nautical miles (fig. 7).
d_U	Similar to d_D, but for undesired station.
d_l	Great circle distance from ground terminal to reflection point in statute miles (fig. 65).

List of symbols (Continued)

d_2	Great circle distance from reflection point to aircraft in statute miles (fig. 65).
D	Dimensionless divergence factor (sec. I.1).
D/U	Desired-to-undesired signal ratio in dB (sec. 4).
D/U(p)	Cumulative distribution of D/U where levels of D/U(p) correspond to values of D/U that are realized or exceeded p% of the time in dB (sec. 4). This and other cumulative distributions are thus defined as quantiles, the inverse of the cumulative distribution function. Values of D/U(p) for specific p levels become smaller as p increases.
D/U(95)	Value of D/U(p) corresponding to p = 95% in dB (sec. 4).
f_{Mc}	Frequency in Mc/s (sec. I.1).
FALTG	Subroutine used to perform the convolution of two cumulative distributions (sec. II.1).
g_{01}	Relative free space voltage gain (vertical pattern) of ground station antenna in a direction corresponding to γ_{01}, a dimensionless quantity (ILS sec. I.1; VOR sec. I.3 and I.1; TACAN sec. I.4 and fig. 5).
g_{r1}	Similar to g_{01}, but for γ_{r1}
G	Gain of ILS localizer carrier array (azimuth pattern) relative to the main lobe maximum in dB (figs. 1 and 2).
h_1	Height of ground station antenna in feet or statute miles as specified (fig. 65).
h_2	Aircraft altitude in feet or statute miles as specified (fig. 65).
h'_1	Height of ground station antenna above a plane tangent to the earth at the reflection point in statute miles (fig. 65).
h'_2	Similar to h'_1, but for aircraft.

List of symbols (Continued)

H_D	Height gain factor used for the desired station in the calculation of C_f in dB (sec. 5.2).
H_U	Similar to H_D, but for undesired station (sec. 5.2 and 5.3).
INTERP	Subroutine used for interpolation (sec. II.1).
k	Dimensionless ratios of the root-mean-square value of the field due to scattering of the reflected ray to that due to the direct ray (sec. I.4).
K	Value of k in dB (sec. I.4).
L_m	Reference transmission loss in dB (ILS sec. I.1 and I.2; VOR I.3 and I.1; TACAN sec. I.4).
L(p, d)	Cumulative distribution of transmission loss where levels of L(p, d) correspond to transmission loss values that are not exceeded during p% of the time in dB (sec. I.1). Values of L(p, d), for specific p levels become larger as p increases.
$L(p, d_D)$	Cumulative distribution L(p, d) when $d = d_D$ in dB (sec. II.1).
$L(p, d_U)$	Cumulative distribution L(p, d) when $d = d_U$ in dB (sec. II.1).
m	Positive integer (sec. II.1).
M	A real number (sec. 5.5).
n	Positive integer (sec. II.1).
N{D/U(95)}	Cumulative distribution corresponding to normalized D/U(95) in dB (sec. 5.2 and 5.3).
N_s	Surface refractivity in N-units (sec. I.1).
p	Percentage value, % (sec. 4).

List of symbols (Continued)

P_D	Carrier power radiated by desired station in dBW (ILS table 1; VOR table 2).
P_U	Similar to P_D, but for the undesired station in dBW (ILS table 1; VOR table 2).
q	Dimensionless parameter used by Rice, et al. [1966] to denote a fraction of time (sec. 3 footnote).
r	Dimensionless ratio of the root-mean-square value of the field due to the ray reflected from the counterpoise to that due to the direct ray (sec. I.4).
r_D	Range of aircraft from desired station in nautical miles (fig. 64).
r_U	Similar to r_D, but for undesired station in nautical miles (fig. 64).
r_o	Length of direct ray path in statute miles (fig. 65).
r_1	Length of ray path from ground station antenna to reflection point in statute miles (fig. 65).
r_2	Length of ray path from reflection point to aircraft in statute miles (fig. 65).
R	Radius of circular D/U(95) locus in nautical miles (fig. 64).
$\|R\|$	Dimensionless magnitude of reflection coefficient (sec. I.1).
R_A	Ratio of ILS aircraft antenna gain in the direction of the desired station to that in the direction of the undesired station in dB (sec. 2.1).

List of symbols (Continued)

$R_A(p)$	Cumulative distribution of R_A where levels of $R_A(p)$ correspond to R_A values that are exceeded for p% of the occurrences in dB (fig. 3). Values of $R_A(p)$ for specific p levels becomes smaller as p increases.
$\lvert R_C \rvert$	Dimensionless magnitude of reflection coefficient associated with reflection from the counterpoise in the TACAN propagation model (sec. I.4).
S	Separation between desired and undesired stations in nautical miles (sec. 5.2).
V(p, d)	Cumulative distribution corresponding to an empirical time availability function used to estimate the variability of hourly median transmission loss in dB, (sec. 3 footnote). Values of V(p, d) for specific p levels become smaller as p increases.
$V(0.5, d_e)$	A variable used by Rice, et al. [1966] (sec. 3 footnote).
$V(p, \theta)$	Approximately equivalent to V(p, d), but expressed as a function of θ instead of d and defined over a smaller range of d (sec. 3 footnote).
V(p, d or θ)	Used to indicate the use of either V(p, d) or $V(p, \theta)$ in dB (sec. I.3).
$V_A(p, \gamma_{02})$	Cumulative distribution of aircraft antenna gain in dB (VOR fig. 4; TACAN fig. 6). Values of $V_A(p, \gamma_{02})$ for specific p levels become smaller as p increases.
$V_C(p, r)$	Cumulative distribution used in accounting for variability associated with reflection from the counterpoise in the TACAN propagation model in dB (sec. I.4). Values of $V_C(p, r)$ for specific p levels become larger as p increases.

List of symbols (Continued)

$V'_C(p, r)$	Cumulative distribution of the resultant of the vector addition of a voltage of unity magnitude and constant phase with a component of magnitude r and a uniformly distributed random phase in dB relative to unity component (fig. 66). Values of $V'_C(p, r)$ for specific p levels become larger as p increases.
$V'_C(50, r)$	The value of $V'_C(p, r)$ corresponding to p = 50% in dB (sec. I.4).
$V_F(p, K)$	Cumulative distribution used in accounting for variability associated with short-term (within-the-hour) fading in the TACAN propagation model in dB (sec. I.4). Values of $V_F(p, K)$ for specific p levels become smaller as p increases.
$V'_F(p, K)$	Cumulative distribution based on fading range data and used in the development of $V_F(p, K)$ in dB (sec. I.4). Values of $V'_F(p, K)$ for specific p levels become smaller as p increases.
$V'_F(50, K)$	The value of $V'_F(p, K)$ corresponding to p = 50% in dB (sec. I.4).
$V_F(p, \theta)$	Cumulative distribution used in accounting for variability associated with short-term (within-the-hour) fading in the ILS and VOR propagation models in dB (sec. I.1). Values of $V_F(p, \theta)$ for specific p levels become smaller as p increases.
$V'_F(p, \theta)$	Cumulative distribution based on fading range data used in the development of $V_F(p, \theta)$ in dB (sec. I.1). Values of $V'_F(p, \theta)$ for specific p levels become smaller as p increases.
$V'_F(50, \theta)$	The value of $V'_F(p, \theta)$ corresponding to p = 50% in dB (sec. I.1).
VPD	Subroutine used to calculate V(p, d) in ILS interference predictions (sec. II.1).
x	Random variable (sec. II.1).

List of symbols (Continued)

$x(p)$	Cumulative distribution of $\mathbf{x}$ (sec. II.1). Values of $x(p)$ for specific p levels become smaller as p increases.
x_i	Value of x used to characterize x in the i^{th} percentage interval (sec. II.1).
y	Random variable (sec. II.1).
$y(p)$	Cumulative distribution of (sec. II.1). Values of $y(p)$ for specific p levels become smaller as p increases.
y_j	Value of y used to characterize y in the j^{th} percentage interval (sec. II.1).
$Y(q, d_e)$	A variable used by Rice, et al. [1966] (sec. 3 footnote).
z	Random variable (sec. II.1).
z'	Random variable (sec. II.1).
$z(p)$	Cumulative distribution of (sec. II.1). Values of $z(p)$ for specific p levels become smaller as p increases.
$z'(p)$	Cumulative distribution of z' (sec. II.1). Values of $z'(p)$ for specific p levels become smaller as p increases.
z_k	A value of z obtained using x_i and y_j (sec. II.1).
z'_k	A value of z' obtained using x_i and y_j (sec. II.1).
α	Azimuth angle in degrees (figs. 1 and 2).
β	An angle shown in figure 65 in radians.
γ_{01}	Elevation angle for direct (0) ray at ground (1) station in degrees or radians as specified (fig. 65).

List of symbols (Continued)

γ_{02}	Elevation angle for direct (0) ray at aircraft (2) in degrees or radians as specified (fig. 65).
γ_{r1}	Elevation angle for reflected (r) ray at ground (1) station in degrees or radians as specified (fig. 65).
γ_{r2}	Elevation angle for reflected (r) ray at aircraft (2) in radians (fig. 65).
Δ	Difference in direct and reflected ray path lengths expressed in radians of electrical phase (sec. I.1).
ϵ	Relative dielectric constant of earth's surface and is dimensionless (sec. I.1).
θ	Angular distance -- the angle between radio horizon rays in the great circle plane defined by antenna locations -- in radians (fig. 7).
θ_0	Central angle associated with the great circle distance d in radians (fig. 65).
θ_1	Similar to θ_0, but for d_1 in radians (fig. 65).
θ_2	Similar to θ_0, but for d_2 in radians (fig. 65).
σ	Conductivity of earth's surface in millimhos per meter (sec. I.1).
ϕ_1	An angle shown in figure 65 in radians.
ϕ_2	An angle shown in figure 65 in radians.
Ψ	Grazing angle at reflection point in radians (fig. 65).
*	An operational symbol used to indicate the combination of two cumulative distributions by convolution (sec. II.1).

INTERFERENCE PREDICTIONS FOR VHF/UHF NAVIGATION AIDS

by

G. D. Gierhart and M. E. Johnson

Desired-to-undesired signal ratio predictions for the VHF Omnirange (VOR), Tactical Air Navigation (TACAN) and Instrument Landing Systems (ILS) air navigation aids are presented in this report. The parameters involved in the various systems are given first. Next propagation mechanisms applicable to the VHF and UHF bands are discussed together with the calculation of transmission loss and its variability. Third, the statistical nature of the desired-to-undesired signal ratio predictions is explained. Finally, the results of the study are presented in graphical form. Aircraft altitudes from 500 to 100,000 feet along with station separations from 20 to 695 nautical miles are considered.

Detailed procedures, mathematical formulas, and computer programs used are discussed in the Appendices.

1. Introduction

Increasing air traffic density together with fast, high-flying jets have made the use of reliable air navigation aids more important than ever before. In expanding the present complex of navigation aids to meet future demands, consideration must be given to potential interference between facilities operating on the same or on adjacent channels. The amount of interference is a function of the desired-to-undesired signal ratio at the aircraft antenna terminals; as both signals vary with time and aircraft location, the ratio varies as well, and interference becomes dependent on time and location. Because of the nature of radio wave propagation in the frequency ranges used, the variations of the received signals and of the interference ratios are best described statistically. The large number of possible conditions requires the use of a digital computer with programs that take into account all variables as well as the fixed equipment parameters.

The air navigation aids treated in this report are the Instrument Landing System (ILS), VHF Omnirange (VOR), and Tactical Air Navigation (TACAN). These aids operate in the very high frequency (VHF; 30-300 Mc/s) and ultra high frequency (UHF; 300-3,000 Mc/s) bands. Most of the information on the ILS contained here has been previously published [Gierhart and Johnson, 1965]. Information similar to that presented here for the VOR and TACAN has also been published [Radio Technical

Commission for Aeronautics, 1955; Decker, 1957]. The range of parameters considered in this study is much larger than that of previous studies.

At VHF/UHF propagation of radio frequency energy is affected by the lower atmosphere (the troposphere), specifically by variations in the refractive index of the atmosphere. The terrain along and in the vicinity of the great circle path between transmitter and receiver also plays an important part.

Within the last decade a number of methods and procedures have been developed to calculate field strength and its variability at VHF/UHF. The work discussed here follows procedures which have been used by the Institute for Telecommunication Sciences and Aeronomy (I. T. S. A., formerly the Central Radio Propagation Laboratory) to predict statistically the effects of terrain and atmosphere on the variability of field strength, and on the performance of radio systems [Rice, et al., 1966]. It is also convenient to use the concept of transmission loss [Norton, 1953 and 1959], which is the ratio of power radiated to the power that would be available at the receiving antenna terminals if there were no circuit losses other than those associated with the radiation resistance of the receiving antenna, and is usually expressed in decibels. Methods used for its calculation as a function of path length, terminal heights, and carrier frequency are discussed in section 3. Computation techniques are discussed in Appendix II.

After some initial calculations, parameters for various systems were assembled into a computer program and desired-to-undesired signal ratios calculated for given probability levels as a function of aircraft location in relation to the desired and the undesired ground stations.

2. System Parameters

Pertinent parameters for the ILS, VOR, and TACAN systems are discussed in this section. The transmission line loss associated with the airborne terminal was considered to affect both the desired and undesired signals equally and was neglected.

2.1 ILS Parameters

The ILS includes a runway localizer, a glide path, and marker beacons. However, this study considers only the localizer since it is most susceptible to co-channel and adjacent-channel interference. The ILS localizer operates in the 108 to 112 Mc/s frequency range and shares this range with the VOR in such a way that VOR facilities must be considered as the source of adjacent-channel interference. Characteristics of three ILS localizers are listed in table 1. Other equipment exists, but consideration of these three examples is sufficient for practical purposes.

TABLE 1

Characteristics of Typical ILS Localizers

	Standard	Directional	Low Cost
Radiated Power *	+ 20 dBW	+ 20 dBW	+ 10 dBW
Array Type	8 - Loop	V - Ring	V - Ring
Antenna Gain *	+ 4 dB	+ 12 dB	+ 12 dB
Array Height Above Ground	5.5 feet	7.5 feet	7.5 feet
Polarization	----------Horizontal----------		

Figures 1** and 2 show relative gain, G, as a function of azimuth angle, α, for the carrier portion of the 8-Loop [Civil Aeronautics Administration, 1957] and V-Ring arrays, [Federal Aviation Agency, 1964 and 1965] respectively.

Aircraft antenna gain statistics were obtained from modeling study data based on an E-cavity type VOR antenna in the vertical stabilizer of passenger-type jet aircraft [Convair, 1959; Commercial Jetstar, 1959]. Only the forward $\pm$ 20° of azimuth were considered in obtaining statistics for gain toward the desired station, but two sets of statistics were developed for gain in the direction of the undesired

* Radiated power refers to the total power radiated from the carrier antenna array, and antenna gain refers to the main lobe free space gain of the carrier antenna array with reference to an isotropic radiator.

** Figures in this report are located at the end of the section in which they are first mentioned.

station. One set considered only the rear + 20° of azimuth and the other considered all azimuth angles as equally likely. From these statistics a single cumulative distribution was established for the ratio of antenna power gain in the direction of the desired station to that in the direction of the undesired station. This ratio, expressed in decibels, is denoted by R_A and the cumulative distribution, $R_A(p)$, used to account for aircraft antenna gain is shown in figure 3. Also shown in figure 3 are two additional cumulative distributions of R_A that resulted from the above mentioned analysis and were used as guides to establish the R_A distribution used in the calculations.

The cumulative distribution involving the rear + 20° of azimuth was developed to assess the effect of constraining azimuth angles to those likely to be given some special attention in the development of aircraft antennas for ILS use.

Free-space gain for the localizer carrier antenna array in the azimuth plane is plotted in decibels relative to the main lobe maximum. The gain of the main lobe maximum relative to an isotropic radiator is 4 dB.

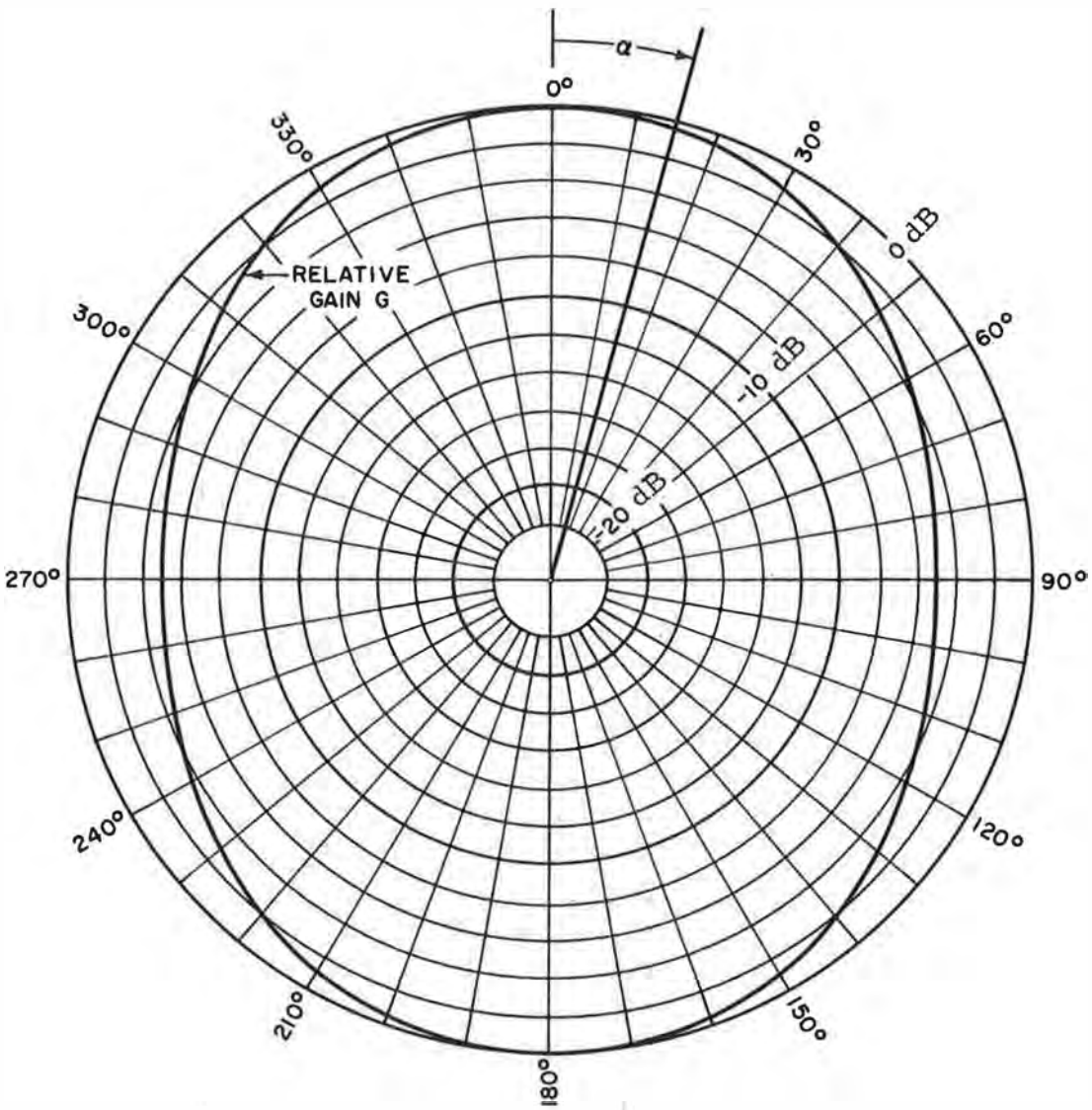

ILS 8-Loop Array Antenna Pattern
Figure 1

Free-space gain for the localizer carrier antenna array in the azimuth plane is plotted in decibels relative to the main lobe maximum. The gain of the main lobe maximum relative to an isotropic radiator is 12 dB

Values plotted are for a V-Ring array (type FA-5549X) with a type III element spacing and current distribution.

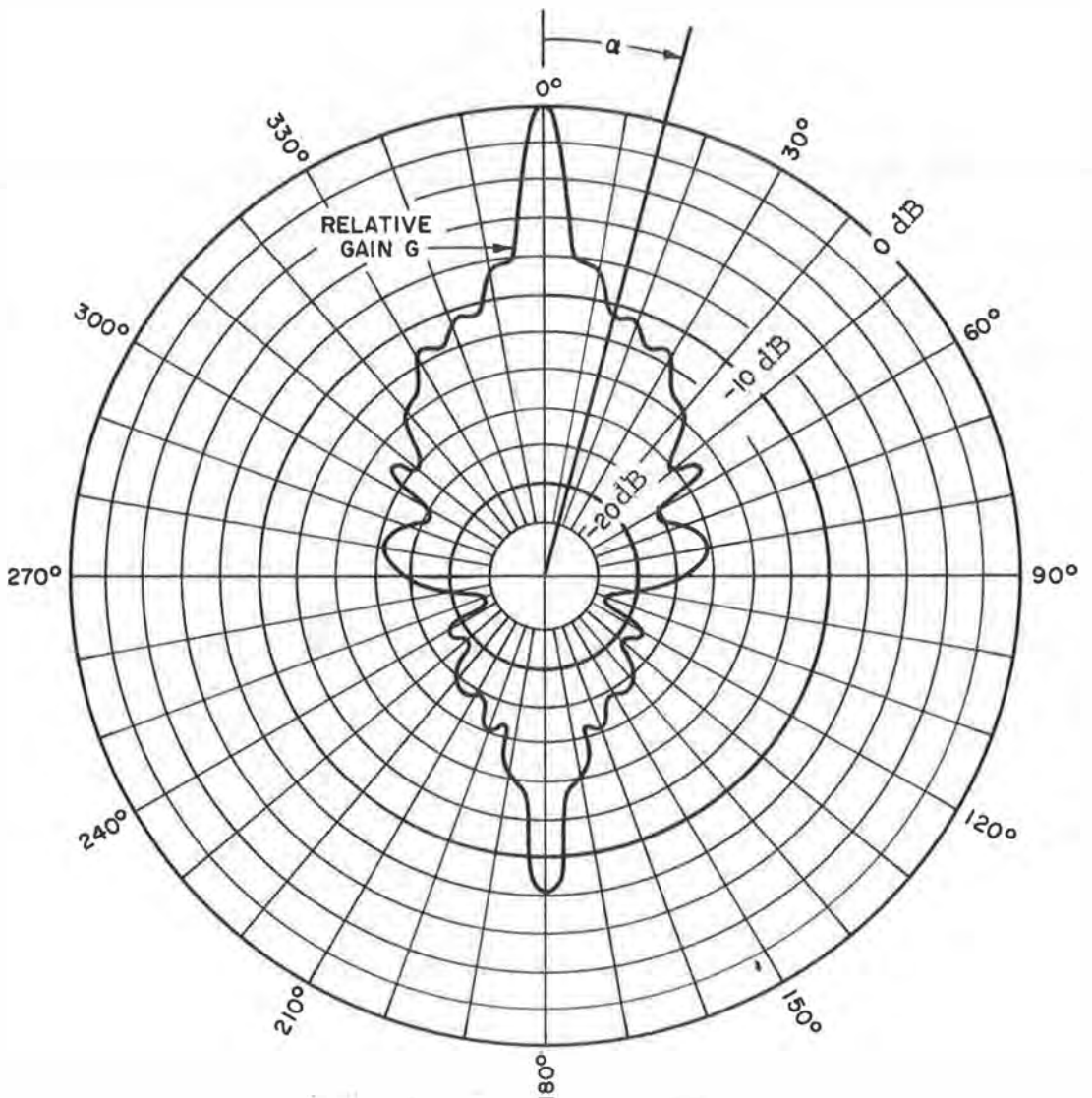

ILS V-Ring Array Antenna Pattern
Figure 2

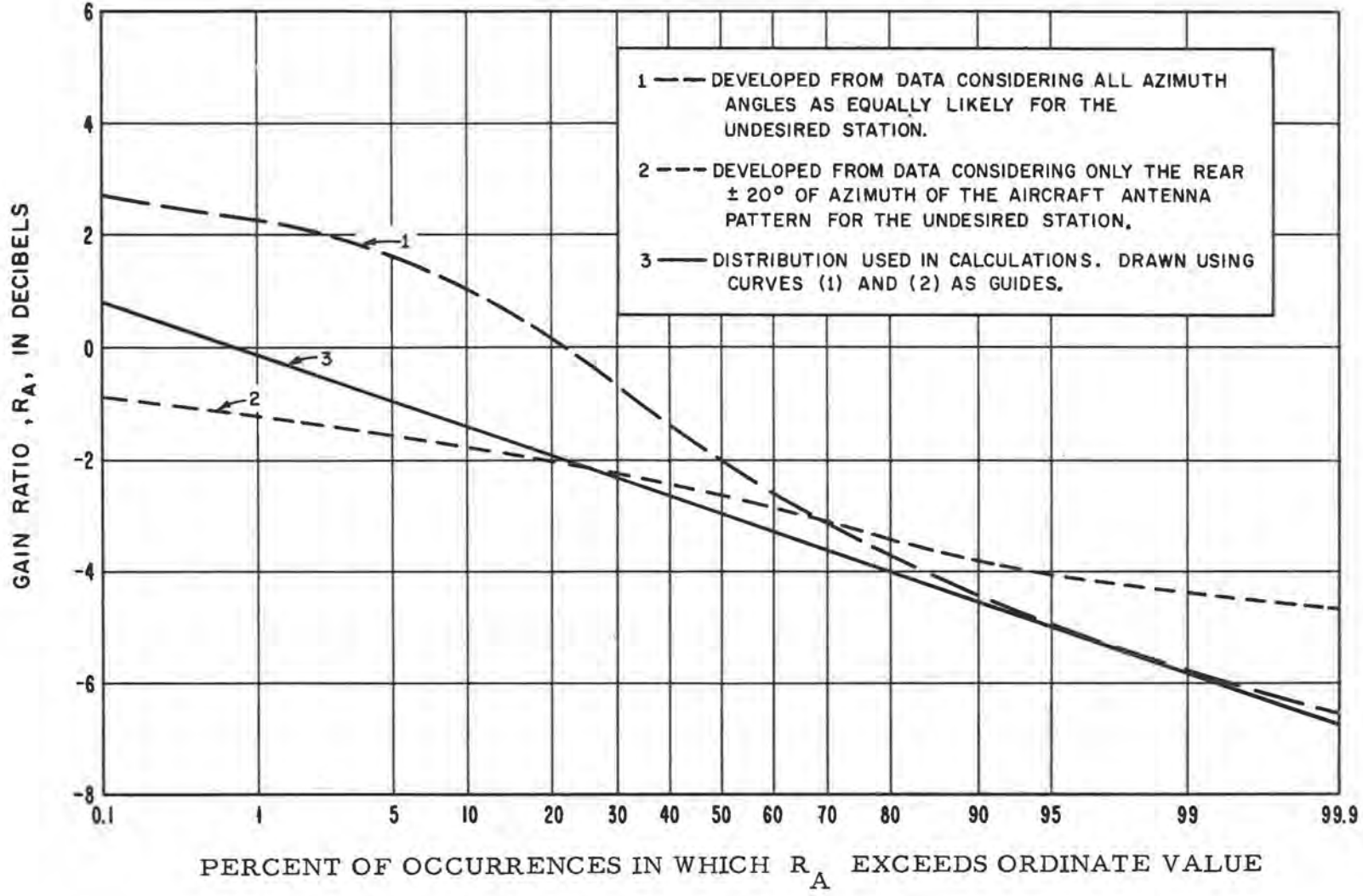

ILS Aircraft Antenna Gain Ratio Distribution
Figure 3

2.2 VOR Parameters

The VOR system operates in the 108 to 118 Mc/s frequency range. Table 2 contains other parameters for the VOR.

TABLE 2

VOR System Parameters

Carrier Power Radiated from Antenna*	20 dBW
Polarization	Horizontal
Antenna Type	4-Loop Array (located above counterpoise)
Maximum Antenna Gain Relative to Isotropic Antenna	2.15 dB
Free-Space Horizontal Pattern	Approximately Circular
Free-Space Vertical Pattern	Similar to a Dipole
Counterpoise Diameter	52 feet
Antenna Height Above Counterpoise	4 feet
Counterpoise Height Above Ground	12 feet

The aircraft antenna gain was determined as a function of azimuth and vertical angle from a modeling study based on an E-cavity type VOR antenna in the vertical stabilizer of a passenger-type jet aircraft [Convair, 1959]. Figure 4 shows the distribution of antenna gains at various vertical angles, together with a sample of the measurement points from which the principal distribution was derived.

* The radiated power is the same as the power delivered to the antenna when other antenna losses are considered negligible when compared with that associated with its radiation resistance.

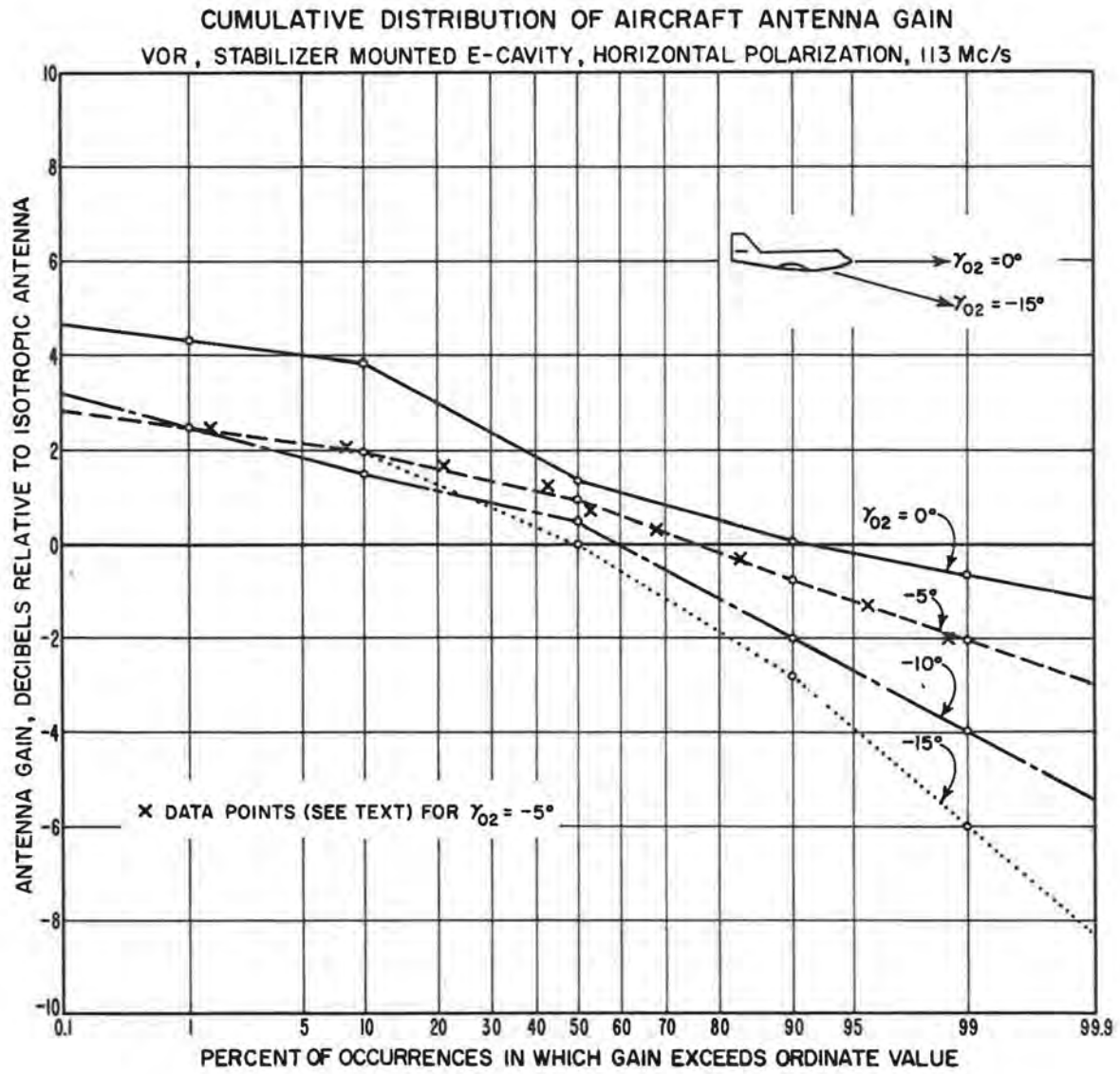

VOR Aircraft Antenna Gain Distributions

Figure 4

2.3 TACAN System Parameters

The TACAN system operates in the 960 to 1215 Mc/s frequency range. Table 3 lists other parameters for the system.

TABLE 3

TACAN System Parameters

Effective Peak Radiated Power *	45 dBW
Polarization	Vertical
Antenna Type	Center Array
Maximum Antenna Gain Relative to Isotropic Antenna	8.15 dB
Free-Space Horizontal Pattern	Approximately Circular
Free-Space Vertical Pattern	See Figure 5
Antenna Height Above Counterpoise	18 feet
Antenna Height Above Ground	30 feet

The effective peak radiated power assumed for the TACAN system includes ground station line loss and transmitter power. The ground station antenna was taken to be the typical center array discussed by Casabona [1956], with its free-space vertical radiation pattern shown figure 5. The aircraft antenna gain was obtained from modeling studies based on an annular slot type DME antenna mounted on the bottom fuselage center line in front of the landing gear of a passenger jet aircraft. Pertinent distributions of antenna gain values for several vertical angles are shown in figure 6, together with a sample of available measurements [Commercial Jetstar, 1959].

* As used here, effective peak radiated power is measured relative to an isotropic radiator at the vertical angle of maximum radiation with peak power delivered to the antenna, and is an average over one or more integral number of antenna revolutions.

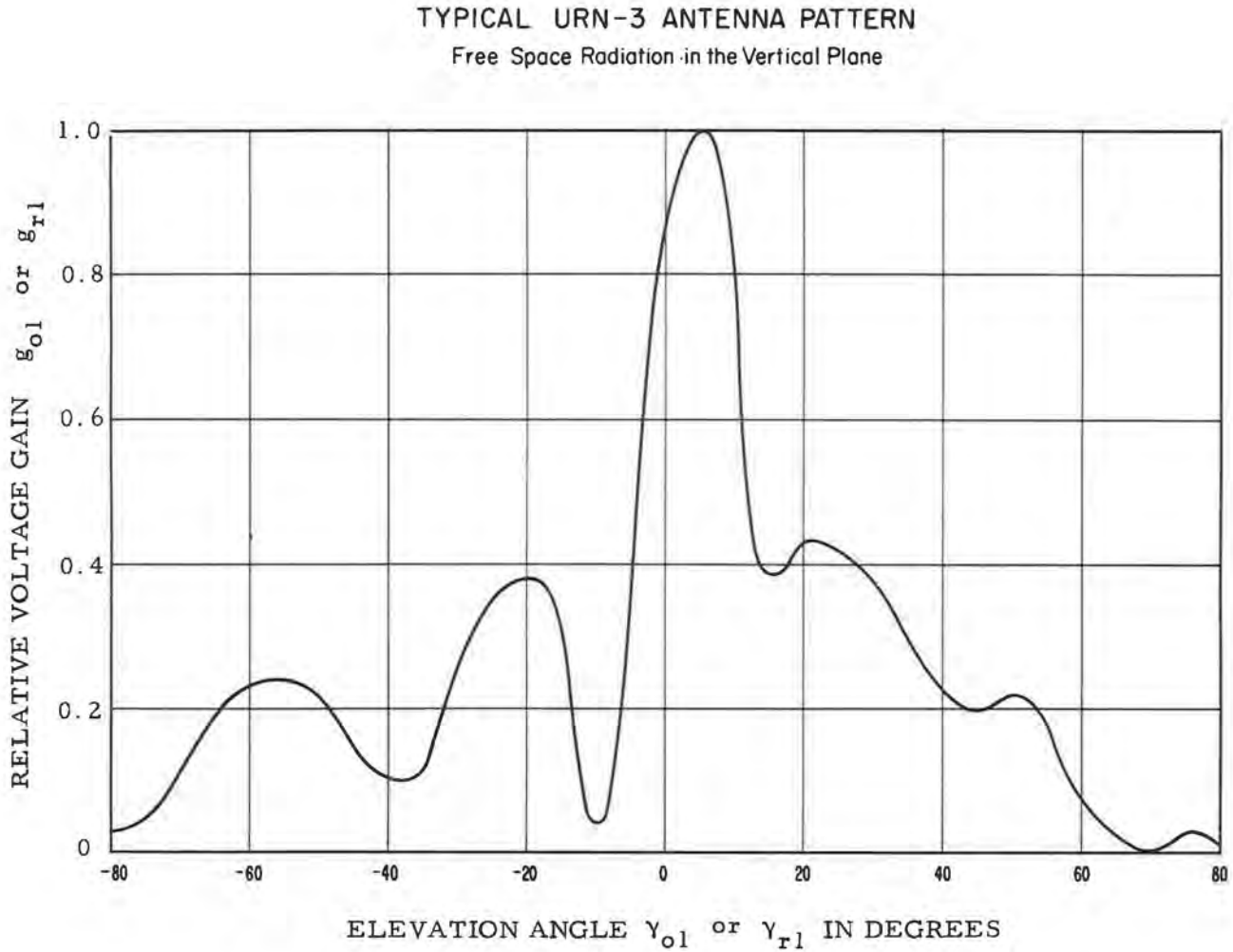

TACAN Ground Station Antenna Pattern

Figure 5

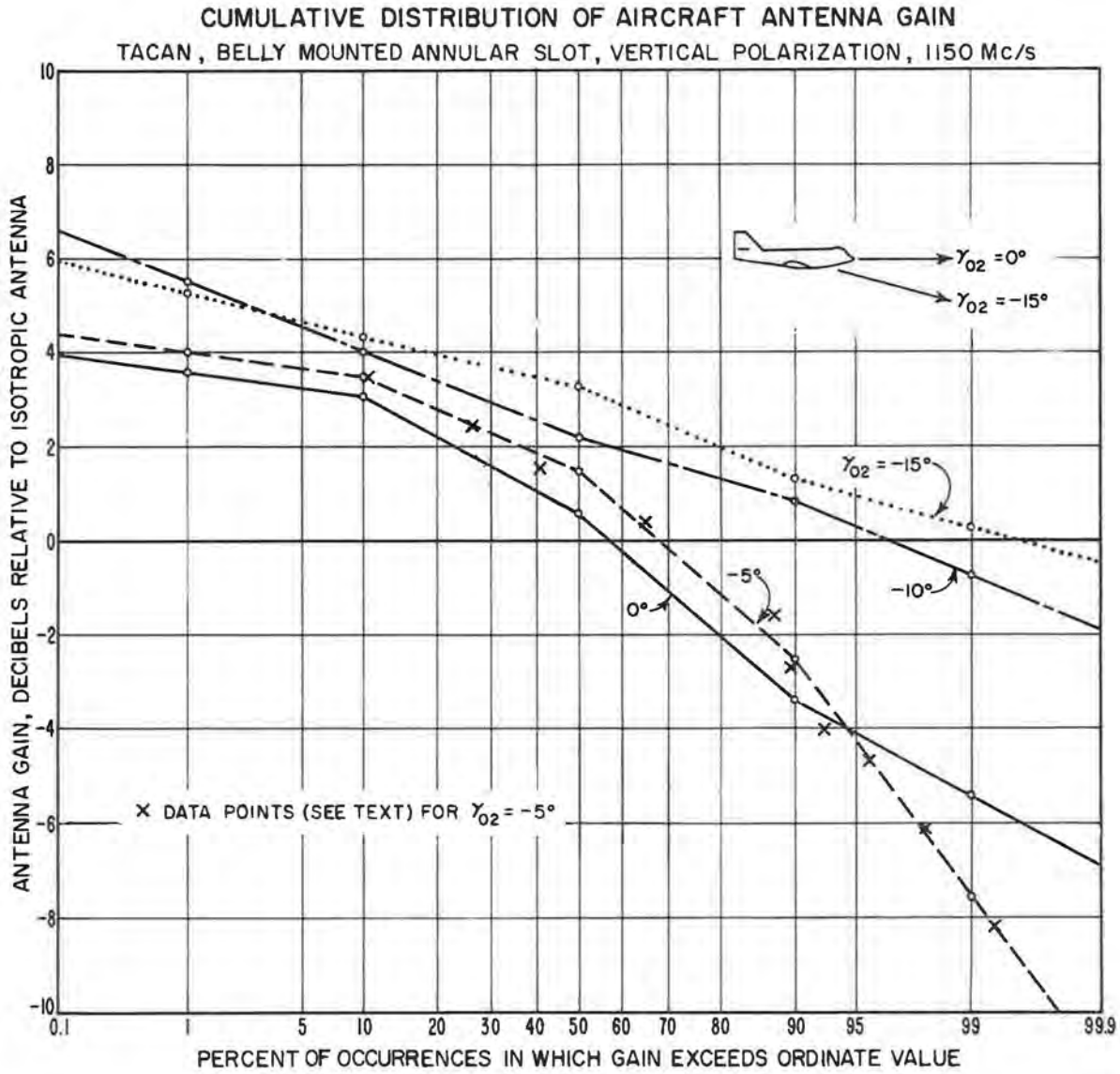

TACAN Aircraft Antenna Gain Distributions

Figure 6

3. Transmission Loss Calculations

The prediction of interference conditons requires a knowledge of the time distributions of transmission loss or field strength at many points in space.

Figure 7 shows a typical configuration of an aircraft (representing the receiving terminal), a desired navigational transmitting facility, and an undesired navigational transmitting facility. All three are aligned along a great circle path, and for simplicity assumed to be above a smooth surface. In the example drawn, the aircraft is within the radio horizon of the desired facility, but beyond the radio horizon of the interfering station. The distances along the great circle path from a point vertically below the aircraft to the desired and the undesired station are denoted by d_D and d_U, respectively. The aircraft is at a height, h_2, above the earth. The angle θ between the horizon rays from the aircraft and the interfering station is an important parameter in the calculation of transmission loss for beyond-the-horizon paths [Norton, et al.,1955a]. Figure 7 is oversimplified because radio rays may only be drawn as straight lines under special conditions, one of which is that h_2 must be less than 5000 feet.

Transmission loss calculations were accomplished by (a) calculating a reference value of transmission loss, (b) calculating a cumulative distribution for long-term variations, (c) calculating a cumulative

distribution for short-term variations, and (d) calculating the cumulative distribution of transmission loss by combining the results of previous calculations. More detail on these four steps follows.

(a) Within the radio horizon, reference transmission loss was calculated using geometric optics methods, including interference between the direct and the ground-reflected ray. For the desired ILS localizer and VOR propagation models, specular reflection was assumed with reflection coefficients equal to -0.9. Because of the irregular nature of the terrain (buildings, etc. included) surrounding the undesired ILS stations, specular reflection from the earth was considered less dominating, and a combination of specular and diffused reflection was assumed. The primary effect of this assumption was to lower transmission loss values associated with the undesired ILS under line-of-sight conditions relative to comparable values for the desired ILS. This is discussed further in Appendix I. In the case of TACAN with frequencies in the 1100 Mc/s range it is more appropriate to assume that the ground-reflected ray is made up of a large number of components having random relative phase. The total contribution from these components can be represented statistically by a Rayleigh distribution [Decker, 1957; McGavin and Maloney, 1959]. Norton, et al. [1955b] have shown how a Rayleigh-distribution component (reflected ray) can be combined with a constant component (direct ray) to obtain a distribution of power at the receiving antenna.

Beyond the radio horizon, reference transmission loss is calculated using smooth-earth diffraction or forward scatter models, depending on the path distance involved. The diffracted field decreases very rapidly for distances beyond the radio horizon, especially at the TACAN frequencies, so that the forward scatter model is more important. Calculations for both models and the method of properly combining diffraction and scatter fields, if they are of comparable magnitude, are based on procedures given by Rice, et al. [1966].

(b) Long-term variations in basic transmission loss were estimated for a continental temperature climate by means of the time availability function $V(p,d)$*. It was used as the cumulative distribution with time of hourly median transmission loss for all hours of the year relative to the reference values calculated under (a) above as functions of path length, terminal height, and carrier frequency.

(c) In addition to the distributions of hourly medians representing long-term variations, short-term (usually within-the-hour) distributions

* The curves presented in this report were developed during the time when prediction methods given by Rice, et al. [1966] were evolving. In particular the function $V(p,d)$, used in all calculations involving the ILS, is identical with the function $V(0.5, d_e) + Y(q, d_e)$ used by Rice, et al. [1966] for a continental temperate climate. An earlier version of this $V(p,d)$ function was used in calculations that involved exclusive consideration of either VOR or TACAN. Early and late versions of $V(p,d)$ are very similar and are identical for beyond-the-horizon paths. Because another function $V(p,\theta)$, similar to $V(p,d)$, was derived primarily from data in the 100 Mc/s range, the recommendation that it be used when $\theta \geq 0.01$ radians [Air Force Technical Order, 1961] was followed in calculations that involved the VOR exclusively.

of the received signal levels had to be estimated. Short-term variations in this particular application are principally due to two causes. One factor is the inherent short-term fluctuation of the tropospheric signal ascribed to phase interference of rays reflected from small layers or scattered from refractive index discontinuities, or to reflections from ground irregularities. The second is the pattern of the aircraft antenna; numerous small lobes cause gain changes with varying bearings which can be represented by a cumulative distribution of antenna gain with time as the aircraft moves through space. In the ILS case, however, it was more efficient to neglect the effect of the aircraft antenna gain in the initial transmission loss calculations, and include it in later calculations as the $R_A(p)$ distribution discussed in section 2. Short-term fading was described by cumulative distributions that are based on fading range data given by Janes [1955].

(d) To obtain the cumulative distribution of transmission loss the functions discussed in a, b, and c above were combined. The mechanics of combining cumulative distributions are discussed in Appendix II.

Note that the 1-hour period taken as the dividing line between long-term and short-term variations is somewhat arbitrary. This is convenient in view of the available empirical time variability functions, which are based on data analysis using hourly median values.

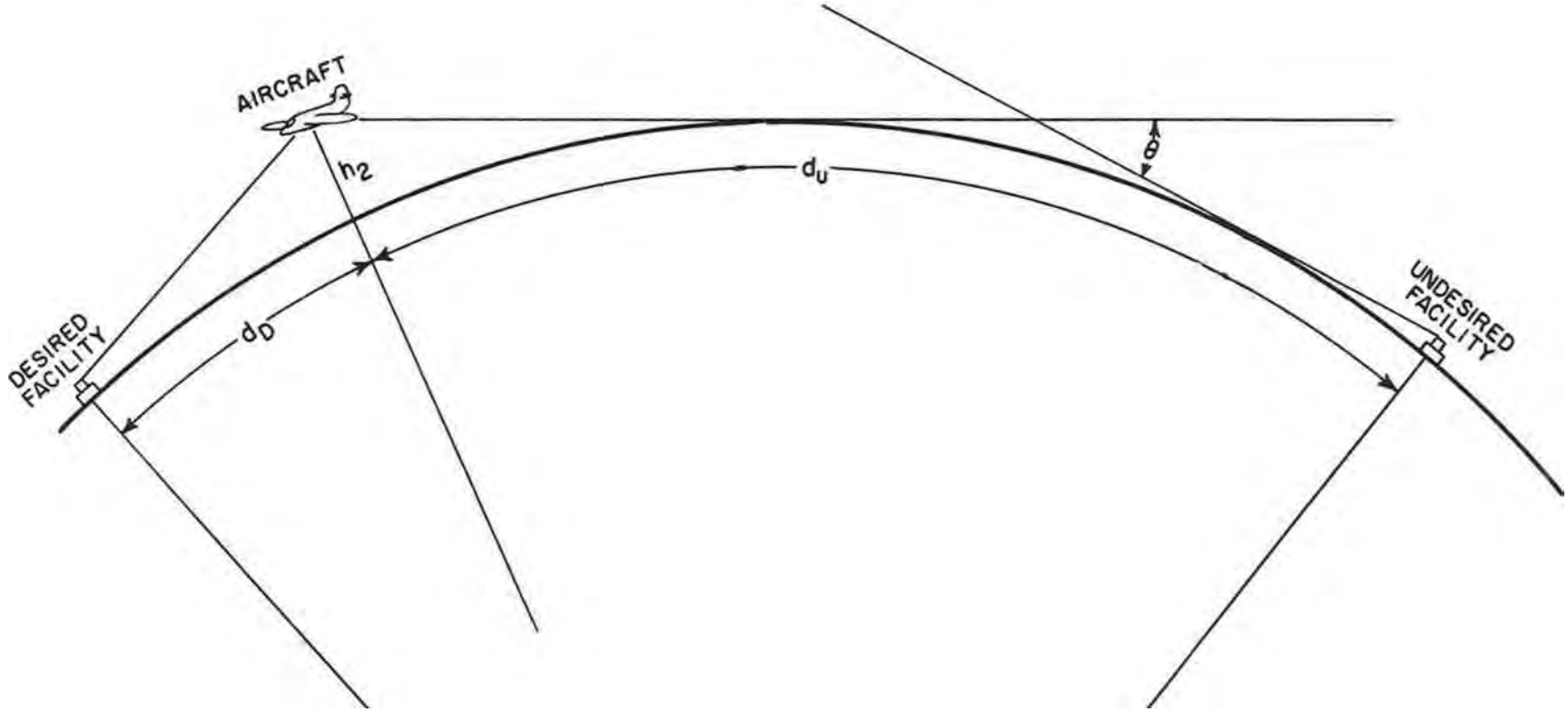

Sketch Showing Relative Positions of Aircraft and Navigational Aids over a Smooth Earth

Figure 7

4. Interference Between Two Stations

As shown by figure 7, both the desired and the undesired signals arrive at the aircraft over propagation paths characterized by the distances, d_D and d_U, and by the aircraft height. The distances are measured along the great circle path. Both signals vary with time, and the distributions of signal levels were calculated in accordance with the procedures outlined in the preceding section. Then the ratio of desired-to-undesired signal exceeded for given percentage-of-time values at a particular aircraft location was determined.

The desired-to-undesired signal ratio can be expressed as the decibel difference of desired and undesired signal levels and is obtained from calculated transmission loss values and other system parameters. The distribution of this ratio will be denoted $D/U(p)$, where p is that percentage of time during which a given value of D/U is realized or exceeded. By virtue of the aircraft being in motion, time variations also include variations in space. Since the actual time distribution of D/U may vary from installation to installation because of terrain characteristics and other factors not taken into account in this analysis, the time availability, p, may be interpreted as an expression of reliability for a typical installation. The concepts of "prediction uncertainty" and "service probability" in the sense defined by Barsis, et al. [1962] were not used explicitly. It is important

to understand that there is an uncertainty associated with the D/U predictions in this study and that this uncertainty will increase under conditions where the assumed propagation models become less valid.

As an example, D/U(95) = 10 dB means that for a typical installation the ratio of the desired-to-undesired signal is equal to or greater than 10 dB during 95% of the time. Values of D/U(95) are associated with the variables used in the calculations. These include: (1) system type (ILS, VOR, or TACAN), (2) interference type (co-channel or adjacent-channel), (3) aircraft altitude, (4) station separation, and (5) aircraft distance from the desired station.

To obtain the time availability of the desired-to-undesired ratio at any point in space it was necessary to properly combine the cumulative distributions of (1) transmission loss from the desired station, (2) transmission loss from the undesired station, and for the ILS case, (3) the antenna power gain ratios, $R_A(p)$. Actually the ILS calculations resulted in a cumulative distribution of a normalized D/U. The process for converting actual D/U to normalized D/U values is discussed in sections 5.2 and 5.3.

5. Results of the Study

Correct interpretation of the prediction curves presented in this section requires some knowledge of the system parameters, propagation models,and computation techniques discussed in previous sections. In

particular, the predictions involve estimates of received power levels or desired-to-undesired signal ratios that are expected to be realized or exceeded 95% of the time (95% reliability). A lower reliability requirement would result in an apparent increase in power received from the desired station. For example, if the difference in power received from desired and undesired ILS stations could be characterized by simply considering the aircraft gain ratio distribution shown by curve 3 on figure 3, then reliabilities of 95, 50, and 5% would correspond to desired-to-undesired signal ratios of -5, -3, and -1 dB, respectively.

The results are in the form of prediction curves. Two basic types of predictions are presented here which involve service limitations due to (1) insufficient power available from the desired station and (2) interference from one co-channel or adjacent channel station with no consideration given to the available power limitation. A single-curve format is used for the first type (sec. 5.1), and three formats are used for second type of predictions (sec. 5.2 through 5.5).

5.1 Available Power Service Limitations

When the service range is not limited by co-channel or adjacent-channel interference, it then is limited by other types of interference or a received power level that is insufficient compared to the noise level of the receiver. The former is beyond the scope of this report, and the latter is the subject of this section.

The radiated power for a ground station may be stated in terms of the power required at the terminals of a reference antenna located at the maximum specified service range. Curves developed show the service range limitations imposed by this type of specification, when the radiated powers discussed in the system parameter section are used. The assumed specifications may be summarized as follows:

VOR and ILS Ground Station Radiated Power

The radiated power shall not be less than that required to insure that the power available at the terminals of a loss-free horizontally polarized half-wave dipole located at the maximum specified range would be -112 dBW or greater 95% of the time.

TACAN Ground Station Radiated Power

The effective peak radiated power* of the pulse envelope shall not be less than that required to insure that the peak pulse power available (mean value) at the terminals of a vertically polarized loss-free half-wave dipole located at the maximum specified range would be -106 dBW or greater 95% of the time.

---

* See footnote in section 2.3.

The combination of available power selected for the VOR specification and a ground station radiated power of 20 dBW results in a maximum range slightly greater than 130 nautical miles at 18,000 feet. Assuming that a VOR receiver with a usable sensitivity of 5 μV across 50 Ω in an airborne environment can be built, then the -112 dBW available power quoted above is excessive by about 11 dB. This "power margin" may be used in engineering the airborne terminal to account for such things as 1) difficulty in obtaining an aircraft antenna with 2.15 dB gain (half-wave dipole), 2) line and mismatch losses, and 3) difficulty in obtaining a usable receiver sensitivity of 5 μV across 50 Ω in an airborne environment.

Since the receiving equipment required for ILS is similar to that for VOR, an identical available power requirement was assumed. This consistency allows the ground station radiated power requirement for the two systems to be covered in a single statement.

The available power selected for the TACAN specification has a "power margin" of 12 dB when a usable receiver sensitivity of -118 dBW in an airborne environment is assumed.

The Federal Aviation Agency is preparing a document describing the "U.S. National Common System Component Characteristics for the VORTAC System". It will contain ground station power requirements similar to those stated above. However, the preliminary version

available to I. T. S. A. expressed the required ground station power in terms of that required to produce a given power density (dBW/m^2) at maximum specified range. To facilitate comparison with documents of this type, table 4 has been prepared where the power density equivalents of the available power requirements are listed for pertinent frequencies.

TABLE 4

Power Density Equivalents

	ILS			VOR			TACAN		
Frequency (Mc/s)	108	110	112	108	113	118	960	1150	1213
$10 \log_{10}$ Eff. area	0.03	-0.13	-0.28	0.03	-0.38	-0.74	-18.95	-20.52	-20.99
Reference power (dBW)	-112	-112	-112	-112	-112	-112	-106	-106	-106
Power density (dBW/m^2)	-112.0	-111.9	-111.7	-112.0	-111.6	-111.3	-87.0	-85.5	-85.0

These equivalents were calculated by subtracting $10 \log_{10}$ of the effective area of a half-wave dipole from the reference power (in dBW). For this conversion method to be valid, the incoming electromagnetic wave must approximate a uniform plane wave over an area somewhat larger than the antenna's effective area, and the antenna must be oriented

so that its maximum gain is utilized. The first requirement is met for regions of interest here*, and the second is met for most regions of interest; e.g., a vertically polarized antenna located directly above a TACAN facility would not be oriented for maximum gain. However, since the half-power beamwidth of a half-wave dipole is about 90°, the error associated with using this conversion for TACAN is less than 3 dB when the distance (along ground) to the reference dipole is greater than its altitude (above ground).

Nominal service ranges for the ILS localizer types mentioned in section 2.1 were calculated using the above specification. Table 5 lists these as a function of altitude.

TABLE 5

Nominal ILS Localizer Service Range

Altitude in feet	Nominal range in nautical miles		
	Standard	Directional	Low Cost
500	22	31	23
1,000	31	39	32
2,000	46	55	47
3,000	59	68	60
4,000	66	78	67
6,250	77	105	79
12,000	95	128	97
18,000	111	153	113

* Some antennas used for tropospheric propagation paths have an effective area so large that their full free-space gain is not realized for the path.

Service volumes defined by the system parameters (sec. 2.2 and 2.3) and the available power requirements of the above specifications are shown in figures 8 and 9 for the VOR and TACAN, respectively. Curves for TACAN effective peak radiated powers (EPRP) of 30 and 39 dBW are also shown in figure 9. Both figures include a plot of the radio horizon. In the volume defined by the revolution of the appropriate curve about its ordinate axis, the reference antenna would deliver the required power at least 95% of the time. However, unsatisfactory service exists in the airspace (cone) immediately above VOR and TACAN ground stations.

* See footnote in section 2.3.

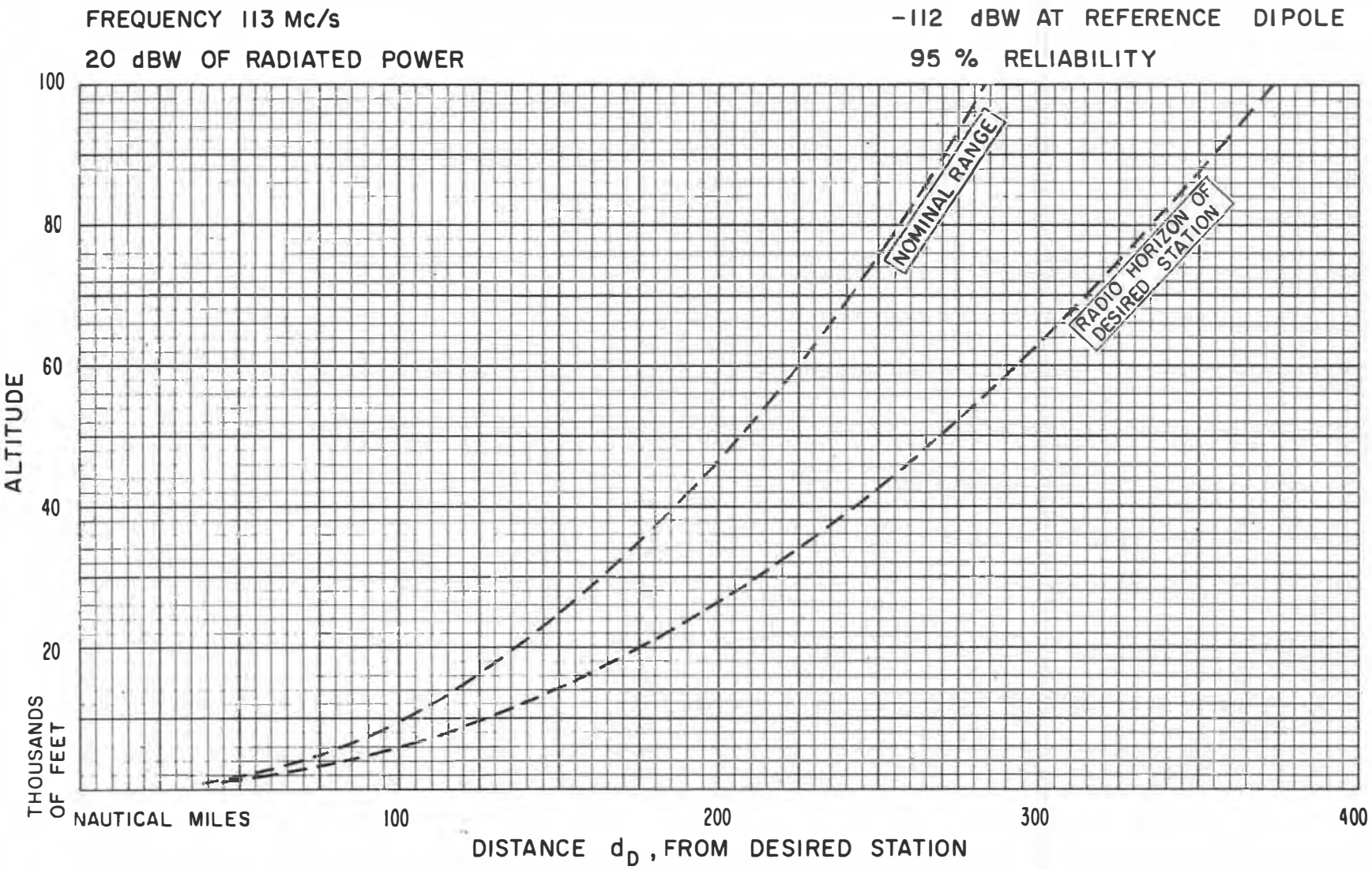

VOR SERVICE VOLUME WITHOUT INTERFERENCE

Figure 8

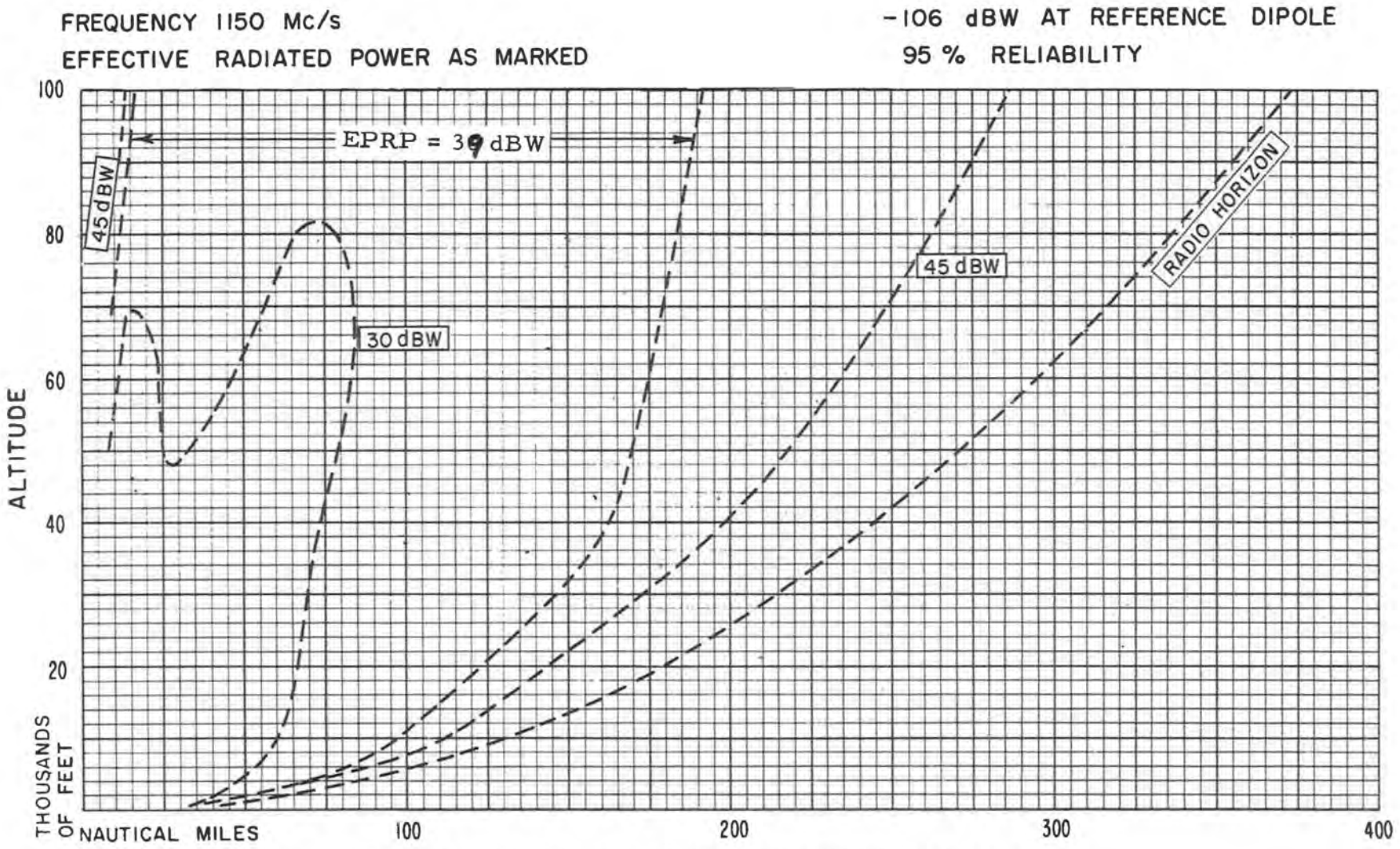

TACAN SERVICE VOLUME WITHOUT INTERFERENCE

Figure 9

5.2 ILS Signal Ratios Due to Co-Channel Interference

The results of the ILS portion of this study are in the form of normalized prediction curves. These curves may be used to estimate the service limitations imposed on ILS installations by co-channel and adjacent-channel interference. Other limitations to service such as man-made noise at the receiver and self interference caused by reflections from airport structures or other aircraft were not considered in this study. As a result an "acceptable" desired-to-undesired signal ratio does not imply that the desired signal is strong enough for operational use (see section 5.1).

Values of normalized D/U(95) will be denoted by the symbol $N\{D/U(95)\}$. These normalized values were calculated for the condition when the two ground stations and the aircraft were on the same great circle arc. Under these conditions D/U(95) will increase as d_D (altitude fixed) is decreased; i.e., a level of D/U(95) at a particular distance from the desired station is sufficient to assure that D/U(95) values larger than this level will be obtained at lesser distances (altitude fixed). In cases where the assumed great circle alignment is not valid $N\{D/U(95)\}$ values can also be obtained by properly interpreting the station separation shown on the curves. Regardless of the shortest distance between the ground stations, the station separation, S, shown on the curves should always be regarded as the algebraic sum of the distance from the aircraft

to the desired station, d_D, and the distance from the aircraft to the undesired station, d_U; i.e., $S = d_D + d_U$. Under these conditions S (also G) will vary with d_D and a level of D/U(95) at a particular distance from the desired station is not sufficient to assure that D/U(95) values larger than this level will be obtained at lesser distances.

Normalized D/U(95) curves for aircraft altitudes of 1,000, 2,000, 3,000, 4,000, 6,250, 12,000, and 18,000 feet are shown in figures 10, 11, 12, 13, 14, 15, and 16 respectively. Desired values of D/U(95), may be converted to values of $N\{D/U(95)\}$ which can be read from the curves by the following procedure.

(a) Determine the value of co-channel station combination factor, C_f from table 6.

TABLE 6

Co-Channel Station Combination Factor, C_f

	Undesired Station Type		
Desired Station Type	Standard	Directional	Low Cost
Standard	0 dB	-10.5 dB	-0.5 dB
Directional	9.5 dB	-1 dB	+9 dB
Low Cost	-0.5 dB	-11 dB	-1 dB

(b) Determine the azimuth angle, α, between main lobe maximum of localizer carrier antenna at the undesired station and the aircraft.

(c) Using α and the antenna pattern (fig. 1 or 2) appropriate for the undesired station type, determine the gain factor, G, of the undesired localizer carrier antenna in the direction of the aircraft.

(d) Calculate $N\{D/U(95)\}$ using

$$N\{D/U(95)\} = D/U(95) - C_f + G \quad . \tag{1}$$

The values of C_f^* in table 6 were calculated from information given in table 1 by using the following equation:

$$C_f = P_D - P_U + A_D - A_U + H_D - H_U \quad , \tag{2}$$

where

P_D = carrier power radiated by desired station in dBW,

P_U = carrier power radiated by undesired station in dBW,

---

* Combination factors given in this report differ slightly from those given earlier [Gierhart and Johnson, 1965]. This occurred because a lower (1.5 dB compared to 2.5 dB) H_D value was selected for the ILS array height of 7.5 feet to provide combination factors that are better suited to the aircraft altitudes considered in this report. More precise combination factors could be obtained by considering H_D to be a function of aircraft altitude (0.5 dB for 500 feet to 2.5 dB for 18,000), but this would further complicate the normalization and require that the conversion factor tables be expanded to several times their present size.

A_D = free-space antenna gain referred to an isotropic radiator for the main lobe of the desired station localizer carrier antenna array, in dB,

A_U = antenna gain similar to A_D, but for undesired station,

H_D = height gain factor for desired station,

H_D = 0 dB for ILS array height of 5.5 feet (8-Loop),

H_D = 1.5 dB for ILS array height of 7.5 feet (V-Ring),

H_U = height gain factor for undesired station,

H_U = 0 dB for ILS array height of 5.5 feet (8-Loop),

H_U = 2.5 dB for ILS array height of 7.5 feet (V-Ring).

Values of G read from figures 1 or 2 represent the gain of the undesired localizer carrier antenna in the direction of the aircraft relative to the gain of the same antenna in the direction of the main lobe maximum. Because of this, values of G are always non-positive and N{D/U(95)} will have its worst (highest) value for a particular pattern when G is 0.

For example, if a co-channel D/U(95) of 12 dB or greater at an altitude of 18,000 feet is required for satisfactory service, then satisfactory service is expected for $d_D \leq 25$ nautical miles when (1) both ground stations are of the "standard" type, (2) the ground stations and aircraft are on the same great circle arc, (3) $G \leq 0$, and (4) $S \geq 130$ nautical miles. This conclusion follows from figure 16 when N{D/U(95)} is determined from (1) with $C_f = G = 0$; i.e., N{D/U(95)} = D/U(95) = 12 dB.

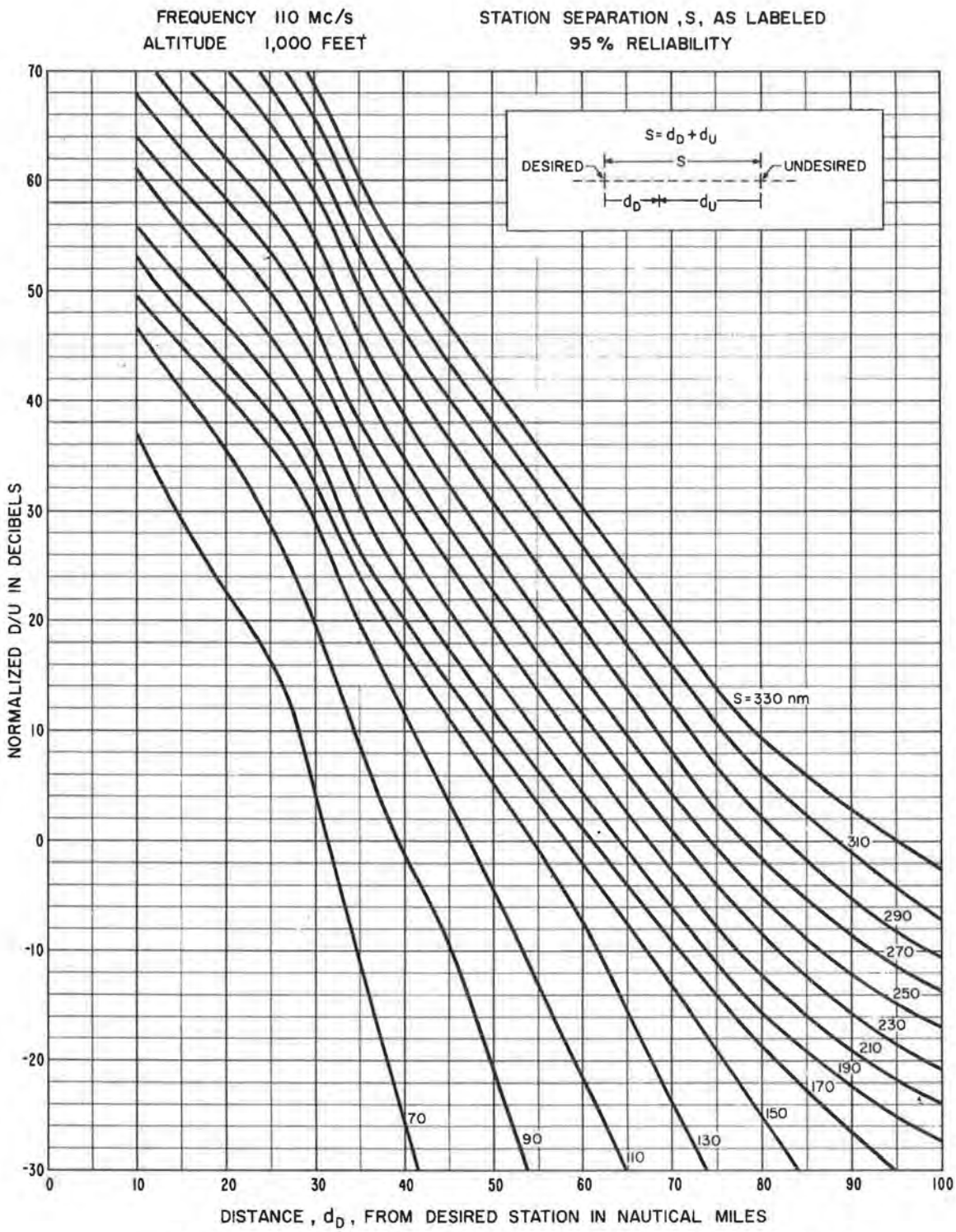

Co-Channel ILS Signal Ratios; Altitude = 1,000 feet

Figure 10

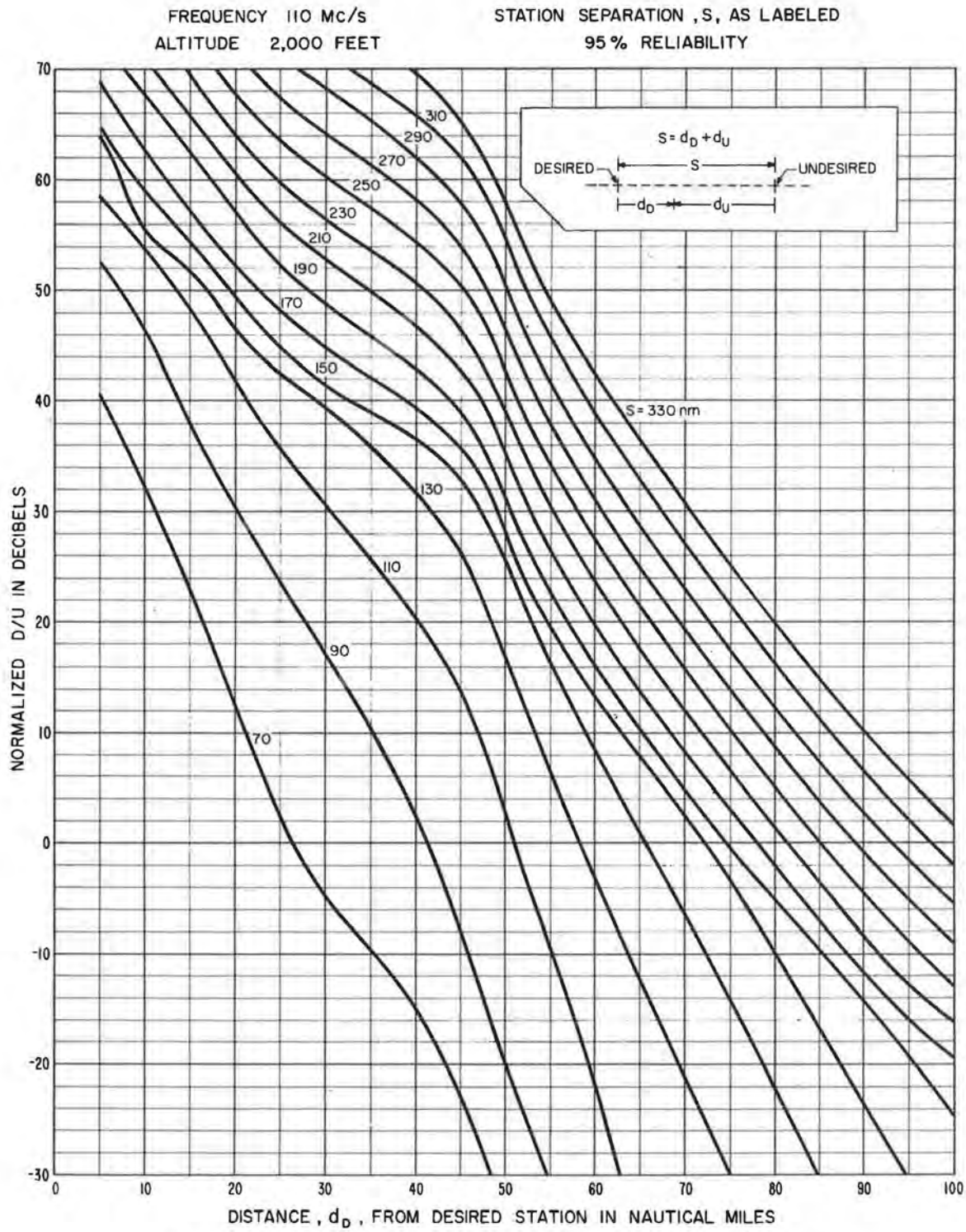

Co-Channel ILS Signal Ratios; Altitude = 2,000 feet

Figure 11

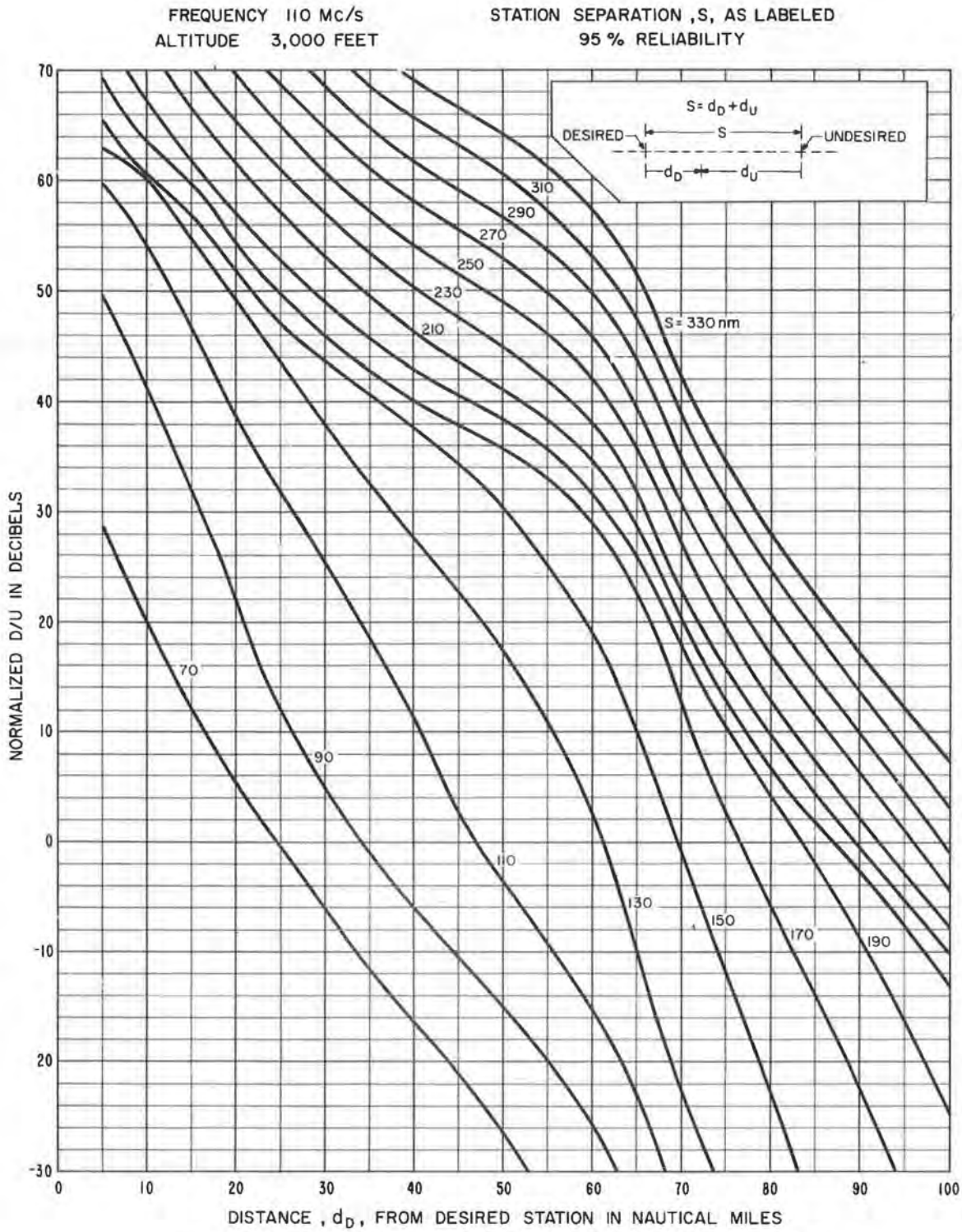

Co-Channel ILS Signal Ratios; Altitude = 3,000 feet

Figure 12

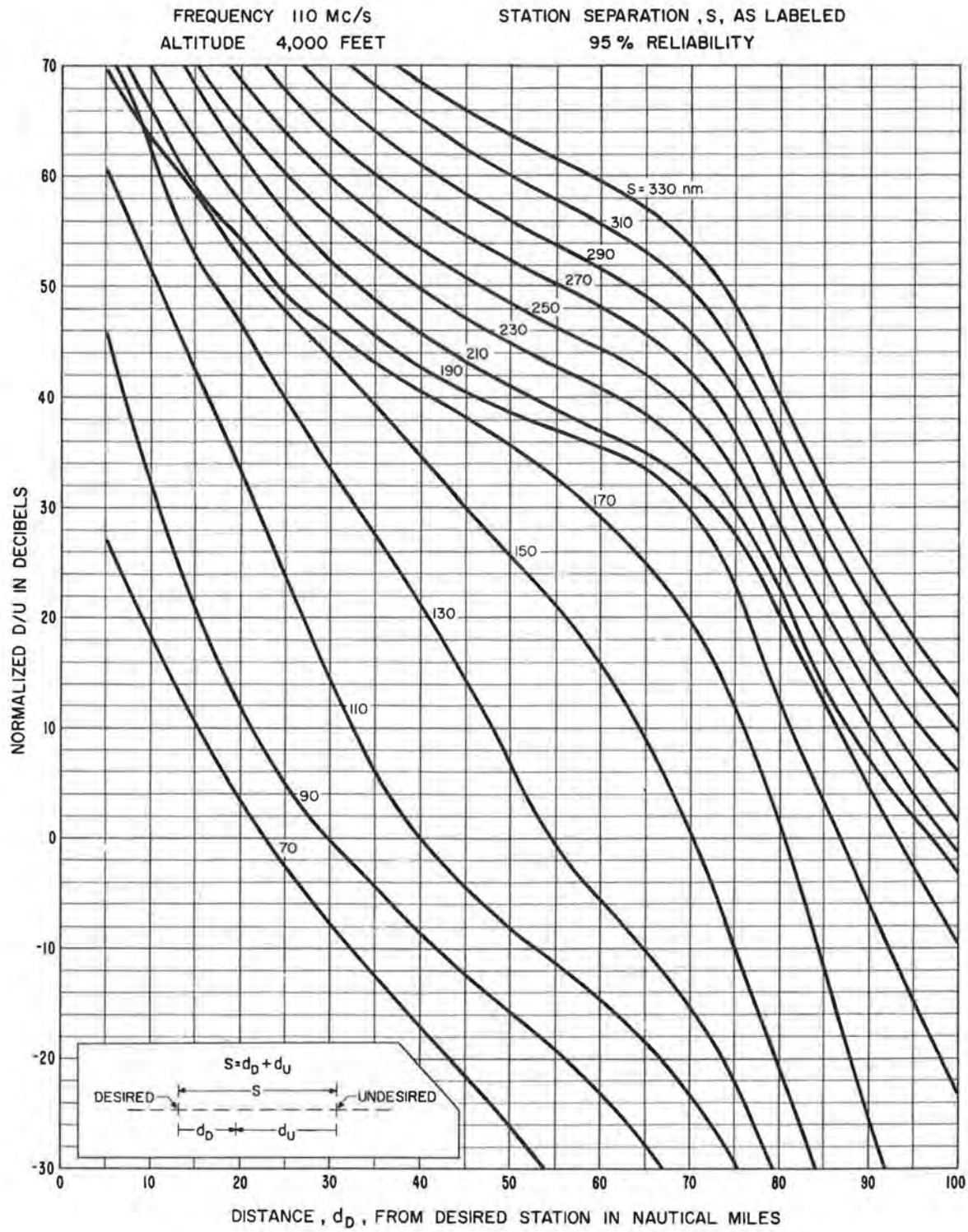

Co-Channel ILS Signal Ratios; Altitude = 4,000 feet

Figure 13

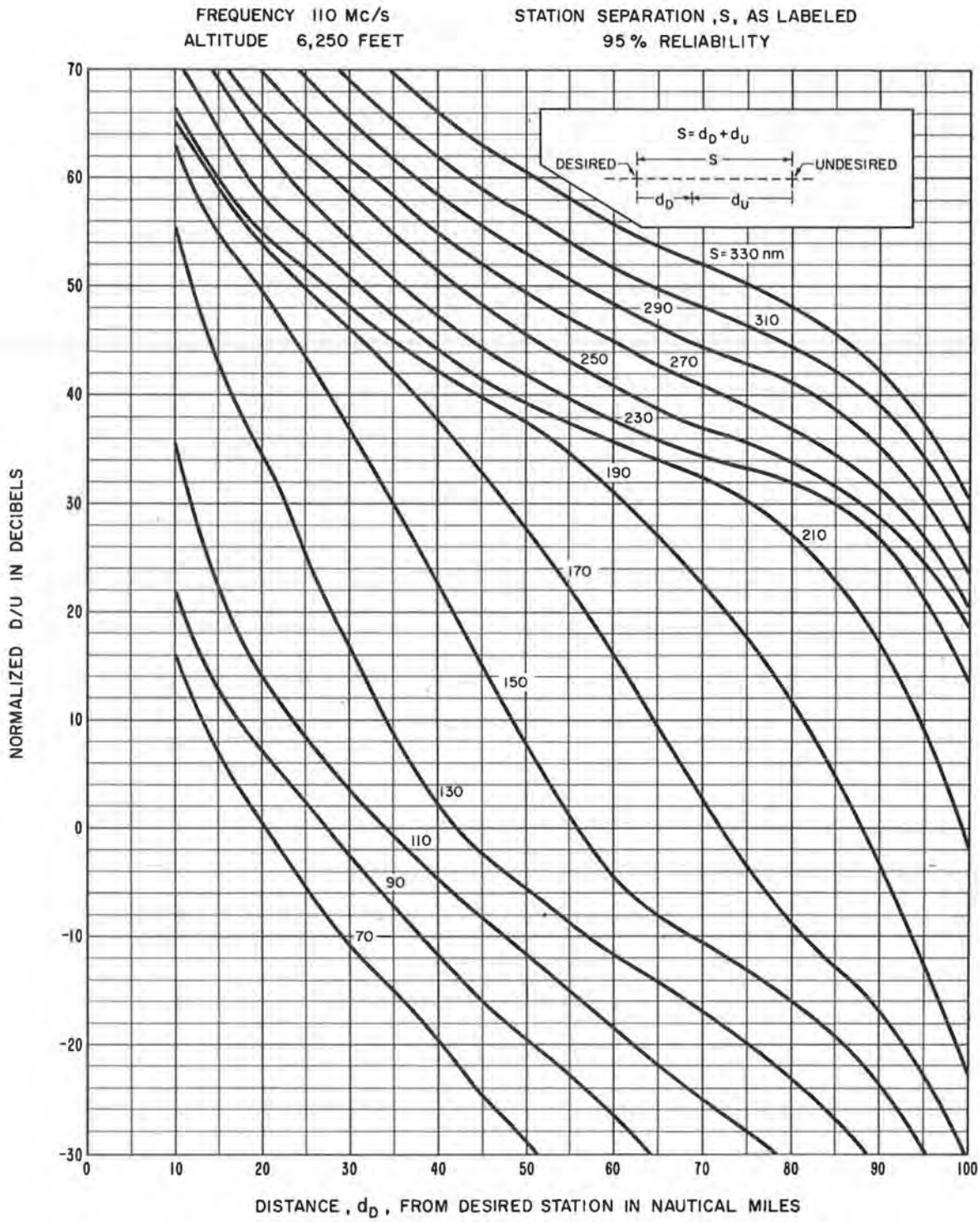

Co-Channel ILS Signal Ratios; Altitude = 6,250 feet

Figure 14

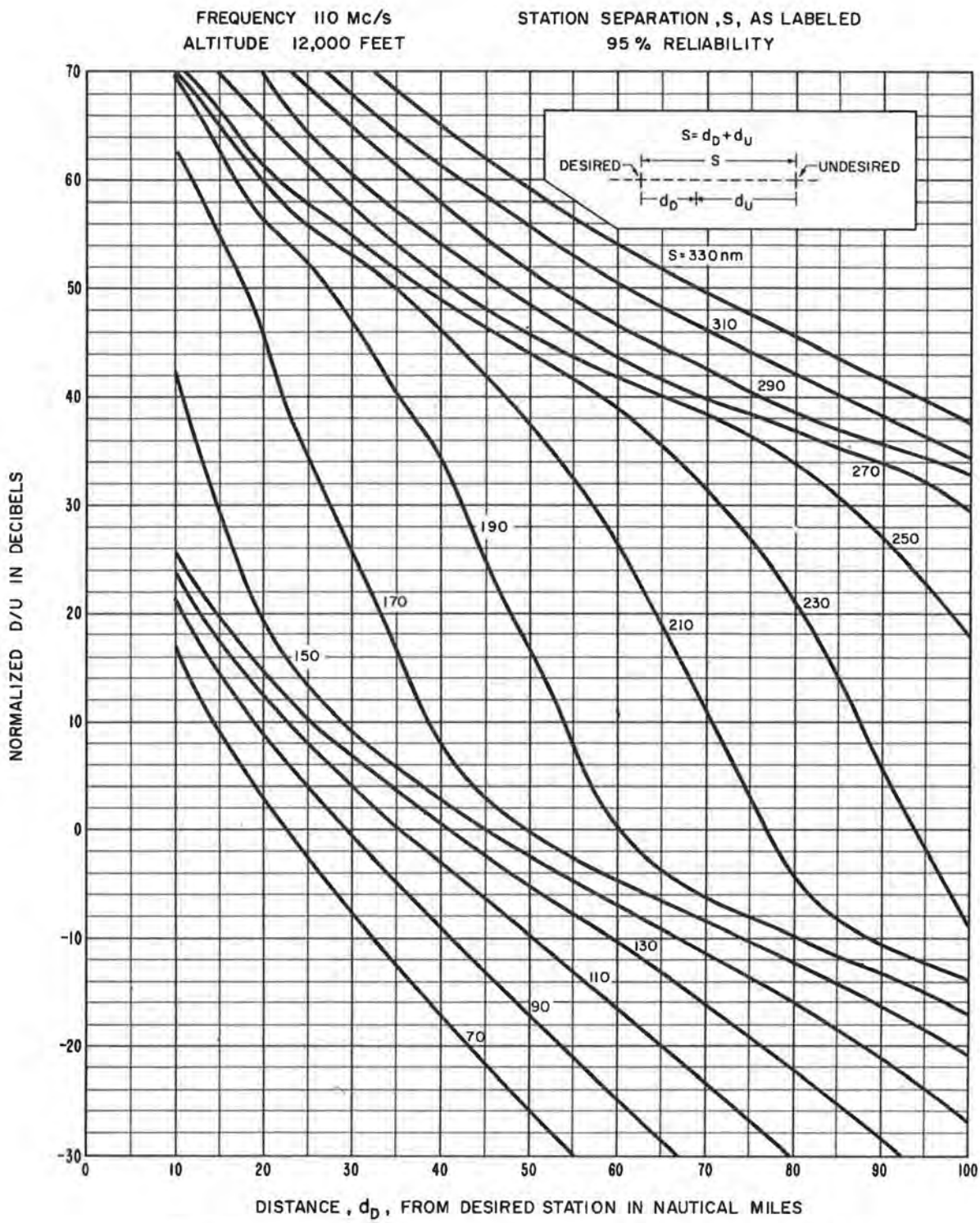

Co-Channel ILS Signal Ratios; Altitude = 12,000 feet

Figure 15

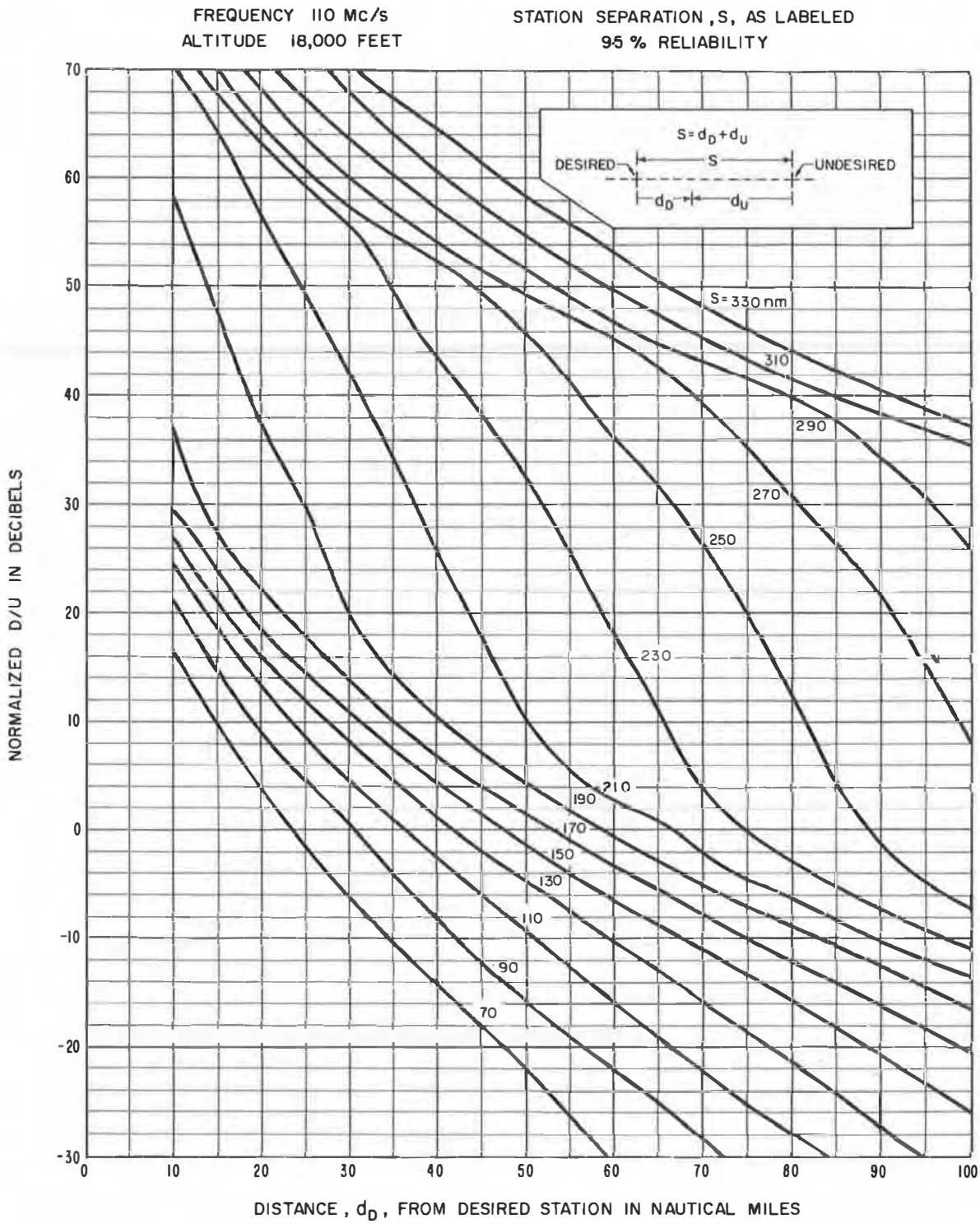

Co-Channel ILS Signal Ratios; Altitude = 18,000 feet

Figure 16

5.3 ILS Signal Ratios Due to Adjacent-Channel Interference

Adjacent-channel N{D/U(95)} curves for aircraft altitudes of 500, 1,000, 6,250, and 12,000 feet are shown in figures 17, 18, 19, and 20 respectively. Values of D/U(95) may be converted to values of N{D/U(95)} which can be read from the curves by the following procedure:

(a) Determine the value of the adjacent-channel station combination factor, C_f, from table 7.

TABLE 7

Adjacent-Channel Station Combination Factor, C_f *

Desired Station Type		
Standard	Directional	Low Cost
1.85 dB	11.35 dB	1.35 dB

(b) Calculate N{D/U(95)} using

$$N\{D/U(95)\} = D/U(95) - C_f . \qquad (3)$$

The values of C_f in table 7 were calculated from information given in tables 1 and 2 by using equation (2) given in section 5.2. (H_U = 0 dB for VOR).

In the adjacent-channel case the calculation of D/U(95) is somewhat simpler than in the co-channel case. This is because the adjacent-channel undesired station is always a VOR and the VOR has an omnidirectional radiation pattern in the horizontal plane; thus, no gain factor is required.

* See footnote for table 6 in section 5.2.

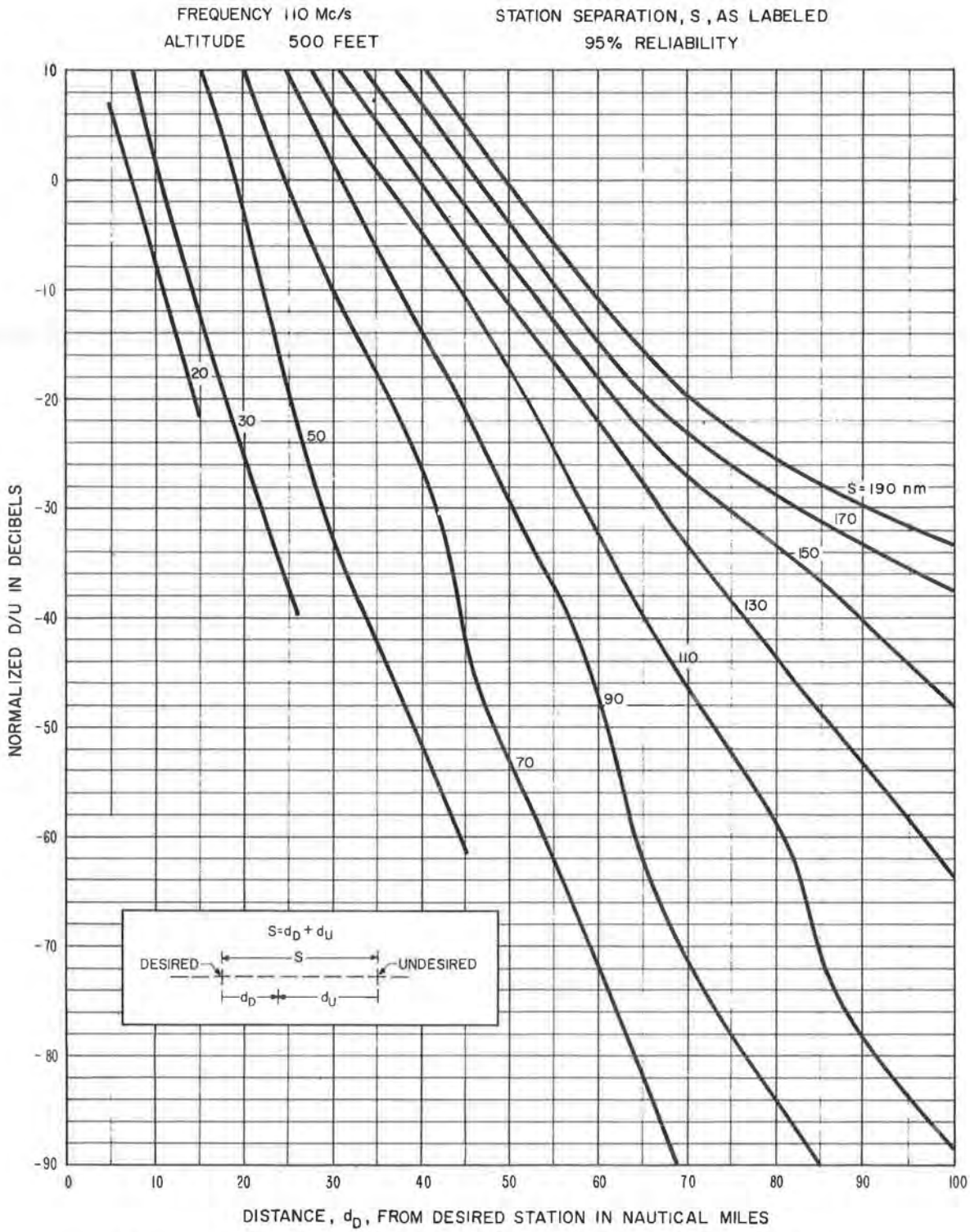

Adjacent-Channel ILS Signal Ratios; Altitude = 500 feet

Figure 17

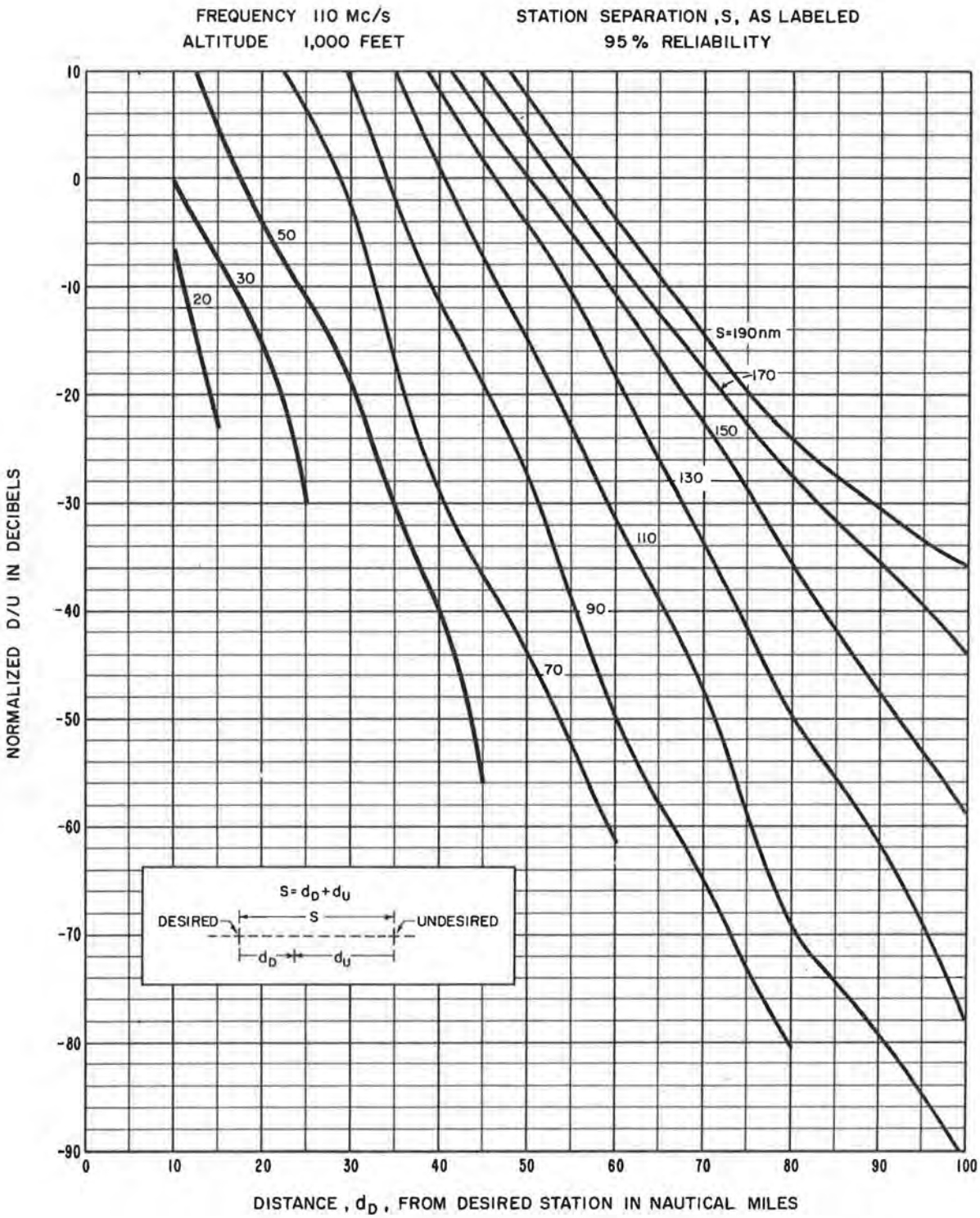

Adjacent-Channel ILS Signal Ratios; Altitude = 1,000 feet

Figure 18

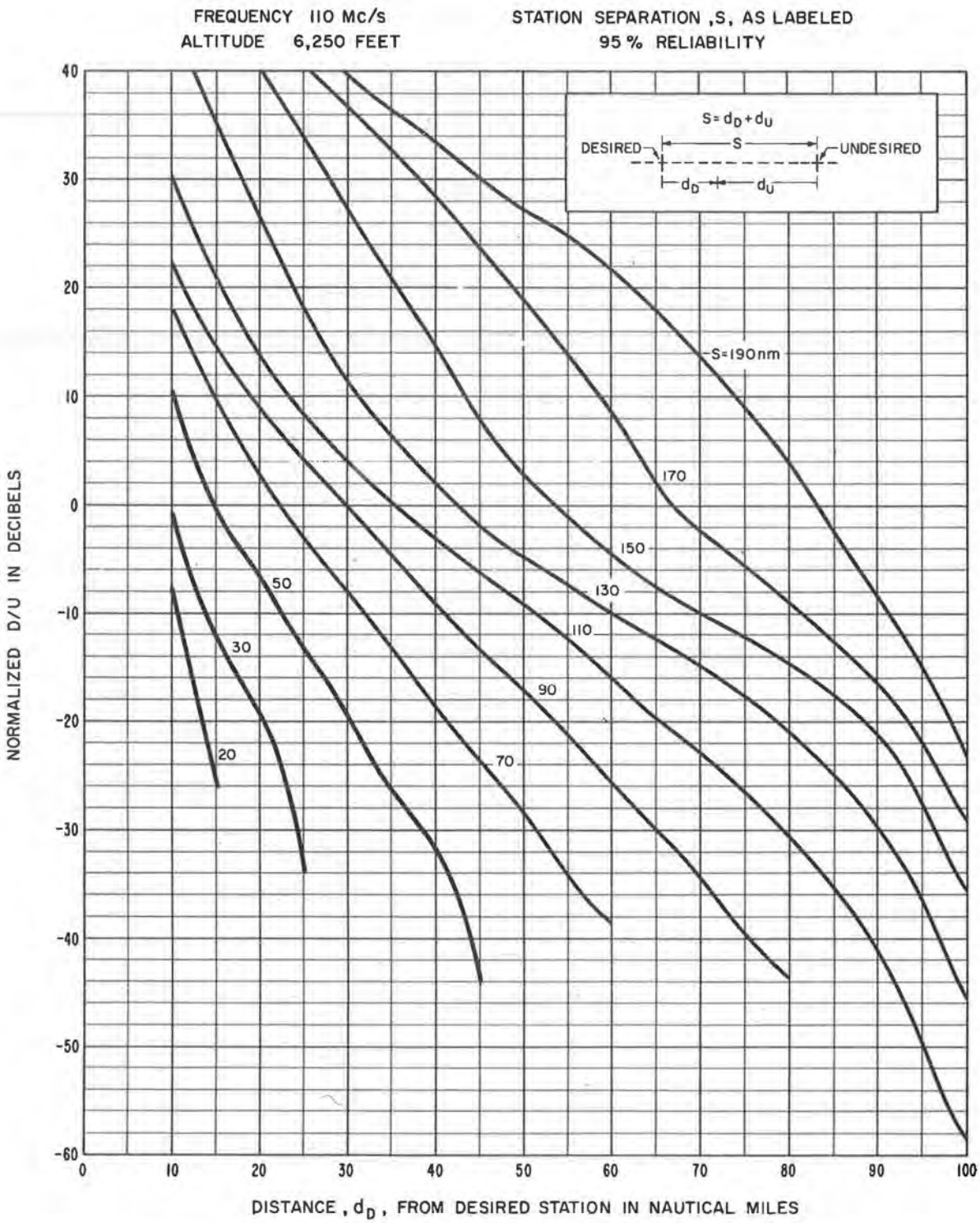

Adjacent-Channel ILS Signal Ratios; Altitude = 6, 250 feet

Figure 19

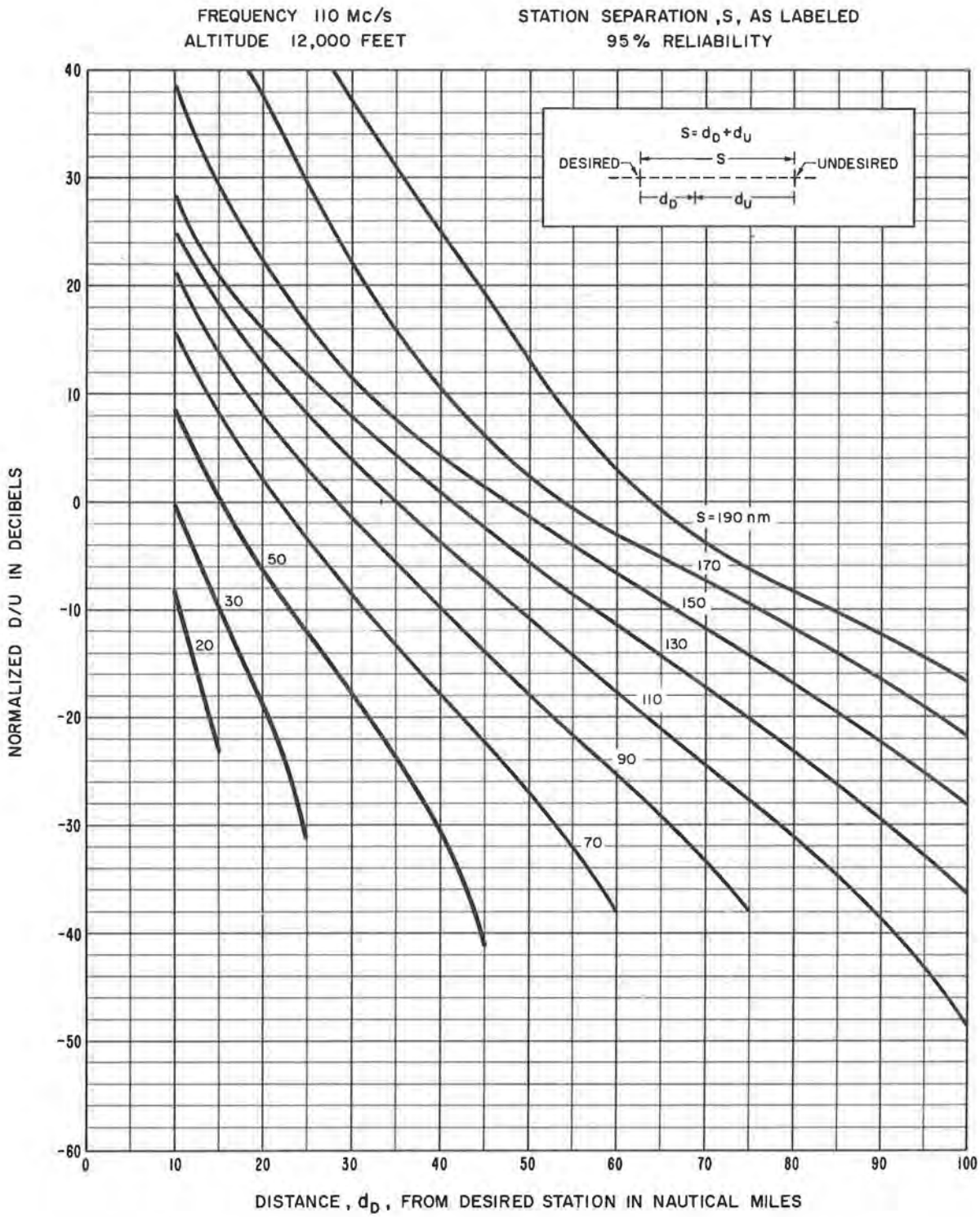

Adjacent-Channel ILS Signal Ratios; Altitude = 12,000 feet
Figure 20

5.4 VOR and TACAN Co-Channel Service Volumes

Service volume curves shown on figures 21 through 27 for VOR and 28 through 37 for TACAN, illustrate the effect of co-channel interference on service volumes when the aircraft is located above the great circle path between the desired and the undesired station at a distance, d_D, from the desired station. The geometry is shown by a small diagram on each figure. Station separations, S, ranging from 70 to 695 nautical miles were considered along with aircraft altitudes ranging from 1,000 to 100,000 feet. Each figure is applicable to a different desired-to-undesired signal ratio, D/U(95). For example, D/U(95) = 14 dB means that the desired signal is at least 14 dB greater than the undesired signal for 95% of the time along the solid curve which forms the boundary of service volume. On these figures the limitation imposed by ground station power output and the available power requirements (see sec. 5.1) is described only by the dashed line labeled "nominal range".

The volume defined by rotating the appropriate curve about the ordinate axis represents a volume in which service reliability (see sec. 4) is 95% or greater by virtue of each curve representing the smallest $d_D + d_U$ value possible for particular ground station separations (see sec. 5.2). Similarly, if service is limited by interference from several co-channel stations, the volume defined by rotating the most restrictive curve (which is the curve appropriate to the closest interfering station) about the ordinate axis represents a volume in which the service reliability is generally 95% or greater, but not always.

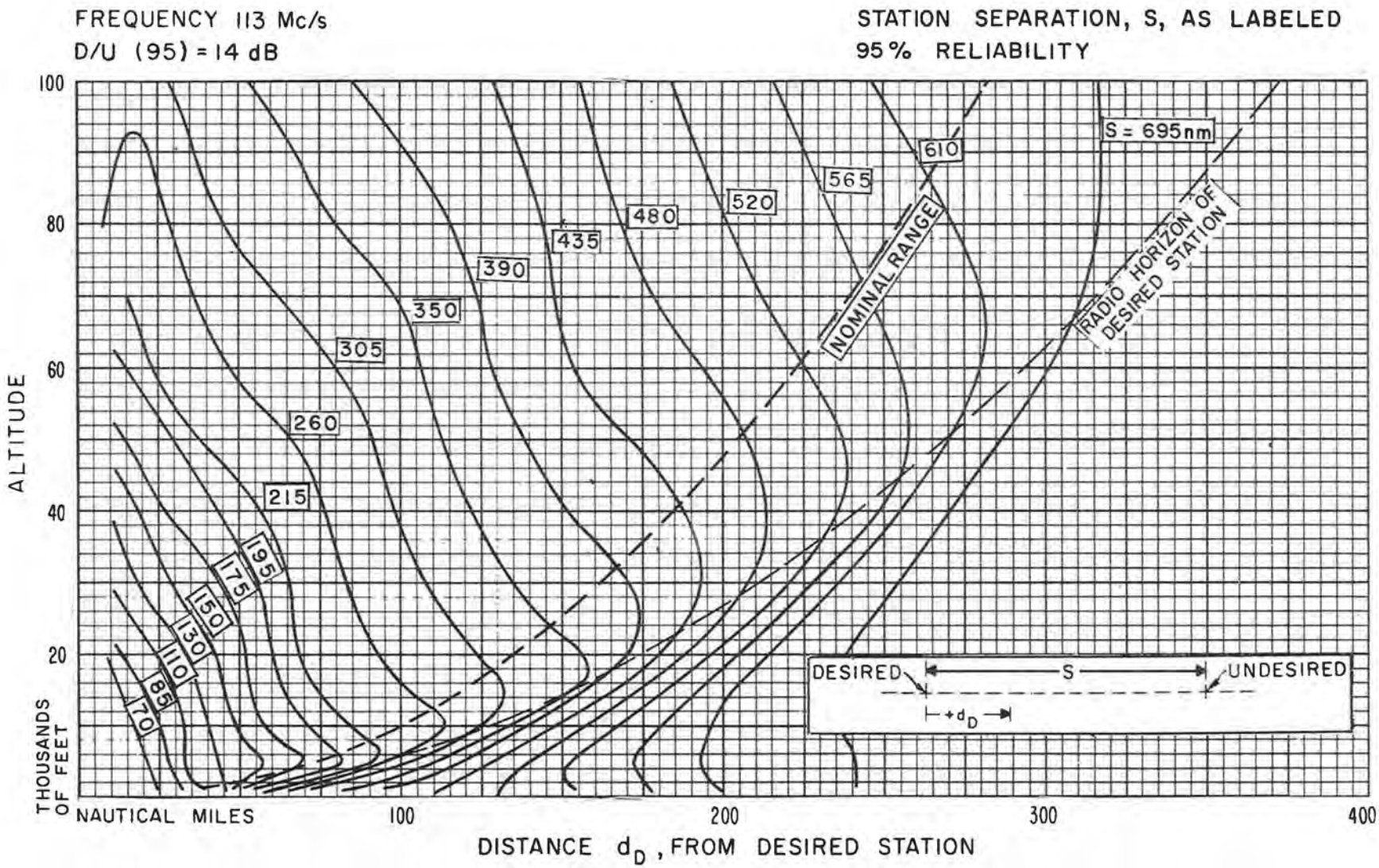

VOR Service Volumes; D/U(95) = 14 dB

Figure 21

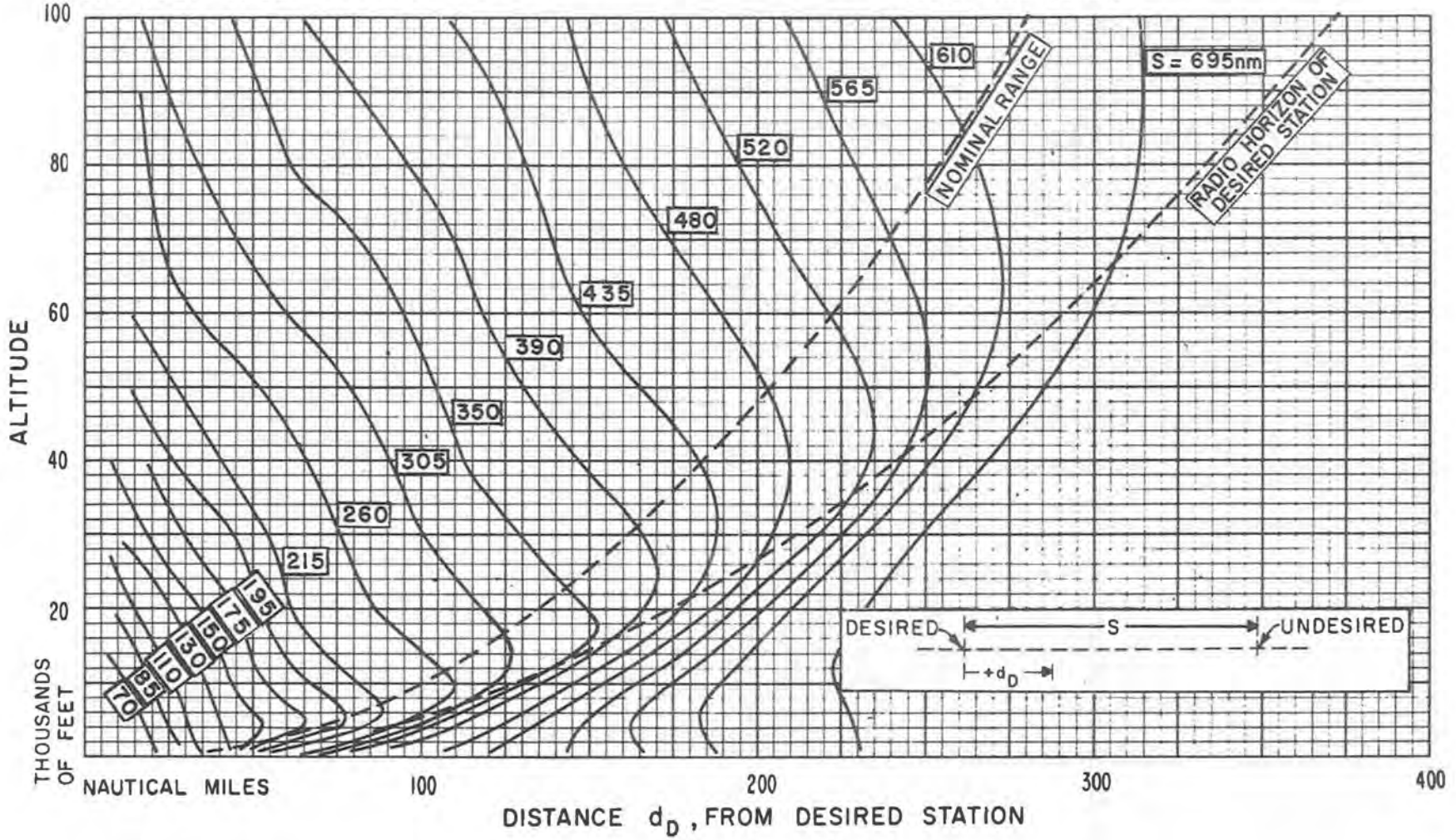

VOR Service Volumes; D/U(95) = 17 dB

Figure 22

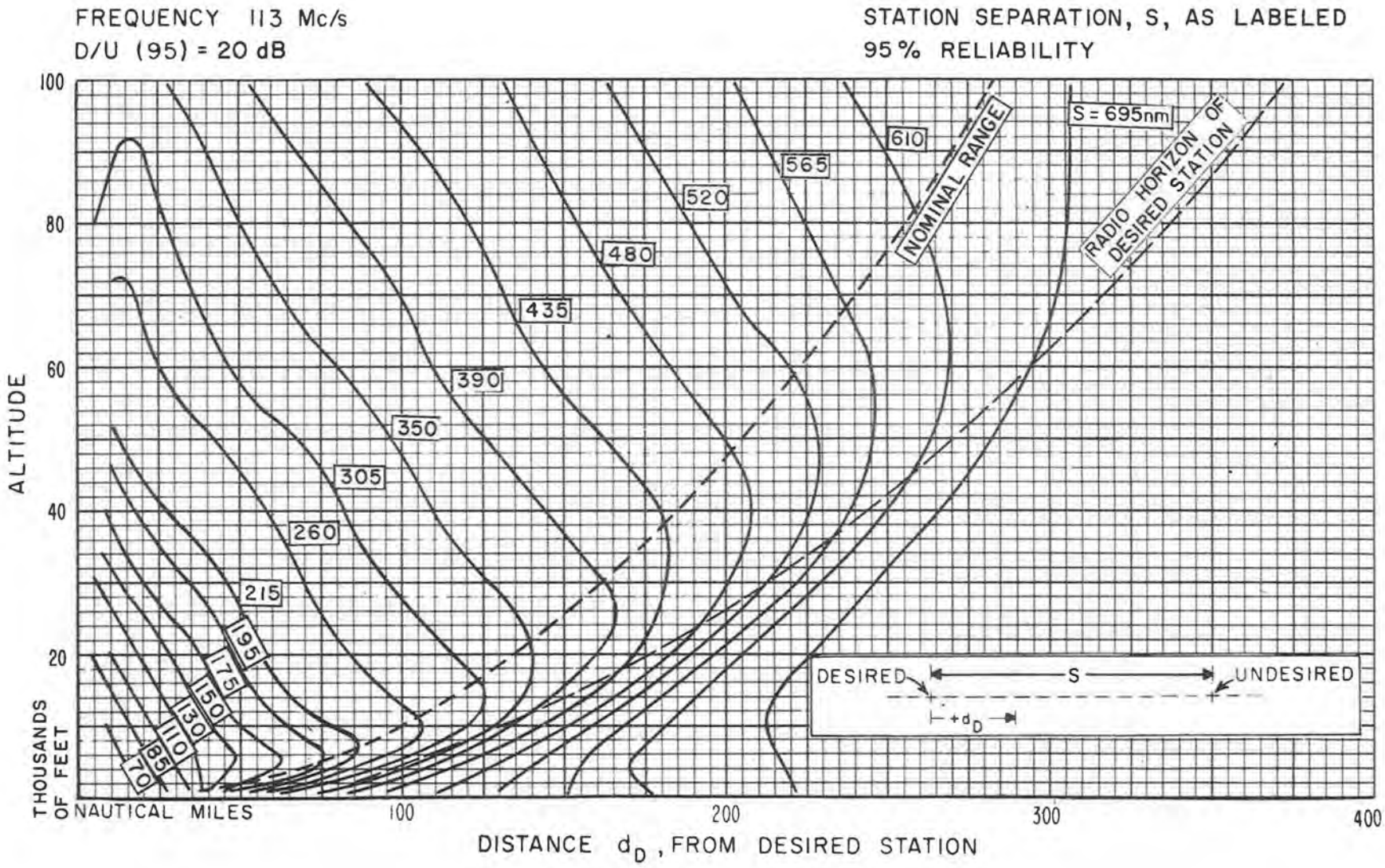

VOR Service Volumes; D/U(95) = 20 dB

Figure 23

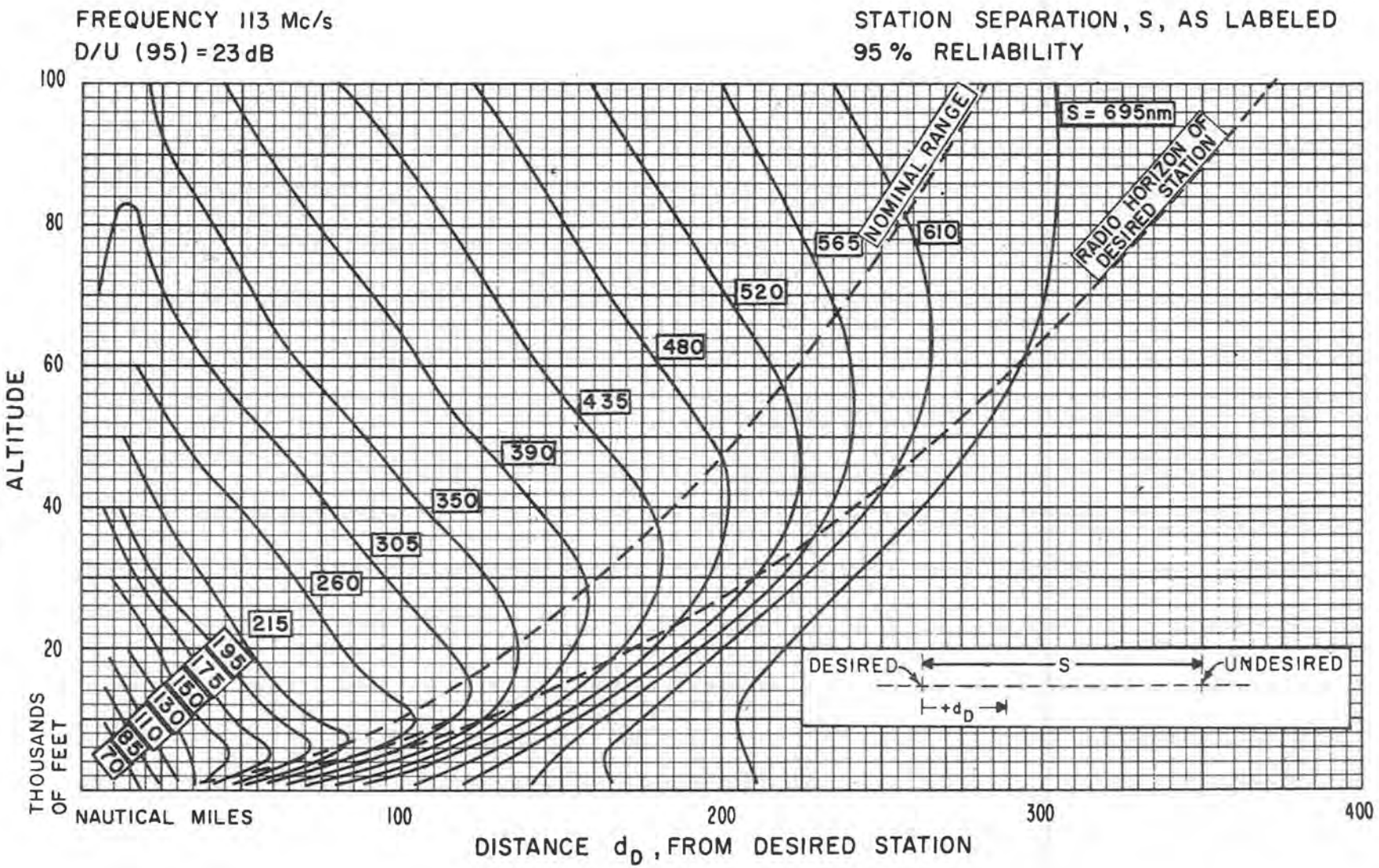

VOR Service Volumes; D/U(95) = 23 dB

Figure 24

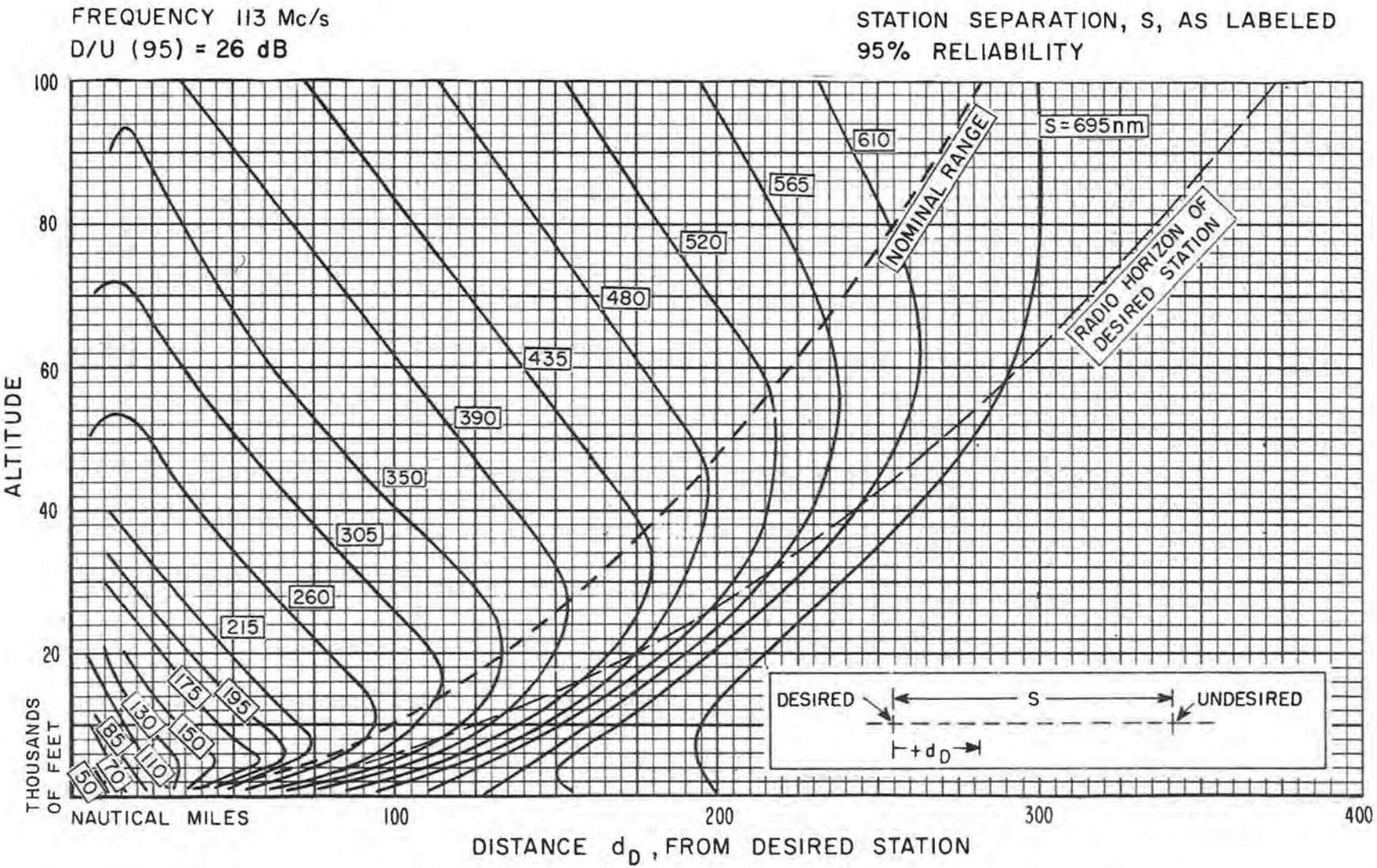

VOR Service Volumes; D/U(95) = 26 dB

Figure 25

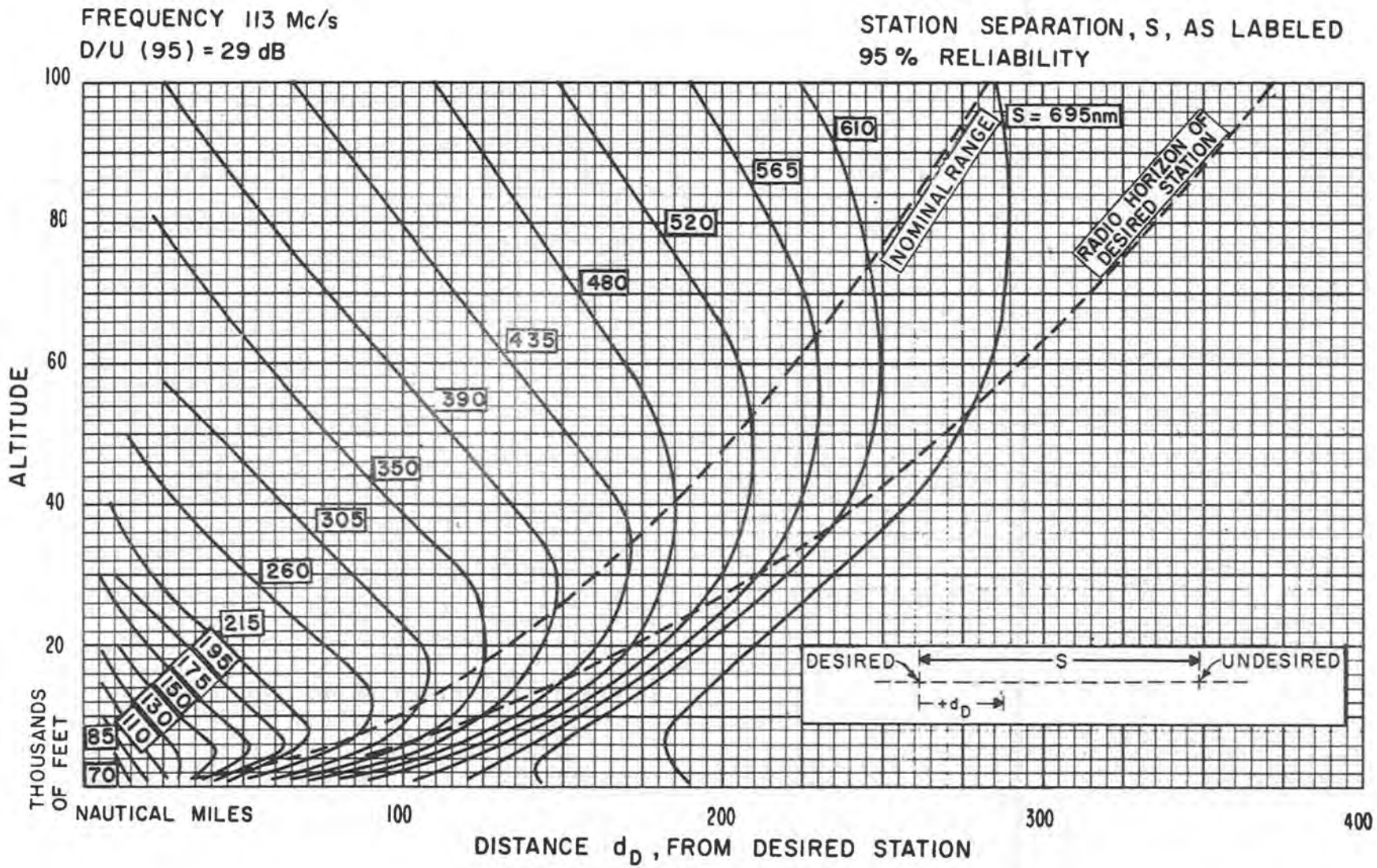

VOR Service Volumes; D/U(95) = 29 dB

Figure 26

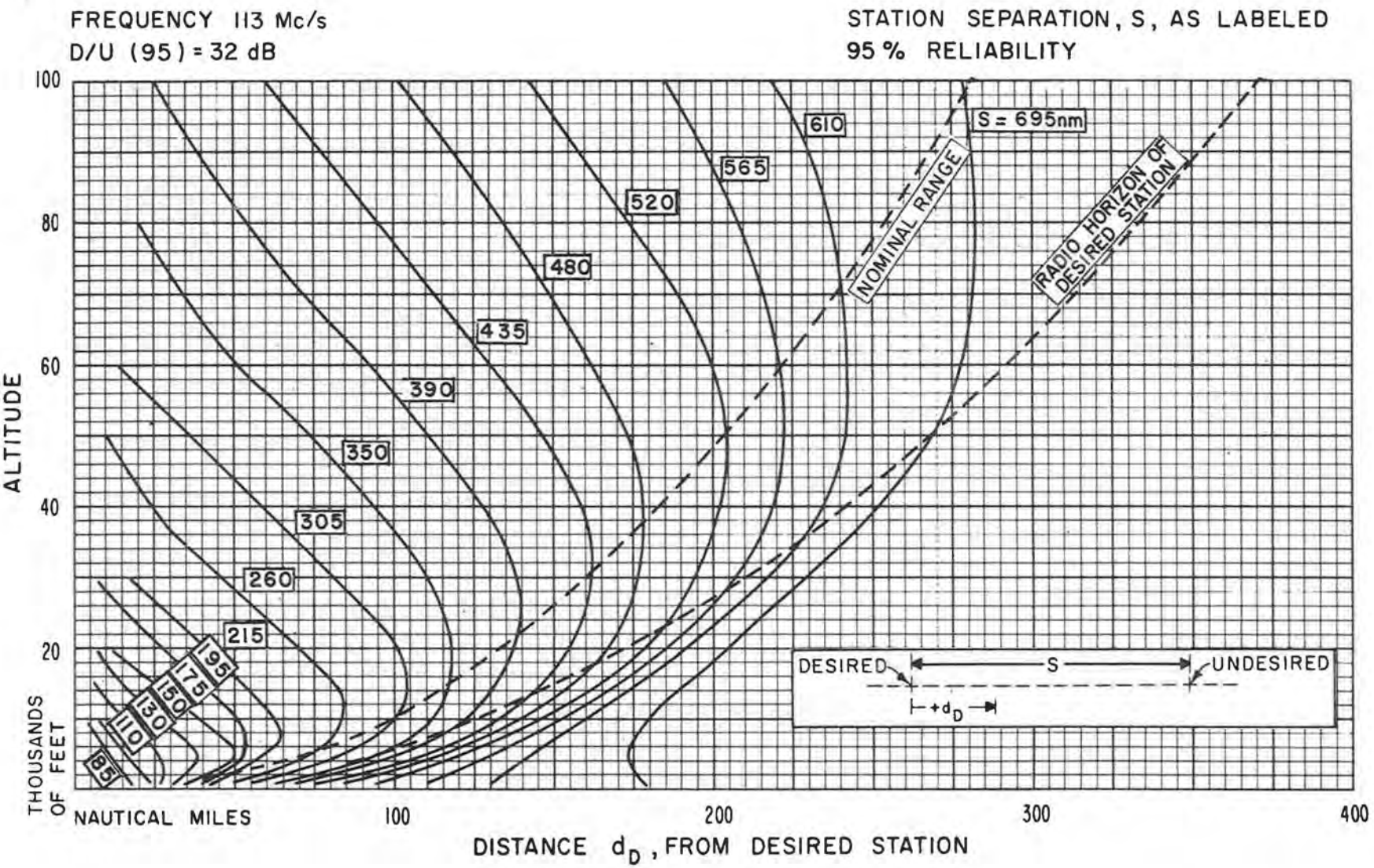

VOR Service Volumes; D/U(95) = 32 dB

Figure 27

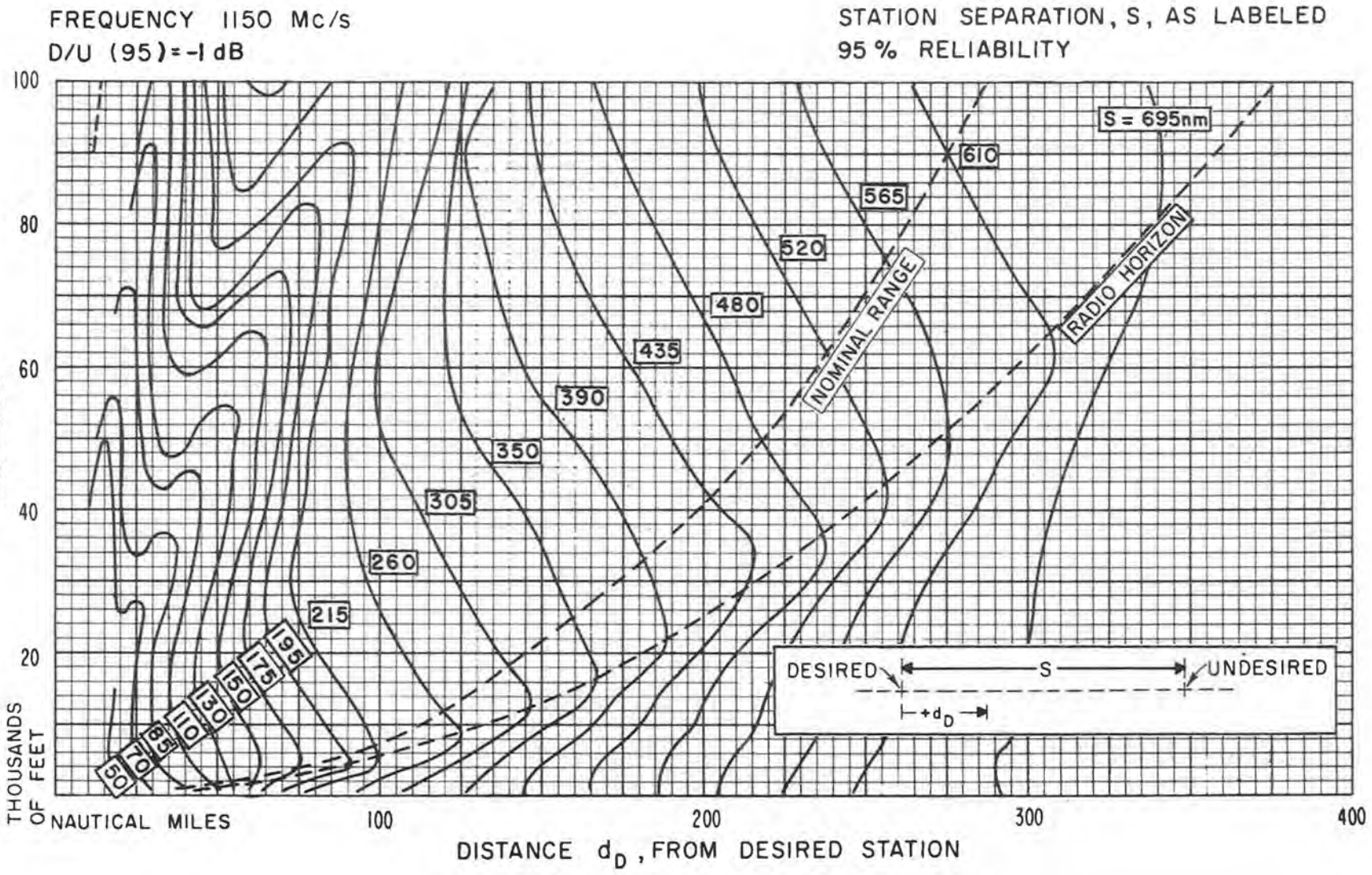

TACAN Service Volumes; D/U(95) = -1 dB

Figure 28

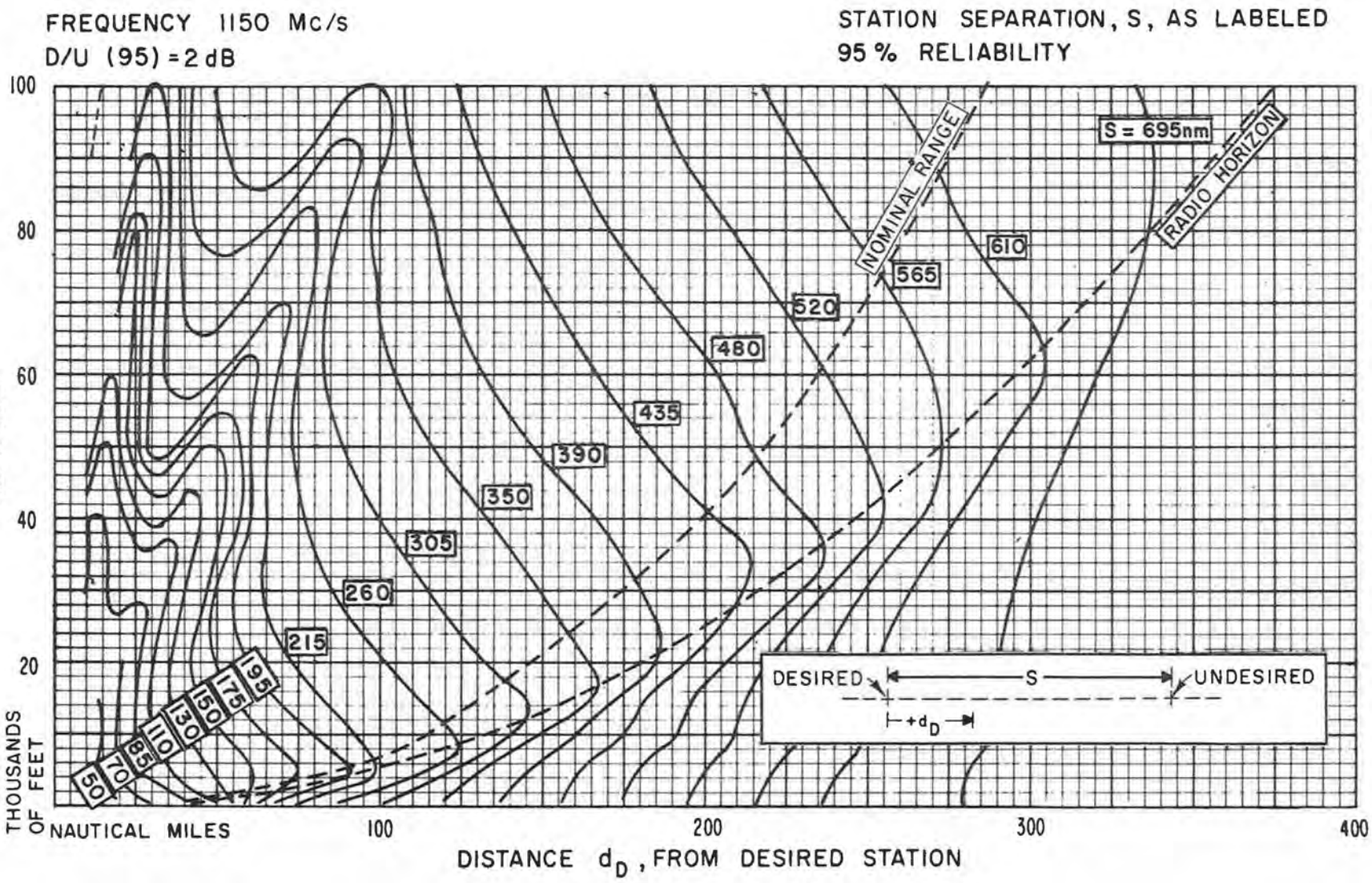

TACAN Service Volumes; D/U(95) = 2 dB

Figure 29

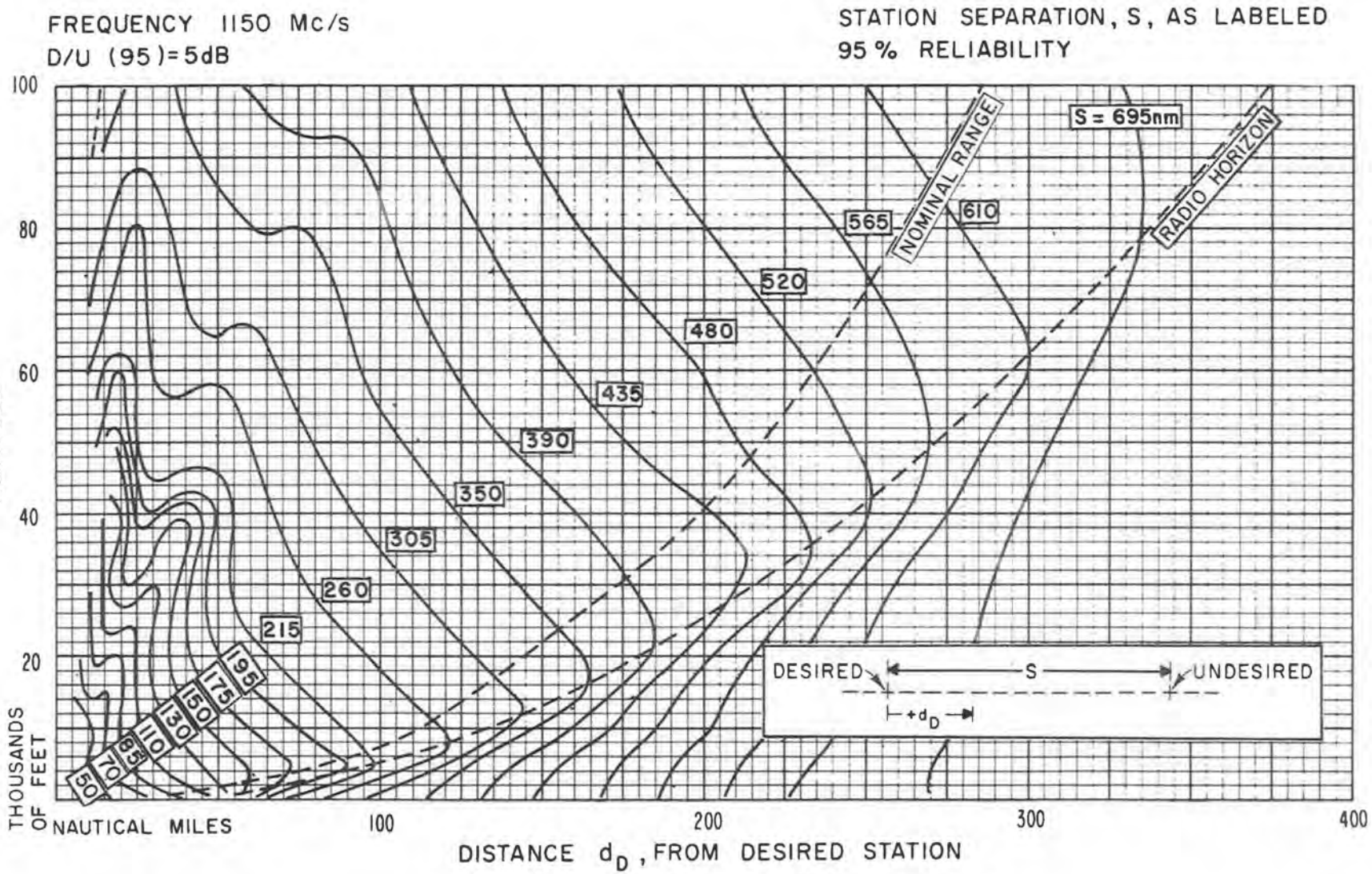

TACAN Service Volumes; D/U(95) = 5 dB

Figure 30

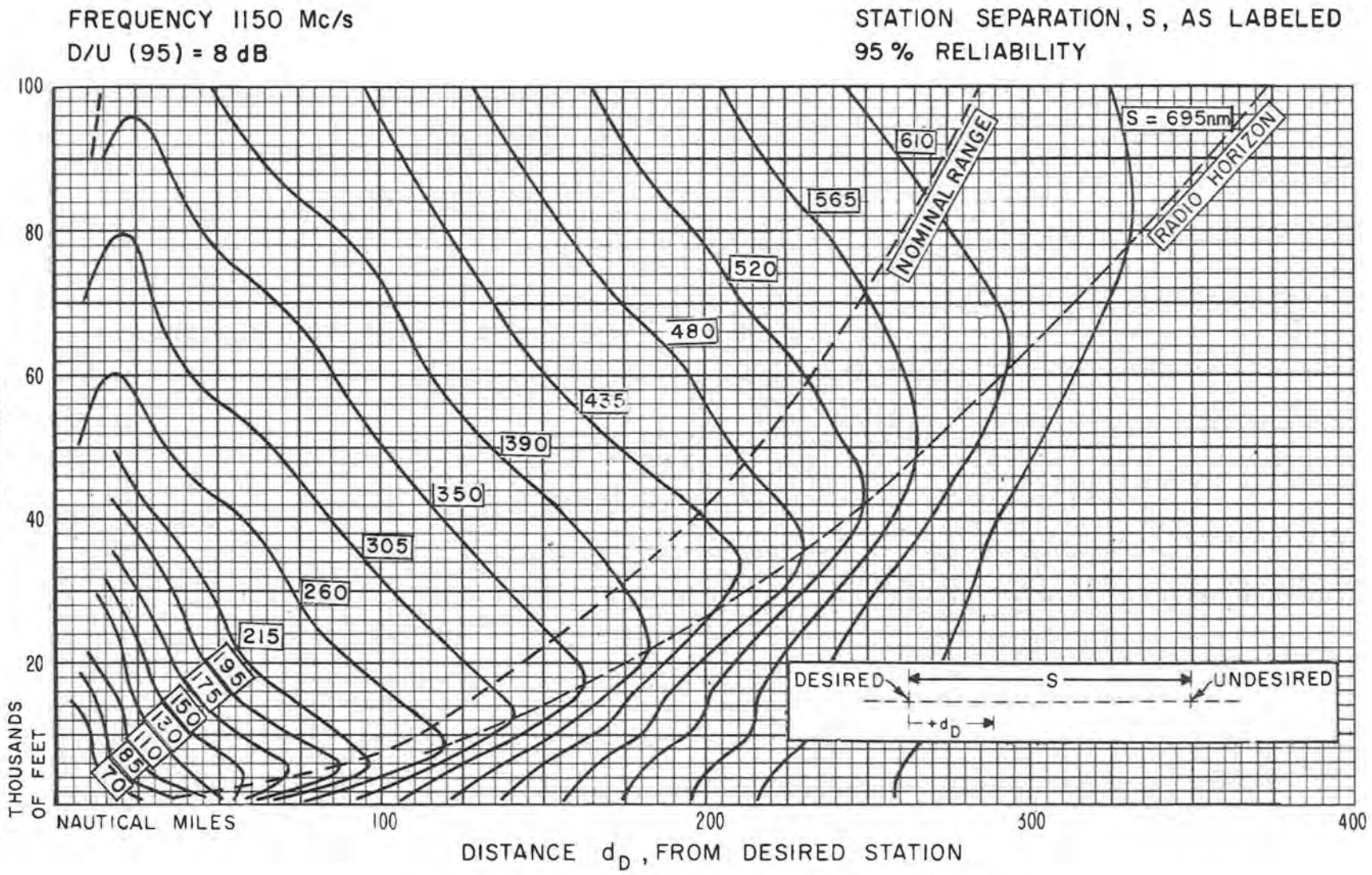

TACAN Service Volumes; D/U(95) = 8 dB

Figure 31

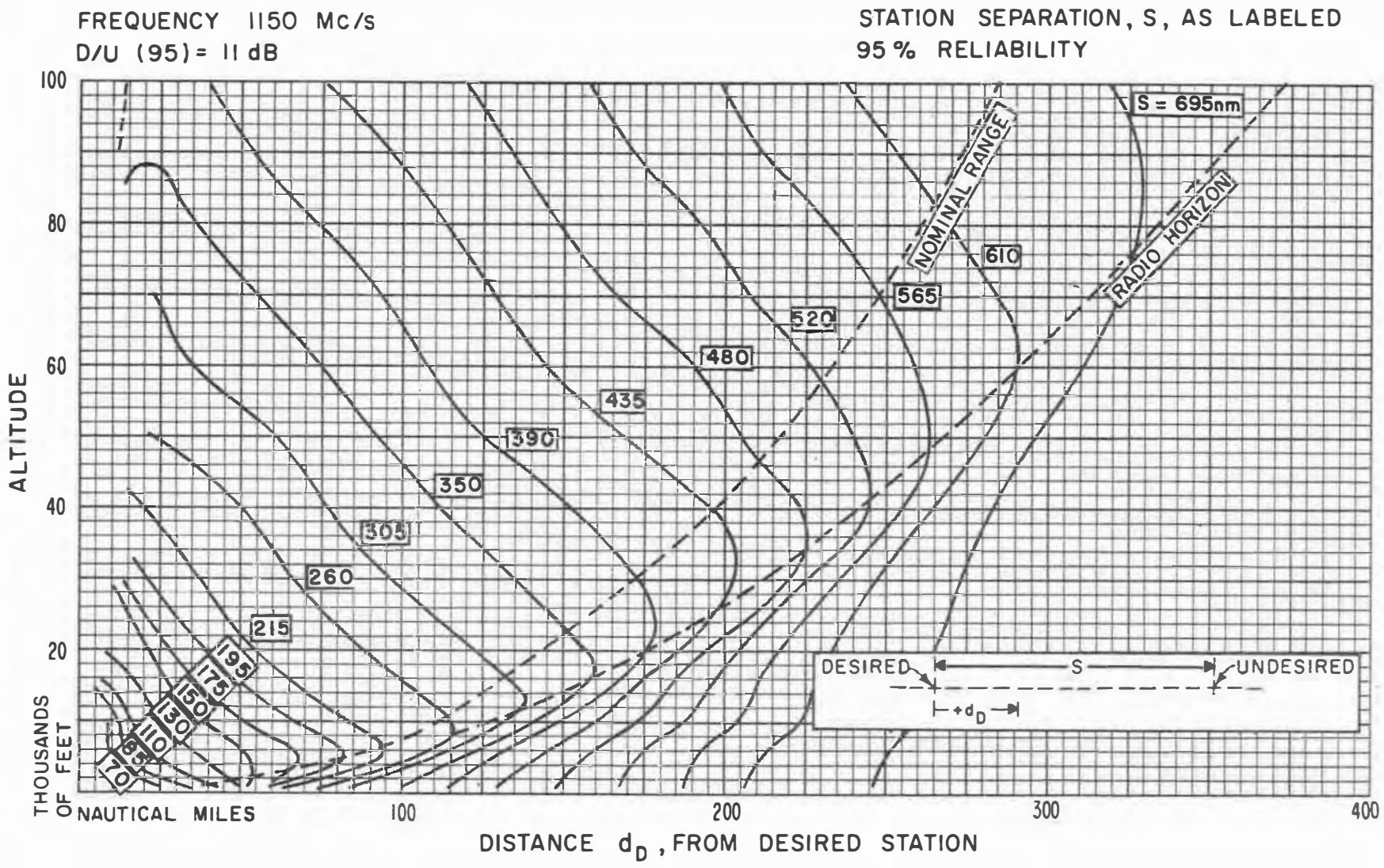

TACAN Service Volumes; D/U(95) = 11 dB

Figure 32

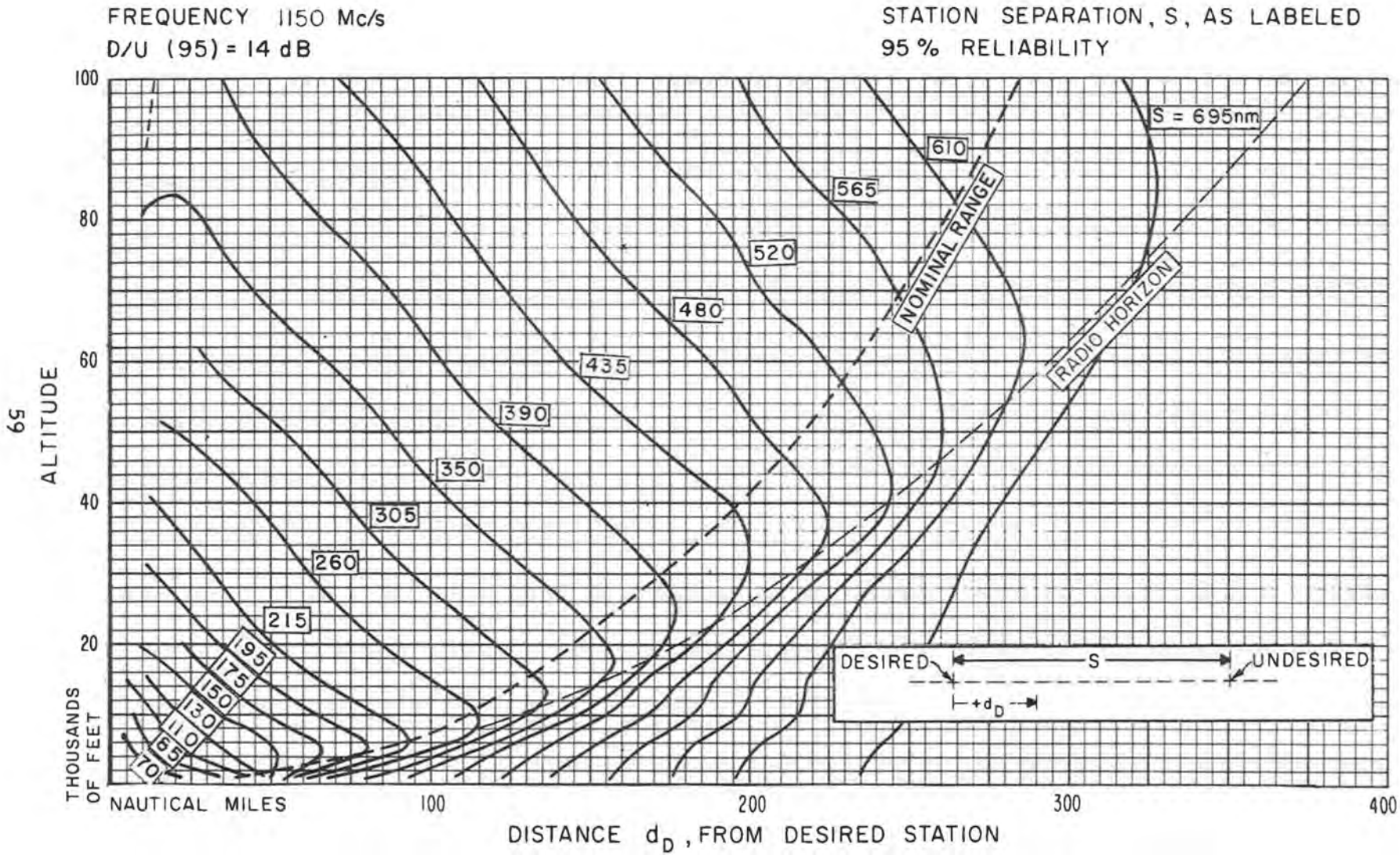

TACAN Service Volumes; D/U(95) = 14 dB

Figure 33

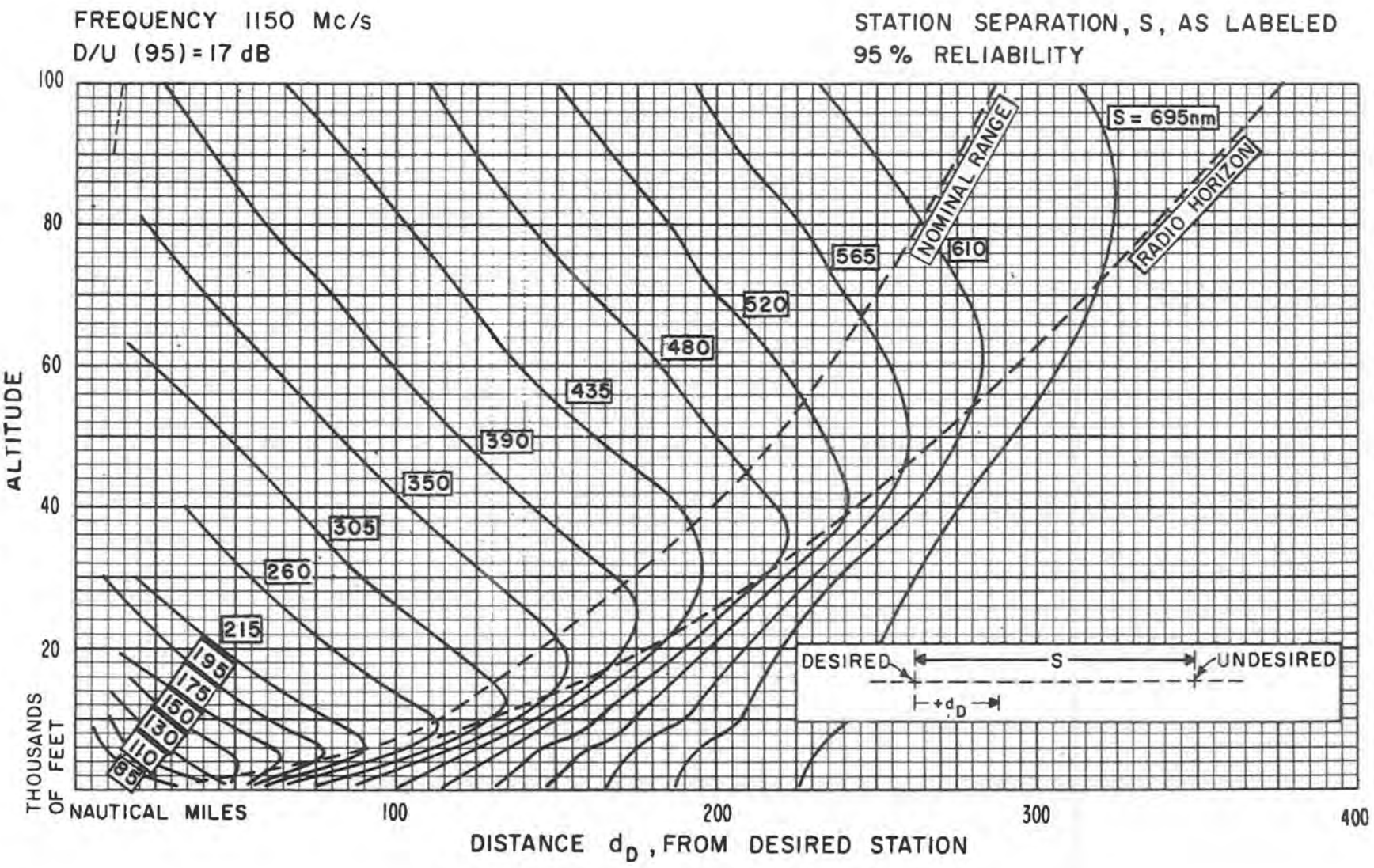

TACAN Service Volumes; D/U(95) = 17 dB

Figure 34

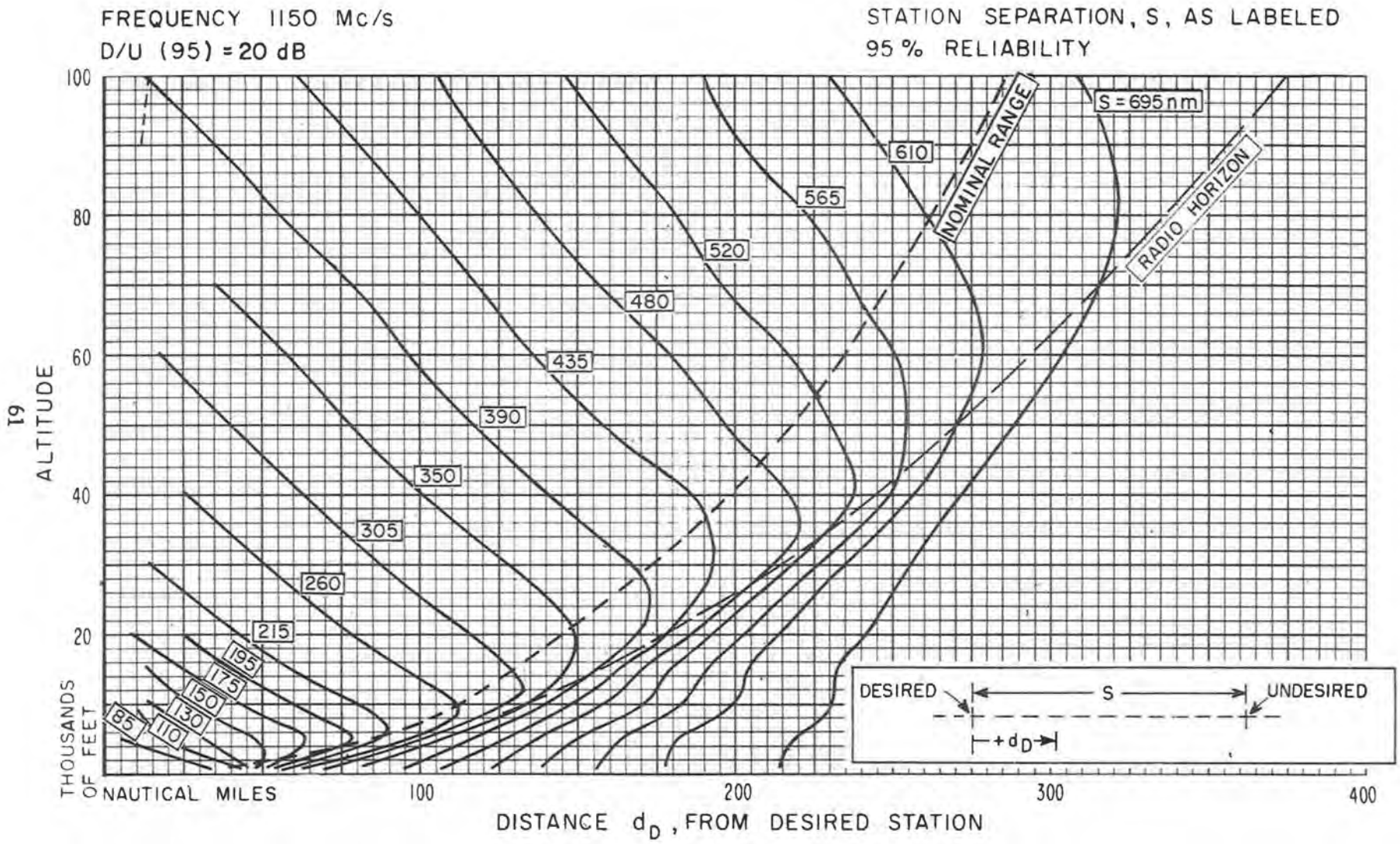

TACAN Service Volumes; D/U(95) = 20 dB

Figure 35

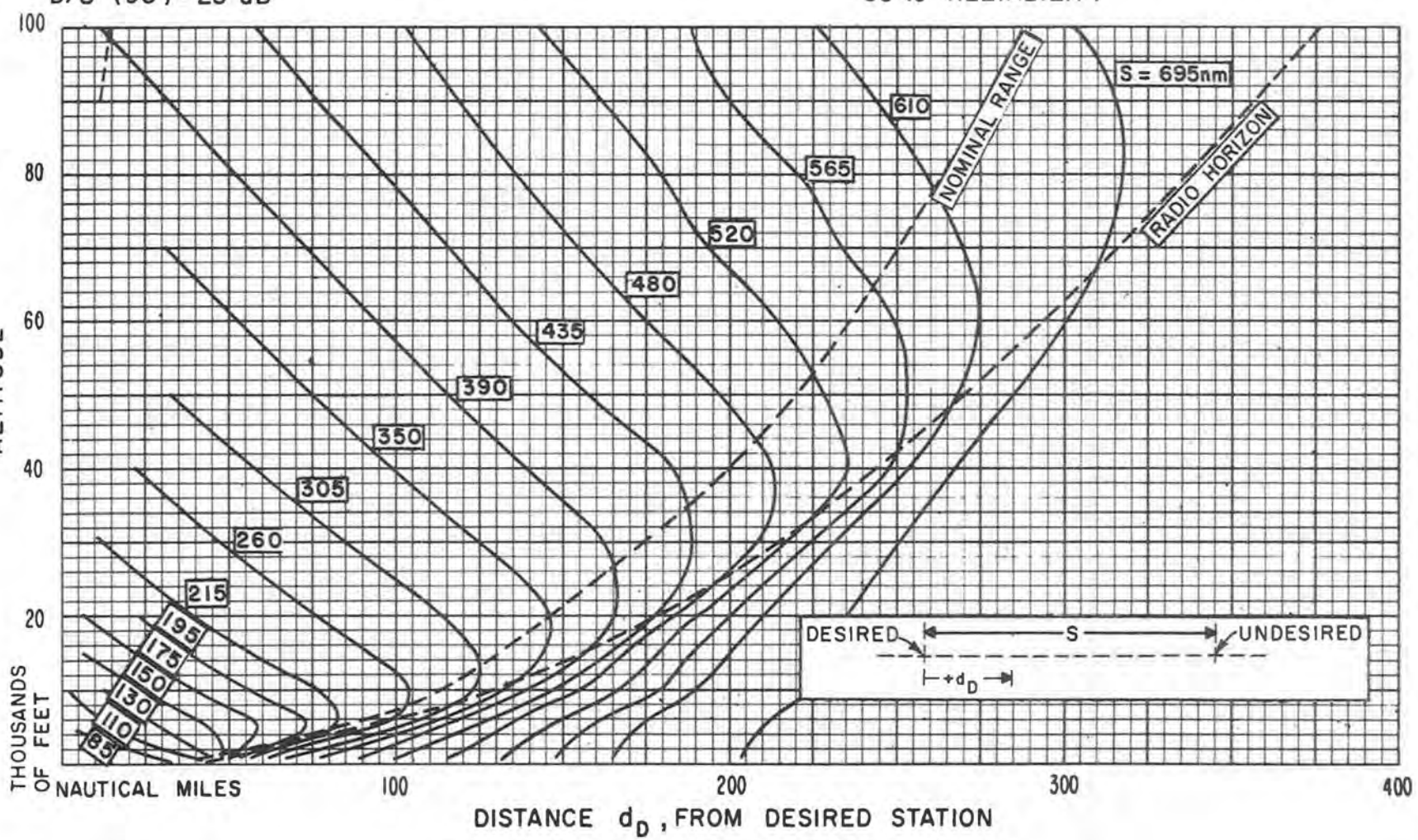

TACAN Service Volumes; D/U(95) = 23 dB

Figure 36

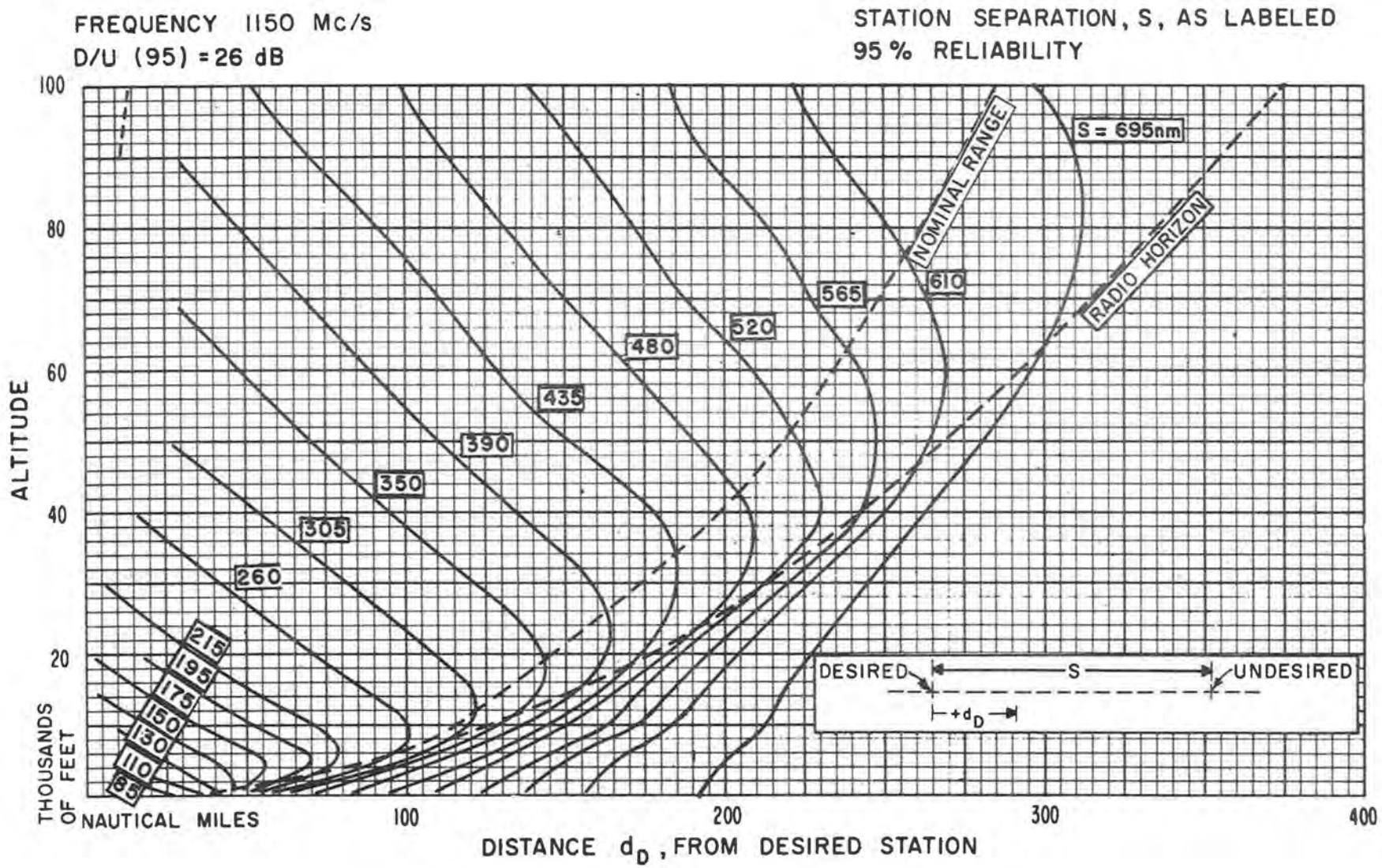

TACAN Service Volumes; D/U(95) = 26 dB

Figure 37

5.5 VOR and TACAN Signal Ratios Near an Interfering Station

Desired-to-undesired signal ratios in the neighborhood of an undesired station are shown in figures 38 through 50 and 51 through 63 for VOR and TACAN, respectively. There is a separate figure for each system-altitude combination with the altitudes ranging from 1,000 to 100,000 feet.

The desired and undesired stations involved in figures 38 through 63 are similar (both either VOR or TACAN). Predictions for the case where the desired station is a VOR and the undesired station is an ILS are not included in this report.

As an example, in figure 38 the intersection of the D/U(95) = -20 dB line at a distance of 43 nautical miles with the curve for S = 70, means that at 1,000 feet the undesired signal exceeds the desired signal by 20 dB for 5% (100-95) of the time at a distance of 27 nautical miles (70-43) from the undesired station. If, in an application to an adjacent channel interference problem, the undesired signal just causes trouble when it is greater than the desired signal by 20 dB, service is available at least 95% of the time where the D/U(95) curve for the station separation and aircraft altitude involved does not become more negative than -20 dB.

The curves on figures 38 through 63 do not show the effect of interference <u>beyond</u> the undesired station or at locations off the great circle path connecting the stations; i.e., the distance d_D shown on the abscissa scales locates the aircraft on the great circle path between the desired and the

undesired station. However, a method of approximating the locus of a constant interference ratio, D/U(95), as a circle enclosing the undesired station has been developed. For a given aircraft altitude, this circle is centered on extension of the line connecting the ground stations concerned, but on the "far" side of the undesired station. The pertinent geometry is shown by a top and a side view in figure 64. Generally, service may be regarded as being unsatisfactory within this circle, even though some locations having satisfactory service may exist above the undesired station because of the vertical pattern of its antenna.

Two basic assumptions must be made as follows:

(a) The geometry represented by figure 64 is treated as plane geometry; i.e., the earth is assumed to be flat and slant range projections, d_U and d_D, onto the horizontal plane are approximately equal to the actual ranges, r_U and r_D.

(b) The interference ratio, D/U(95), is assumed to be proportional to the logarithm of the ratio of the ranges, r_D/r_U ; i.e.,

$$D/U(p) = M \log (r_D / r_U) \tag{4}$$

where M is a constant.

Assumption (a) is reasonable if $d_D > d_U \geq$ (aircraft altitude/1600), where the distances, d_D and d_U, are in nautical miles and the aircraft altitude is in feet. Hence, the problem of finding the locus of r_D/r_U = constant may be solved using plane geometry. This locus is found to be a circle, described by the parameters C and R defined in figure 64 (page 94) and given by the following equations which contain an additional auxiliary parameter, B:

$$B = d_D/d_U = (S - d_U) / d_U \cong r_D/r_U , \tag{5}$$

$$C = \frac{S(B^2 + 1)}{2(B^2 - 1)} , \tag{6}$$

$$R = \frac{SB}{B^2 - 1} \tag{7}$$

As an example, consider the S = 150 nautical miles curve of figure 41, (VOR; 15,000 feet). For a desired-to-undesired signal ratio D/U(95) = - 40 dB which may very well constitute the adjacent-channel interference threshold in a practical case, the distance, d_D = 130 nautical miles, from the desired station (d_U = 20 nautical miles) is read from figure 41. Then B, C, and R are calculated:

$$B = \frac{130}{20} = 6.5 ,$$

$$C = 75(43/41) = 79 \text{ nautical miles,}$$

$$R = 975/41 = 24 \text{ nautical miles.}$$

Thus, inside a circle of radius 24 nautical miles, centered at a point 4 nautical miles beyond the undesired station, VOR service at 15,000 feet aircraft altitude would be expected to be sub-standard.

It should not be overlooked that this method is only approximate. The second assumption, (b) is violated by lobing in the transmission loss versus distance curve, which may occur at any constant altitude due to ground reflections or the ground antenna pattern. The assumption (b) is also violated by a change in the slope of the transmission loss versus distance curve which, as an example, occurs in the vicinity of the radio horizon. However, the use of the smallest d_D corresponding to a particular station spacing and a particular signal ratio from figures 38 through 63 avoids the ambiguity due to lobing. Furthermore, in most applications service is limited by noise rather than by interference if ranges beyond the radio horizon of the desired station are encountered.

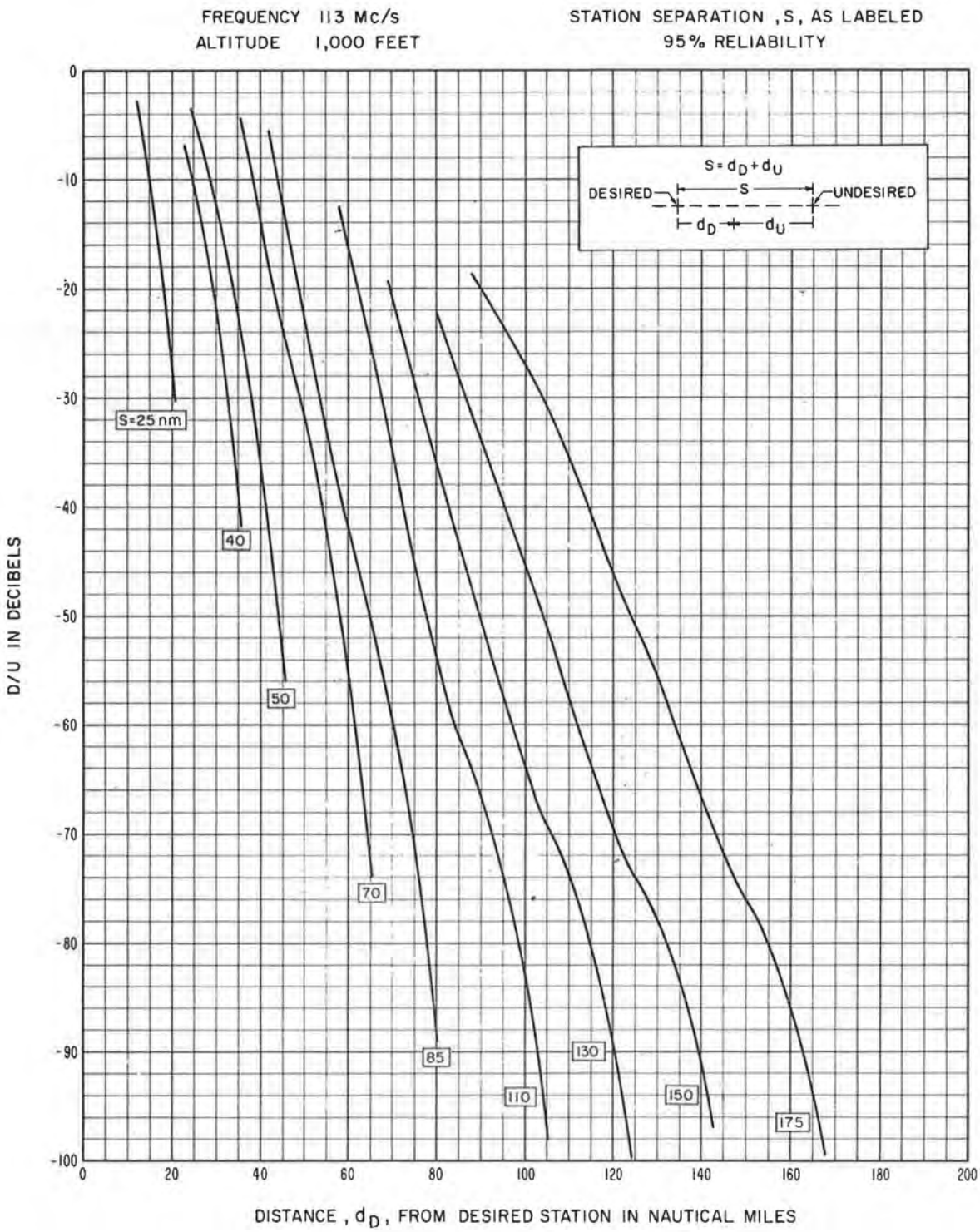

VOR Signal Ratios; Altitude = 1,000 feet
Figure 38

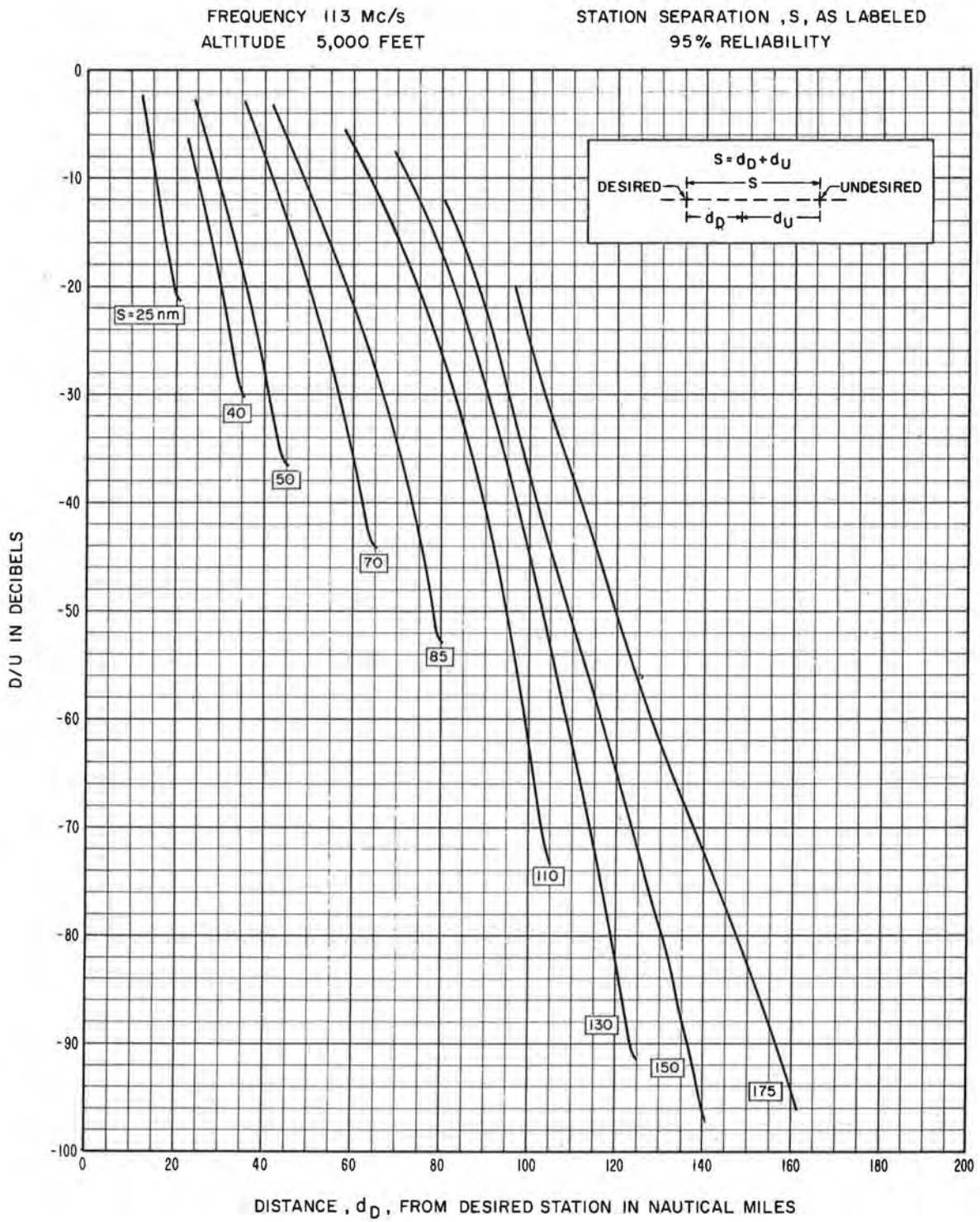

VOR Signal Ratios; Altitude = 5,000 feet
Figure 39

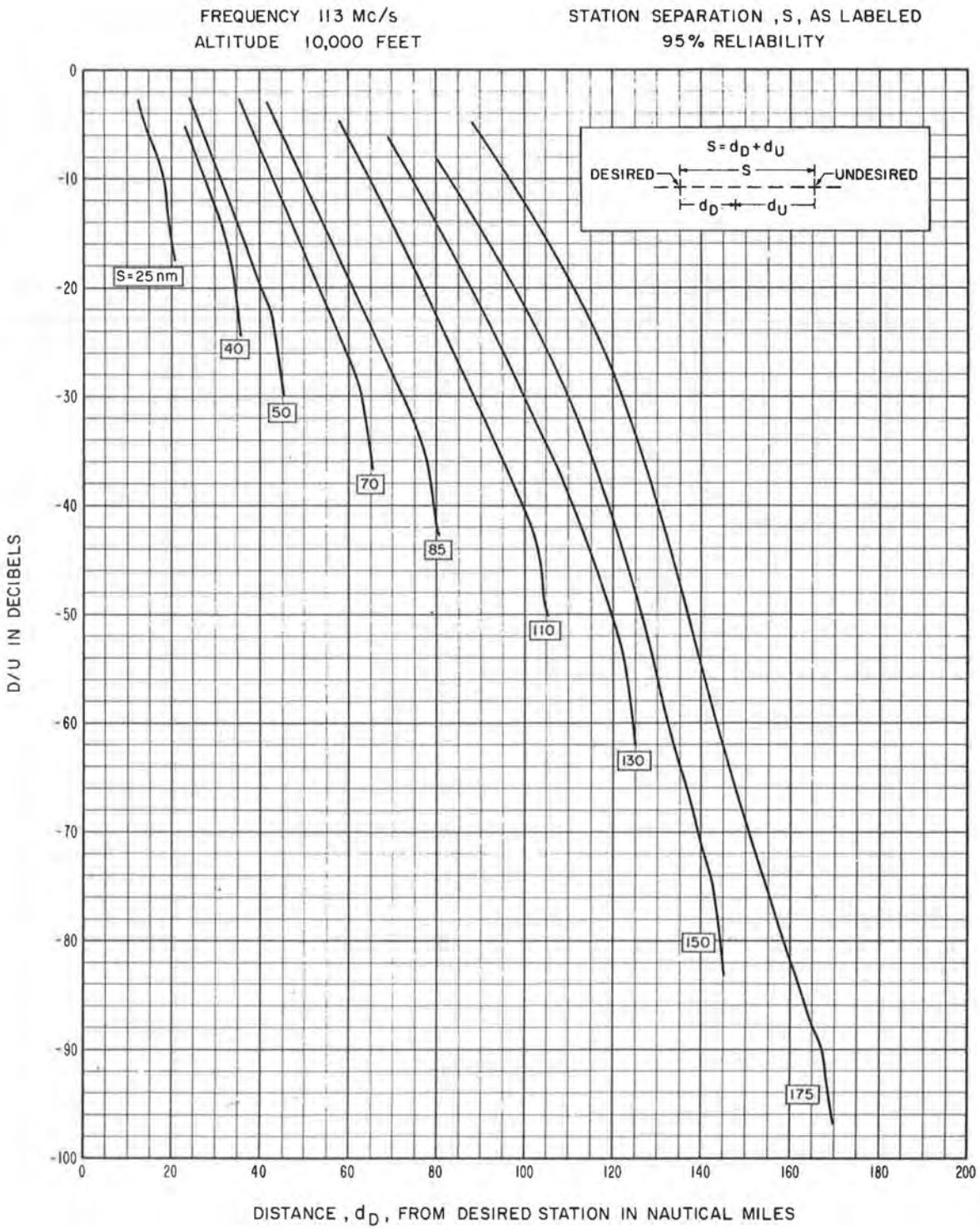

VOR Signal Ratios; Altitude = 10,000 feet

Figure 40

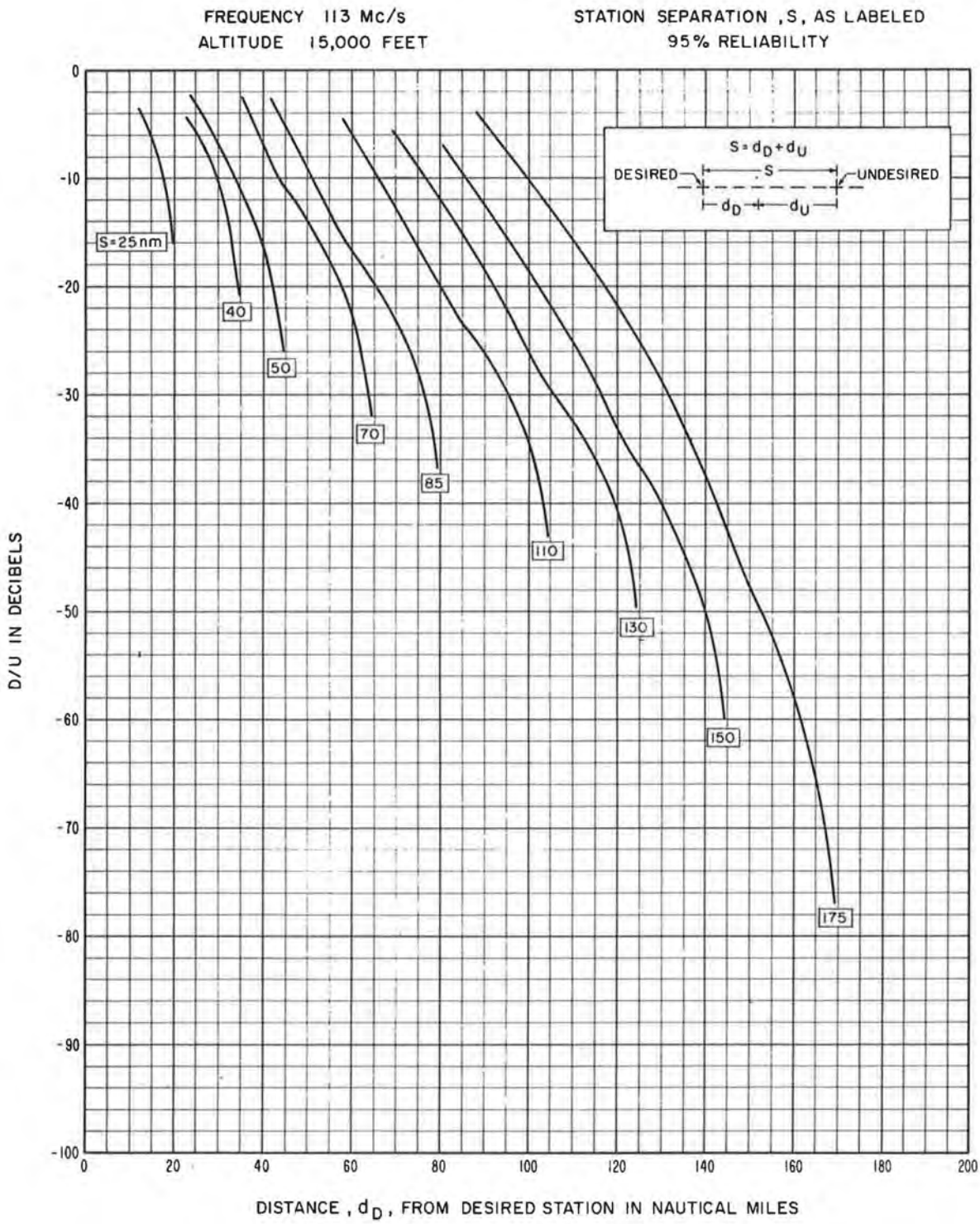

VOR Signal Ratios; Altitude = 15,000 feet

Figure 41

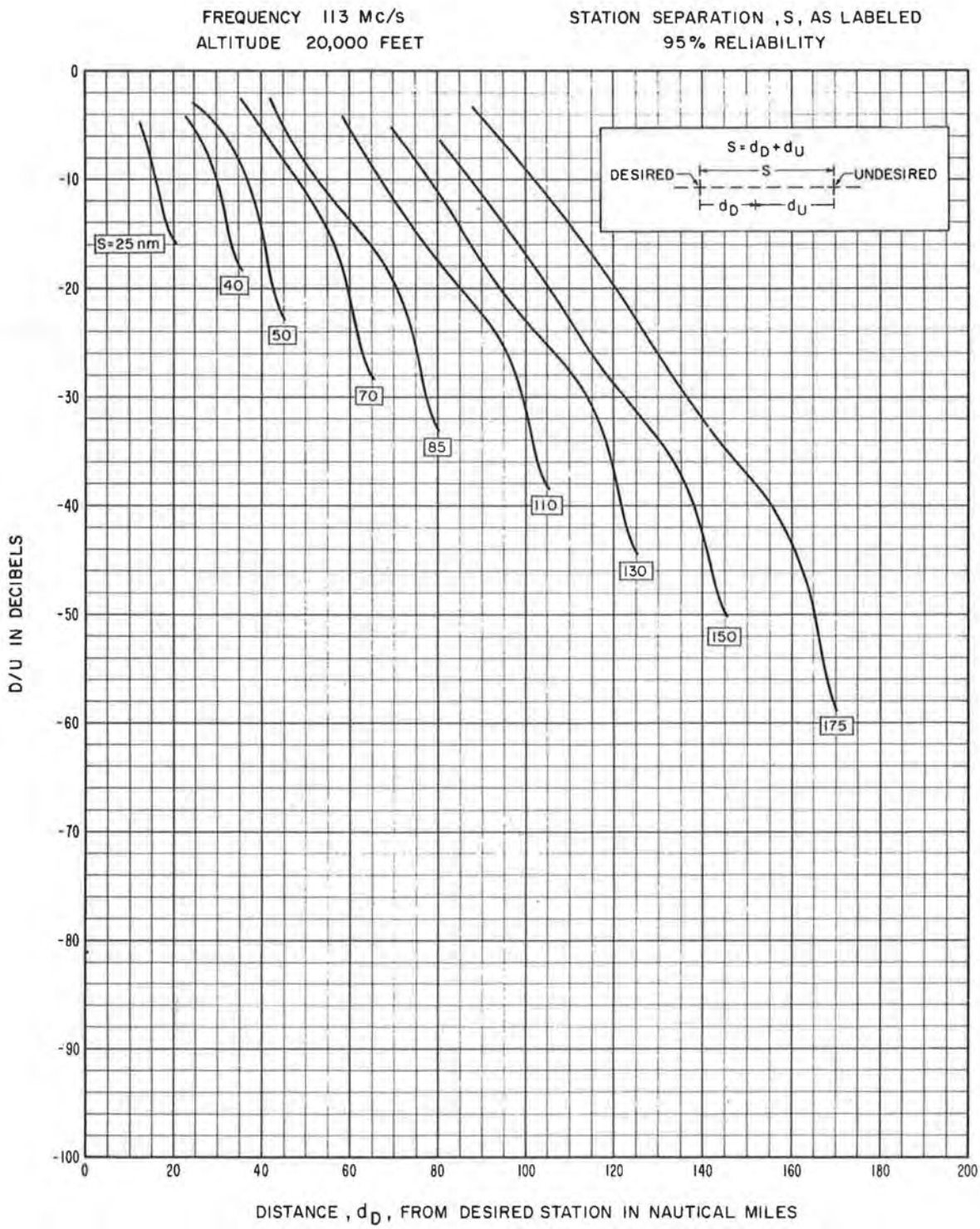

VOR Signal Ratios; Altitude = 20,000 feet

Figure 42

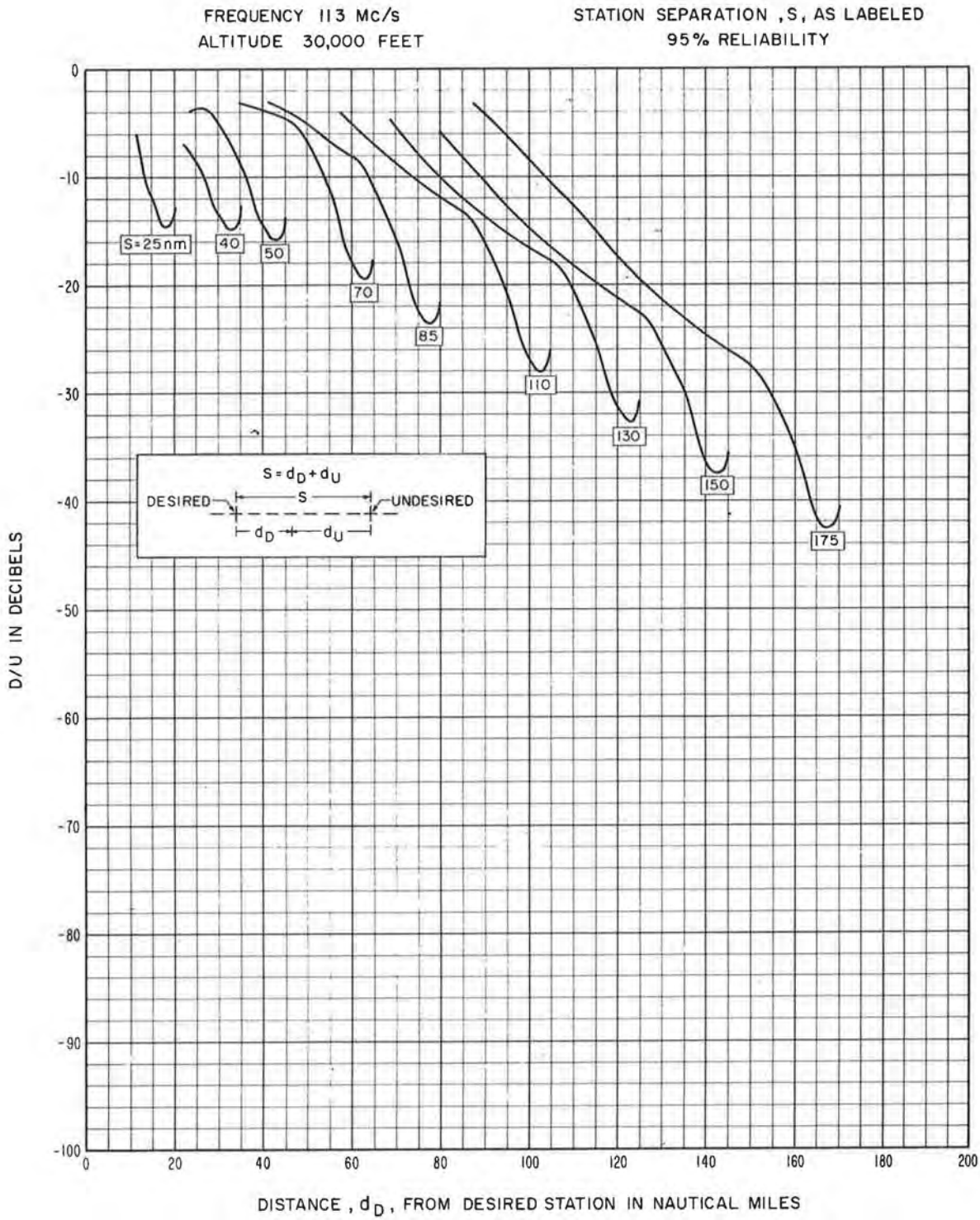

VOR Signal Ratios; Altitude = 30,000 feet

Figure 43

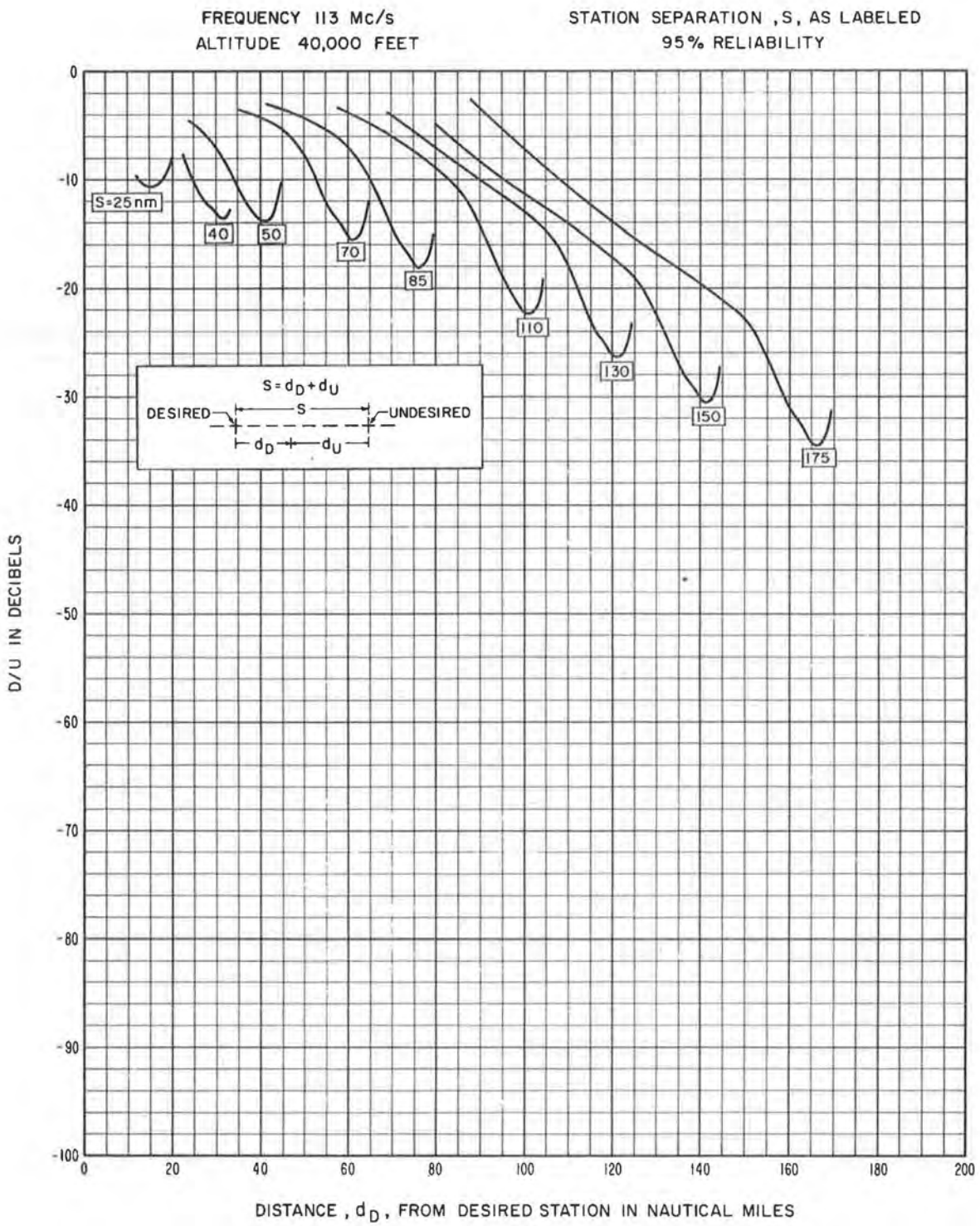

VOR Signal Ratios; Altitude = 40,000 feet

Figure 44

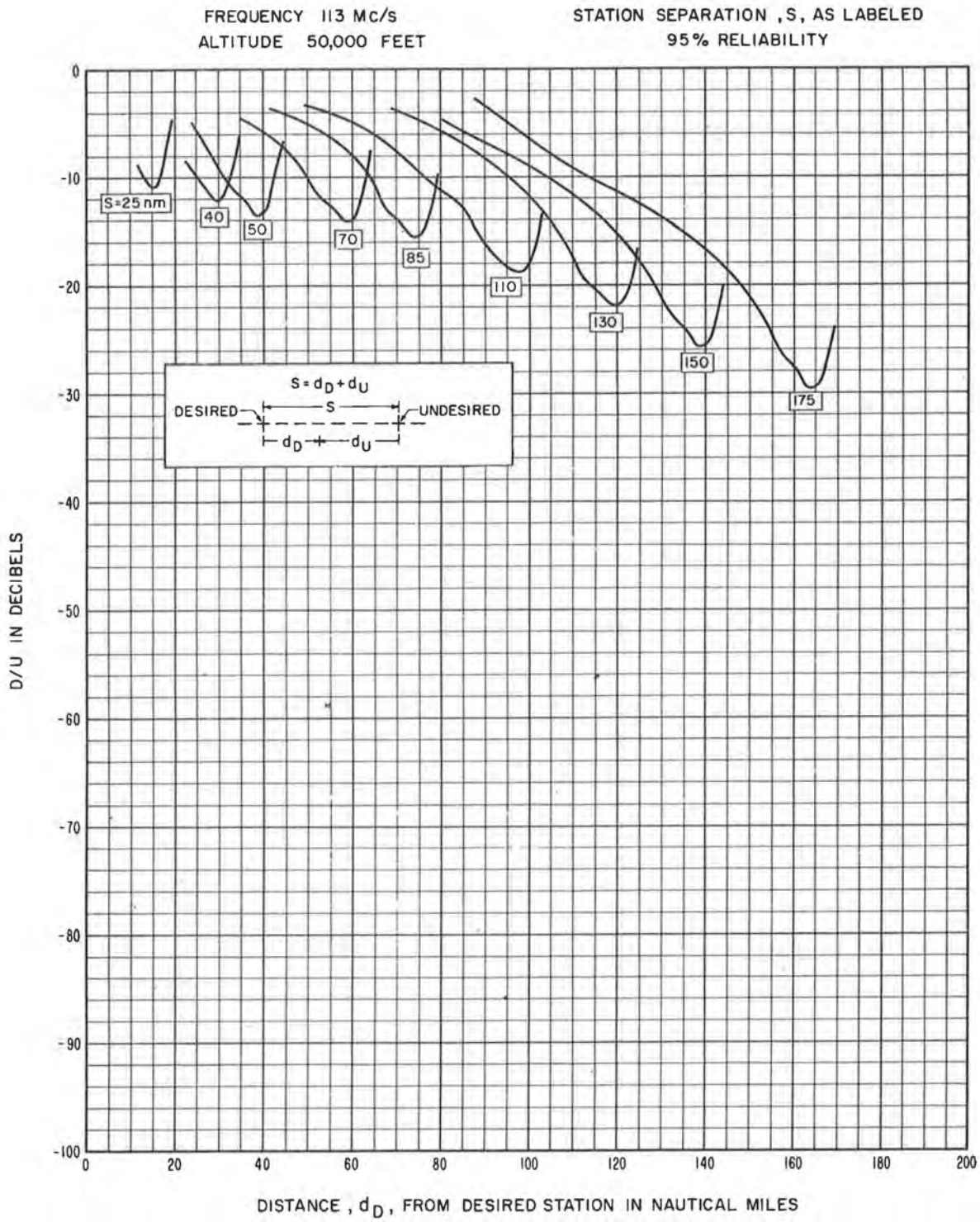

VOR Signal Ratios; Altitude = 50,000 feet

Figure 45

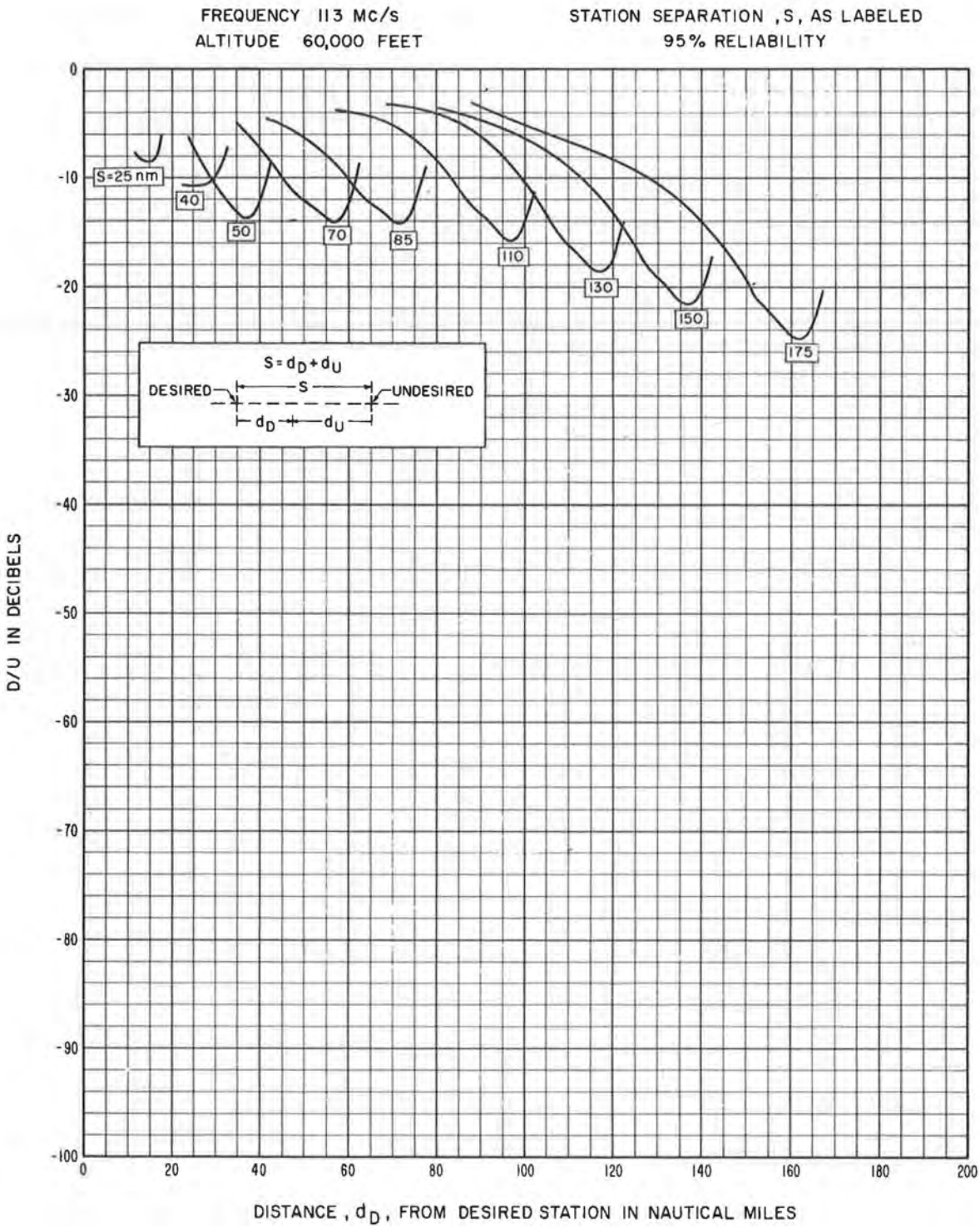

VOR Signal Ratios; Altitude = 60,000 feet

Figure 46

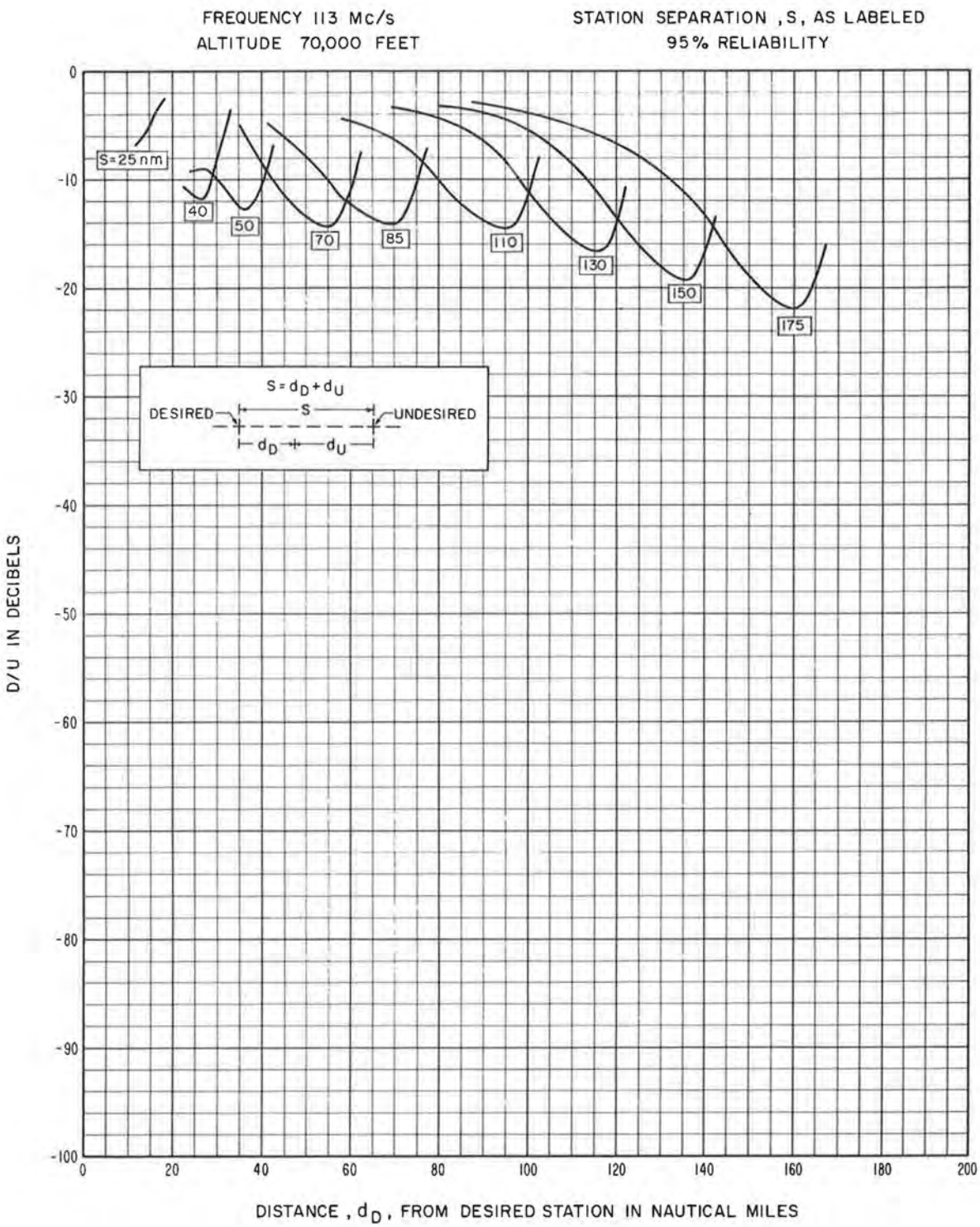

VOR Signal Ratios; Altitude = 70,000 feet

Figure 47

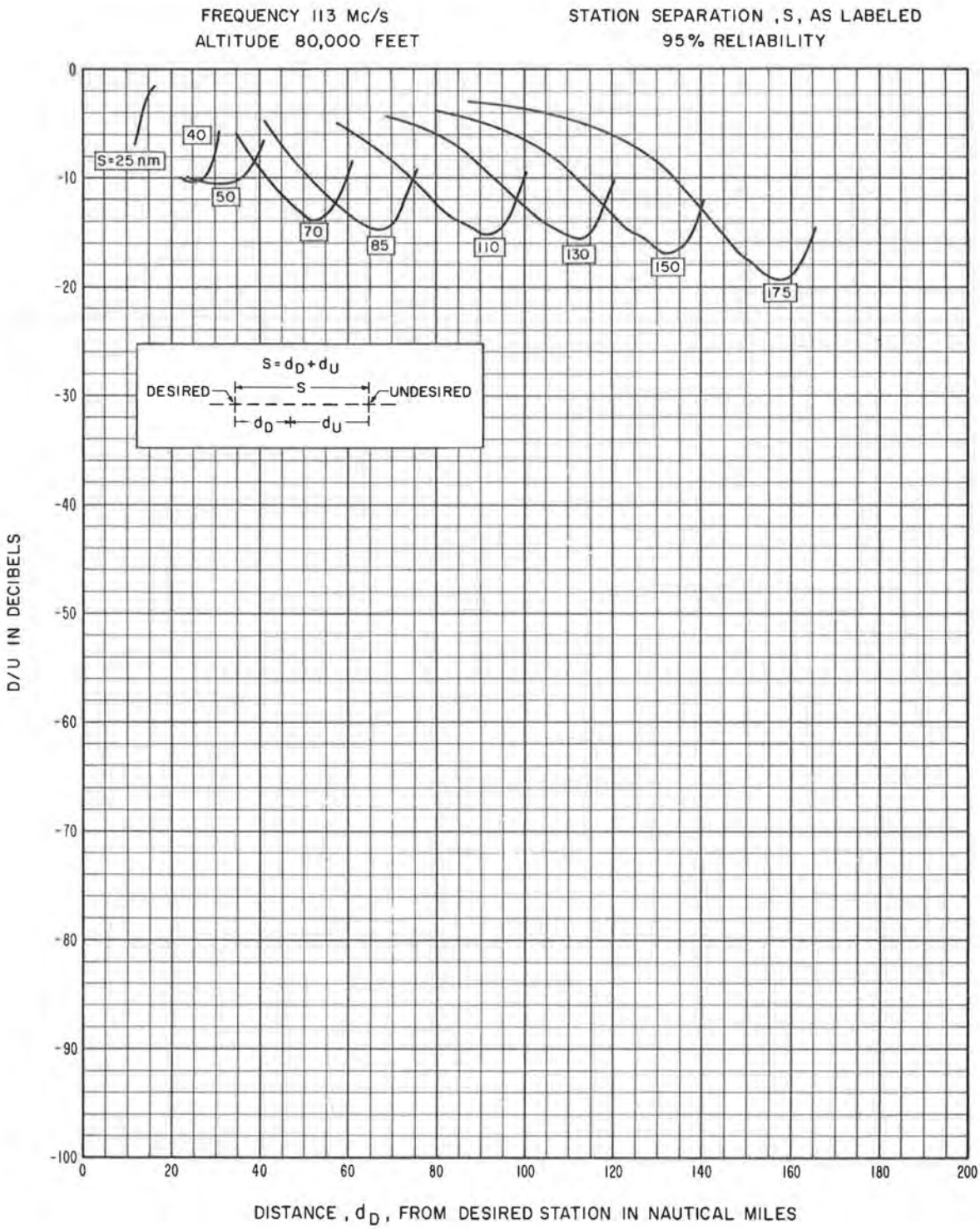

VOR Signal Ratios; Altitude = 80,000 feet

Figure 48

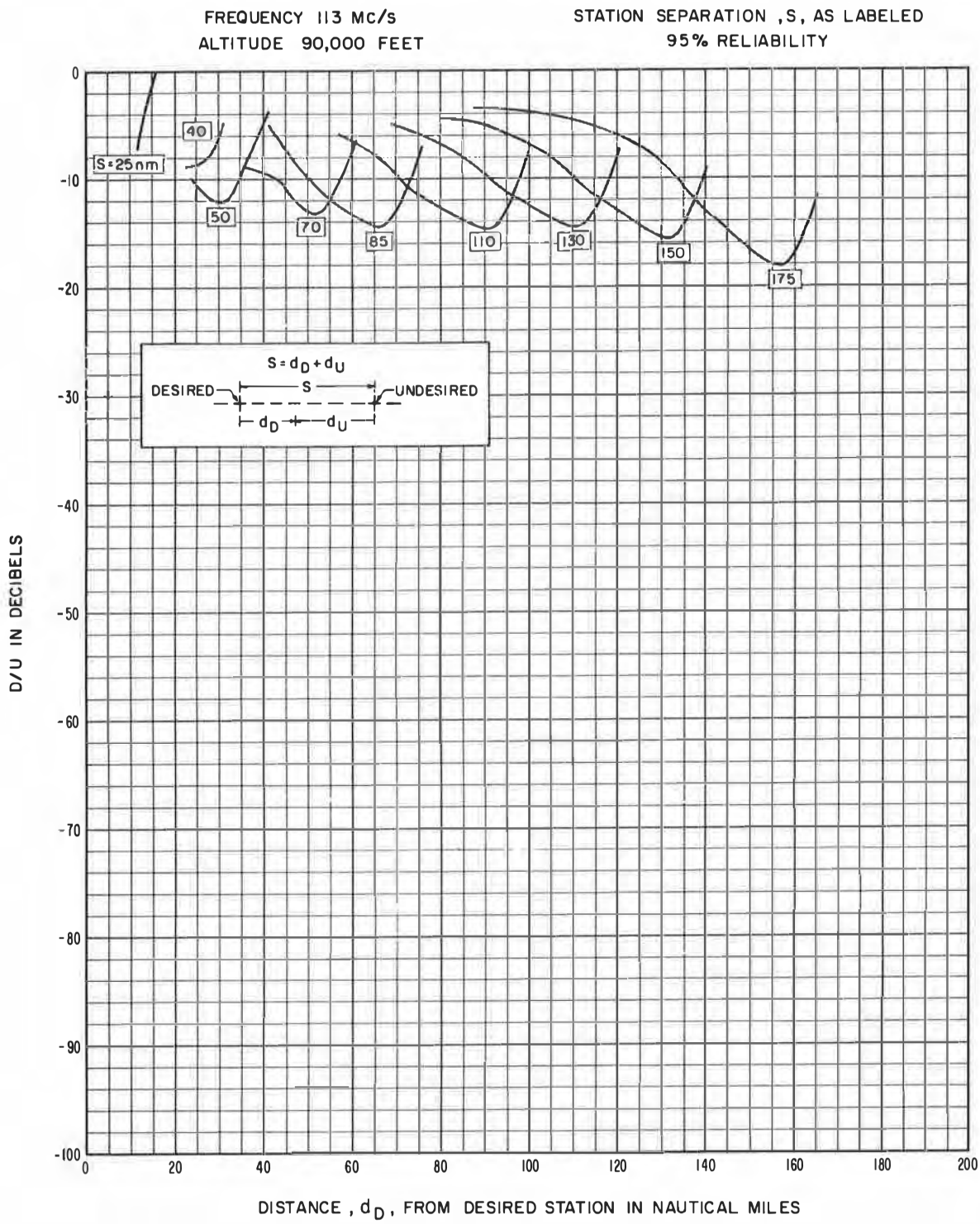

VOR Signal Ratios; Altitude = 90,000 feet

Figure 49

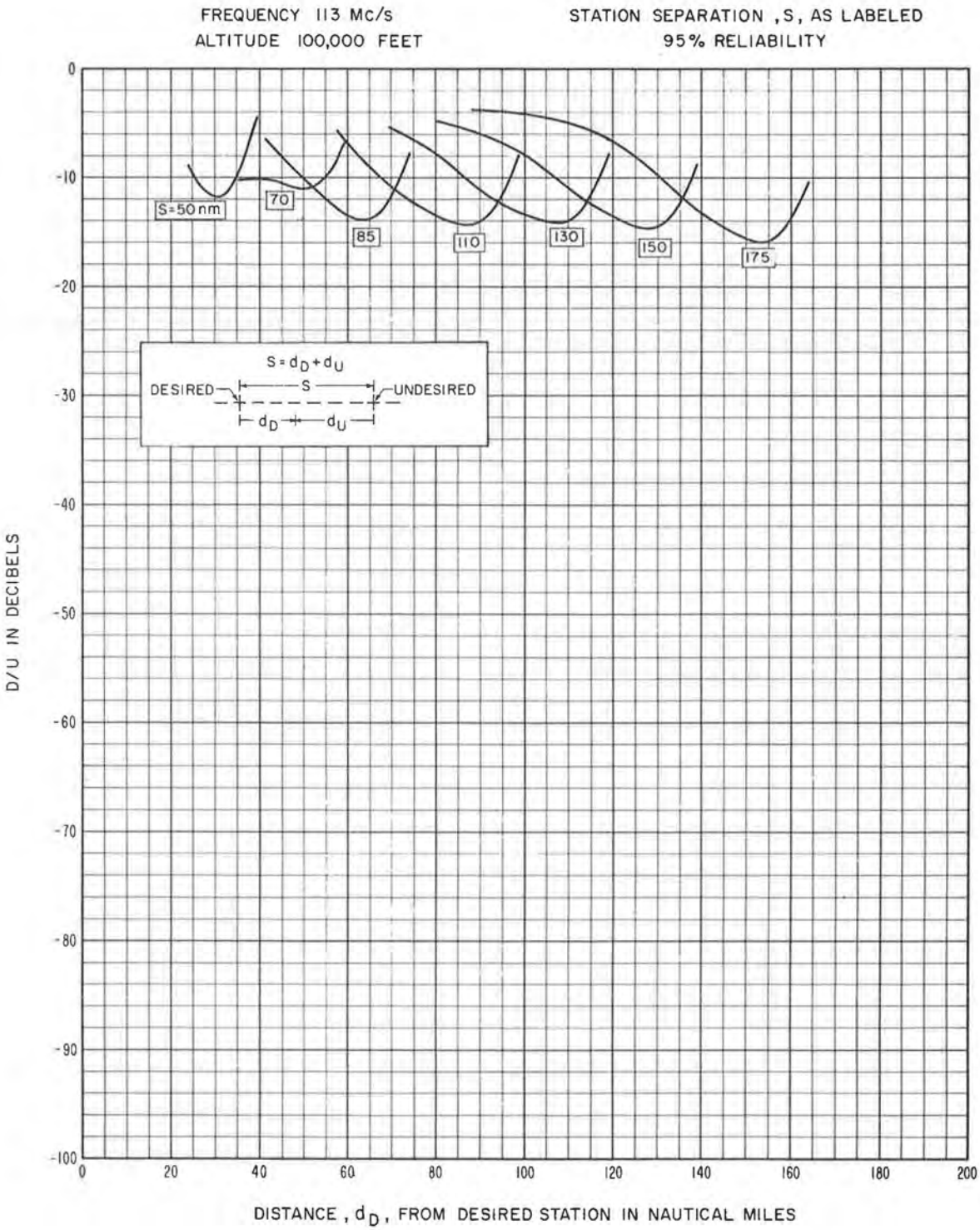

VOR Signal Ratios; Altitude = 100,000 feet

Figure 50

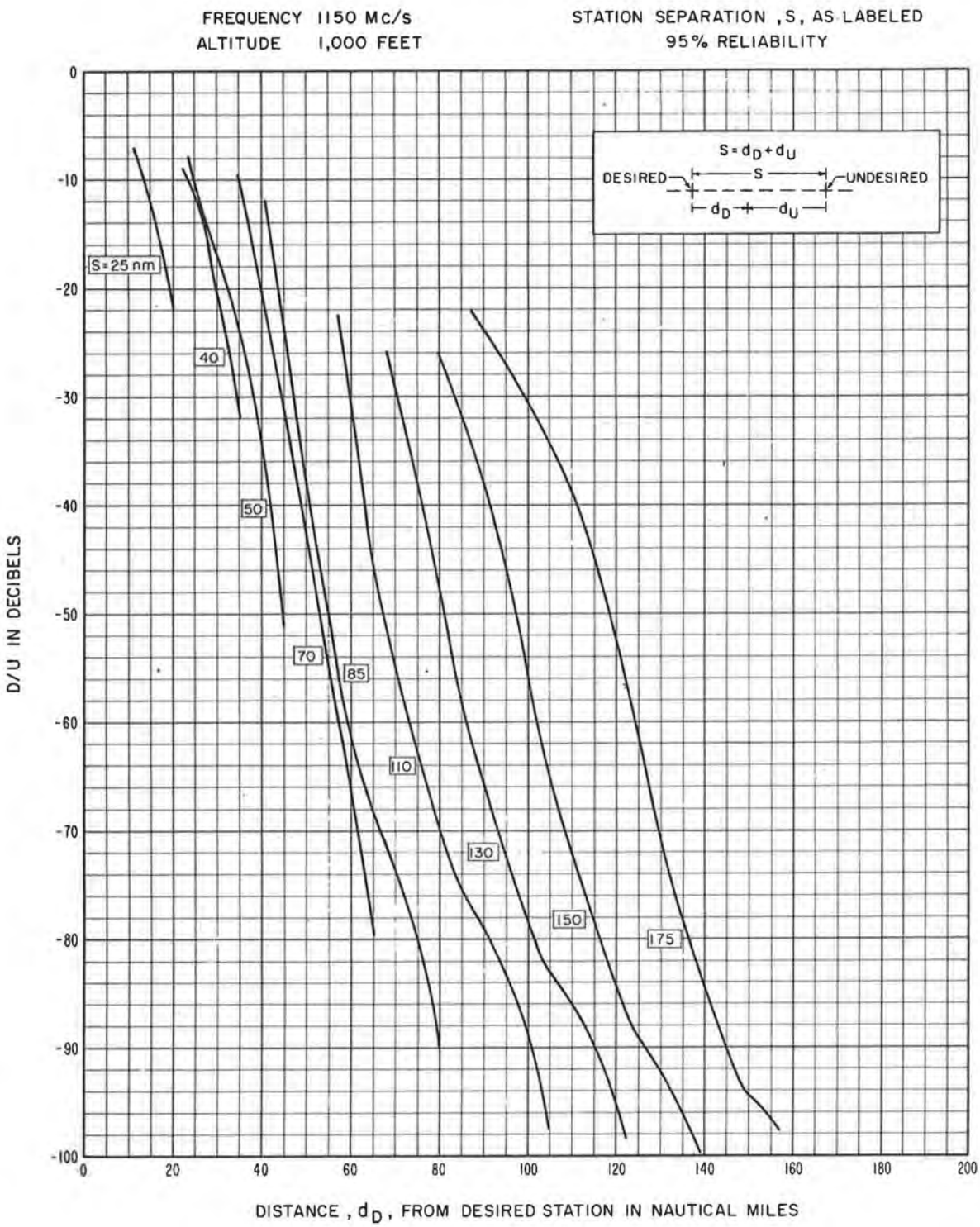

TACAN Signal Ratios; Altitude = 1,000 feet

Figure 51

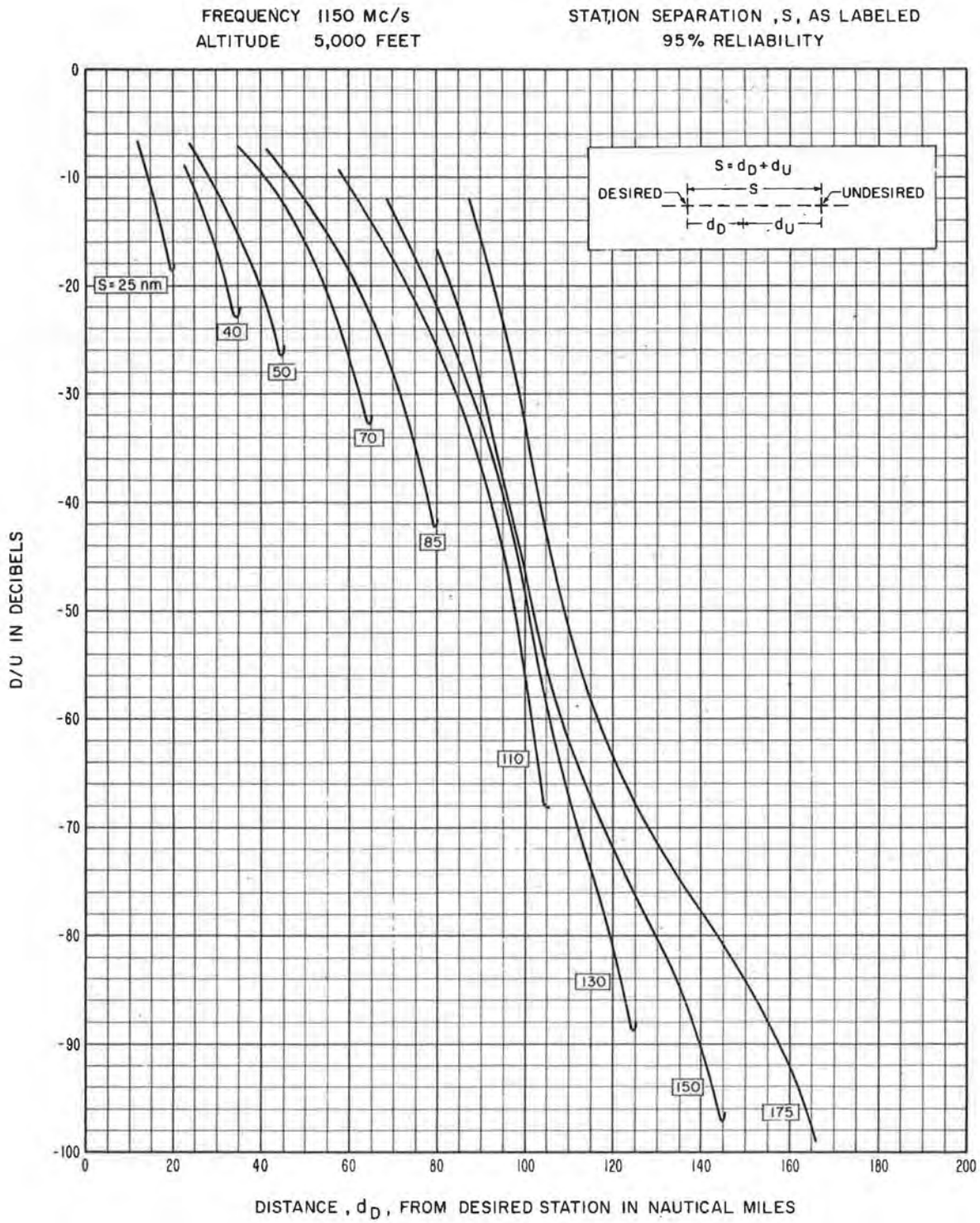

TACAN Signal Ratios; Altitude = 5,000 feet

Figure 52

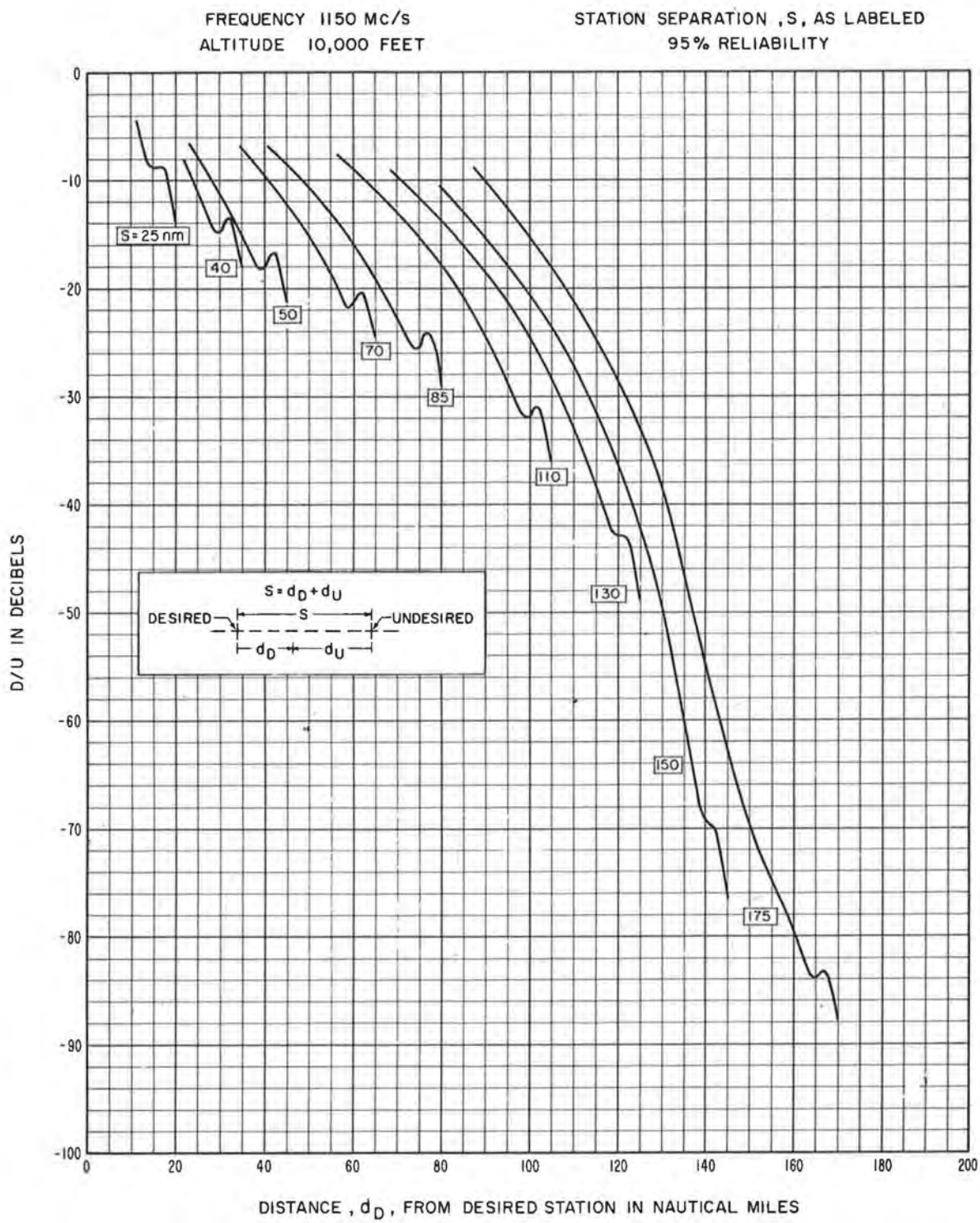

TACAN Signal Ratios; Altitude = 10,000 feet

Figure 53

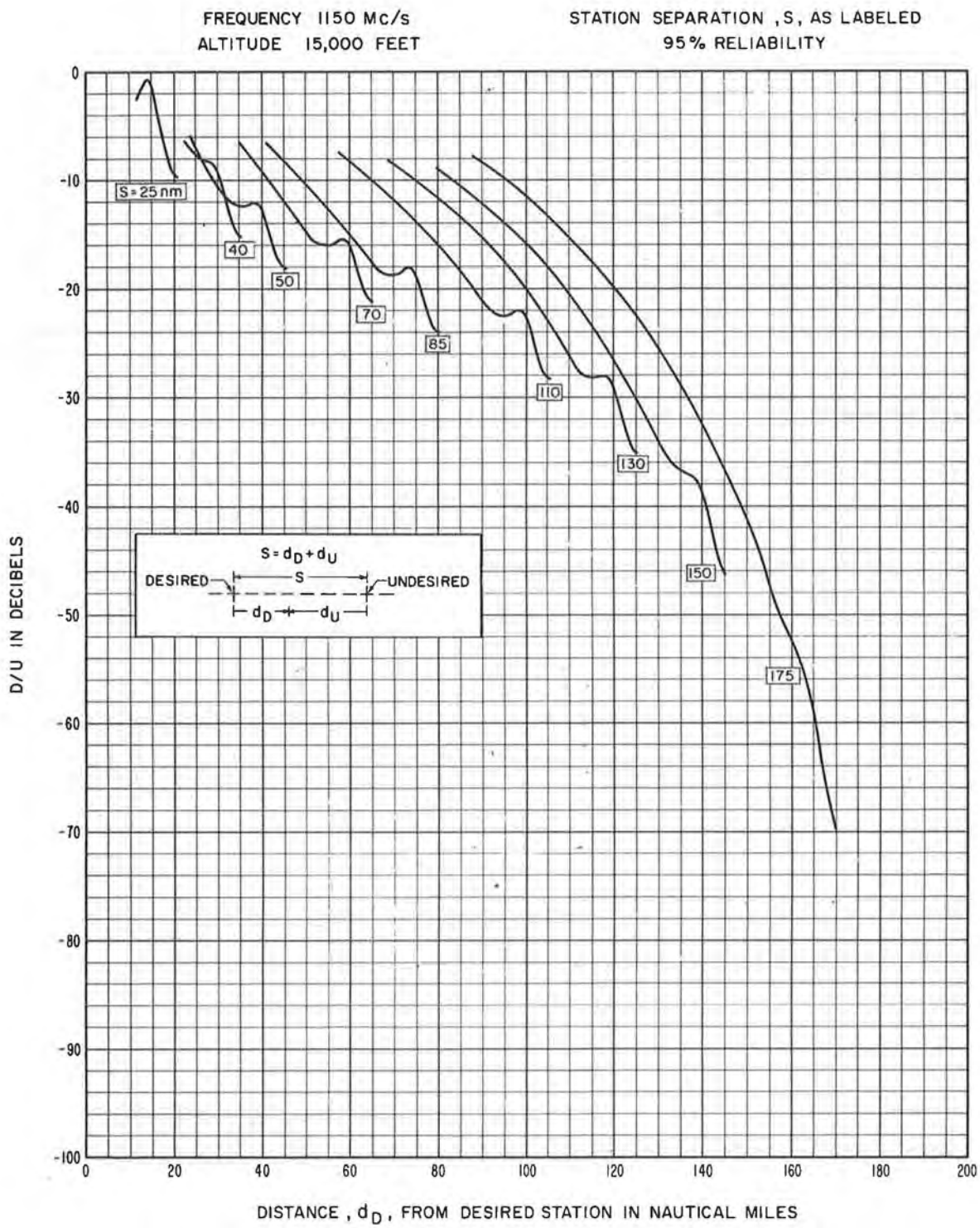

TACAN Signal Ratios; Altitude = 15,000 feet

Figure 54

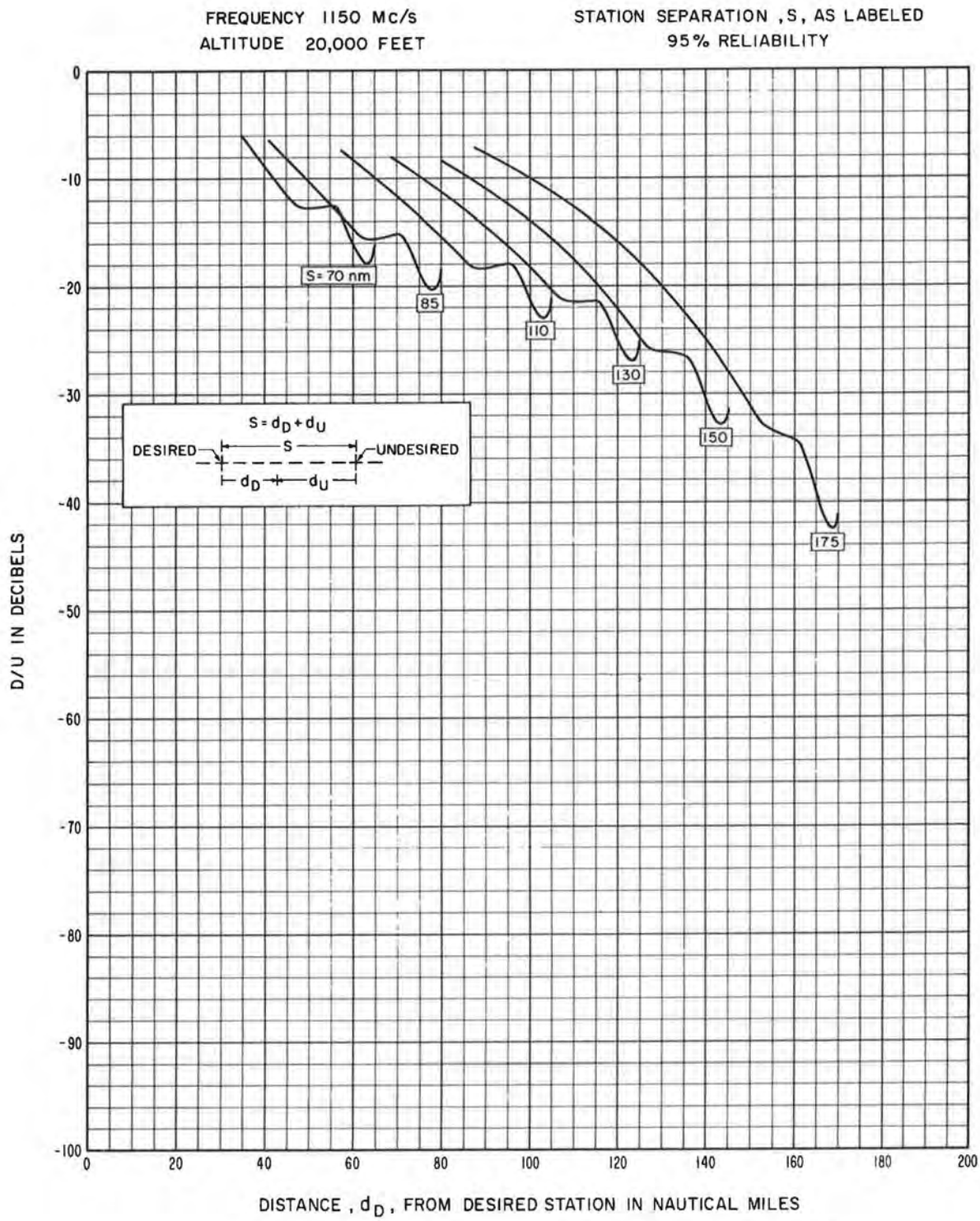

TACAN Signal Ratios; Altitude = 20,000 feet

Figure 55

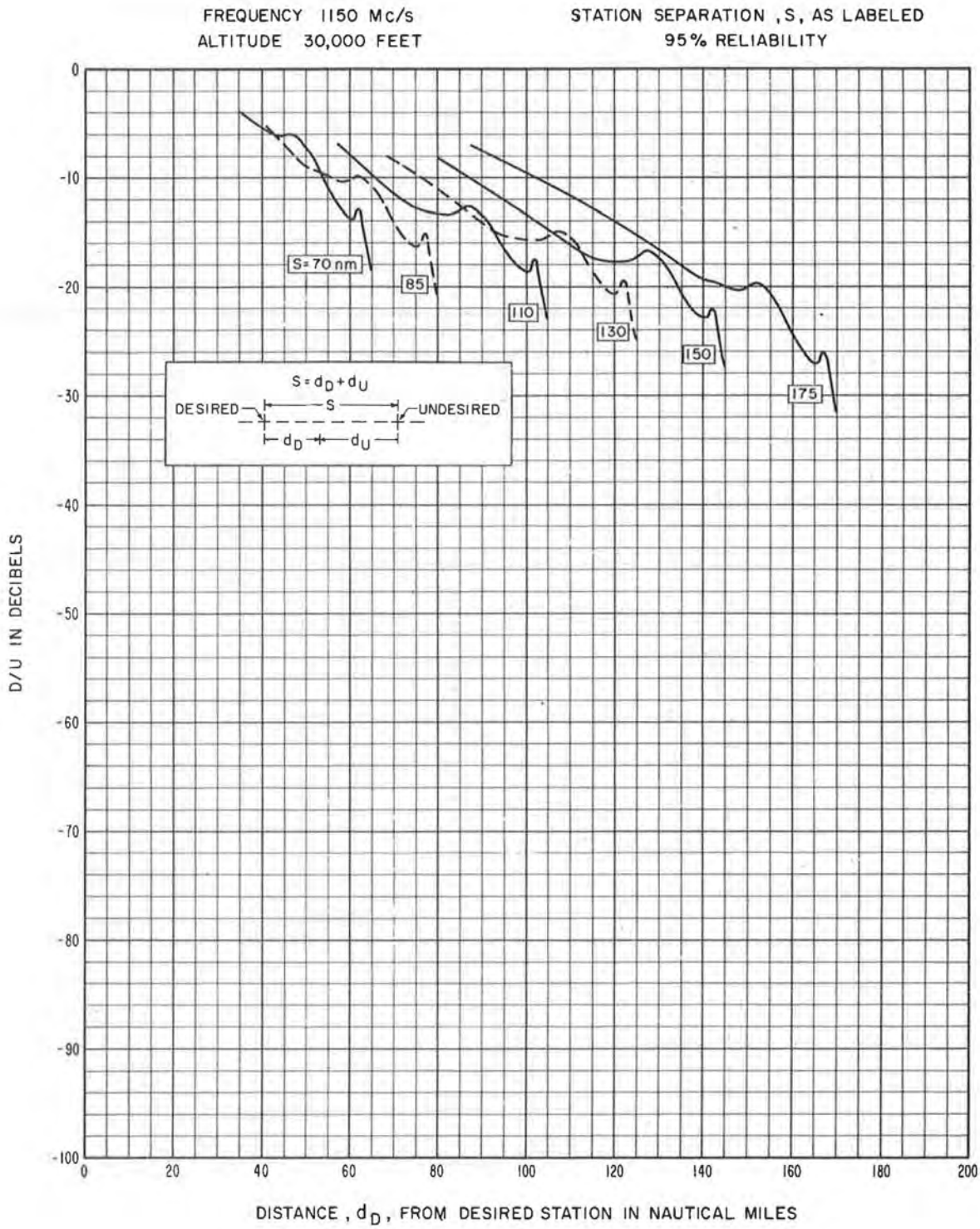

TACAN Signal Ratios; Altitude = 30,000 feet

Figure 56

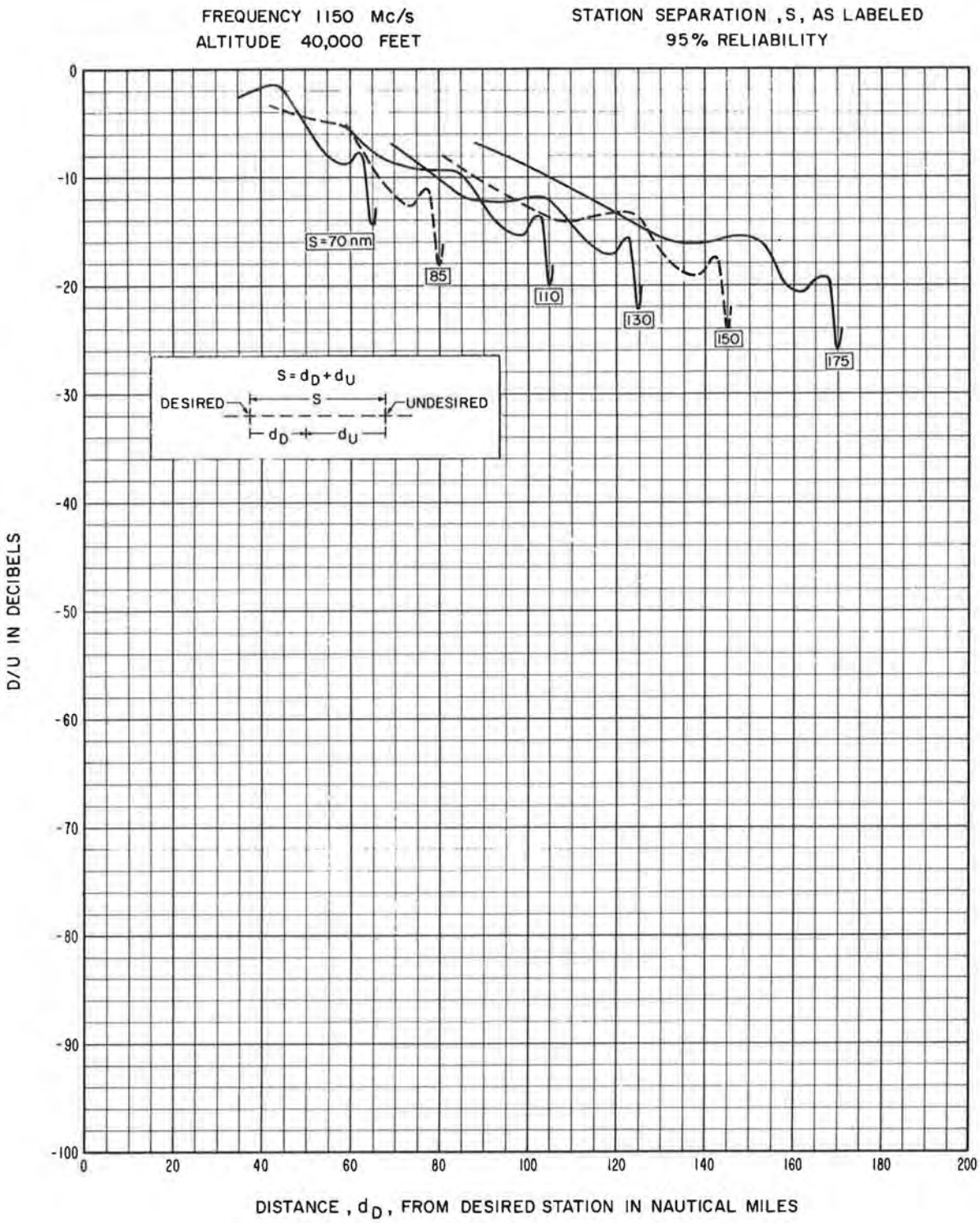

TACAN Signal Ratios; Altitude = 40,000 feet

Figure 57

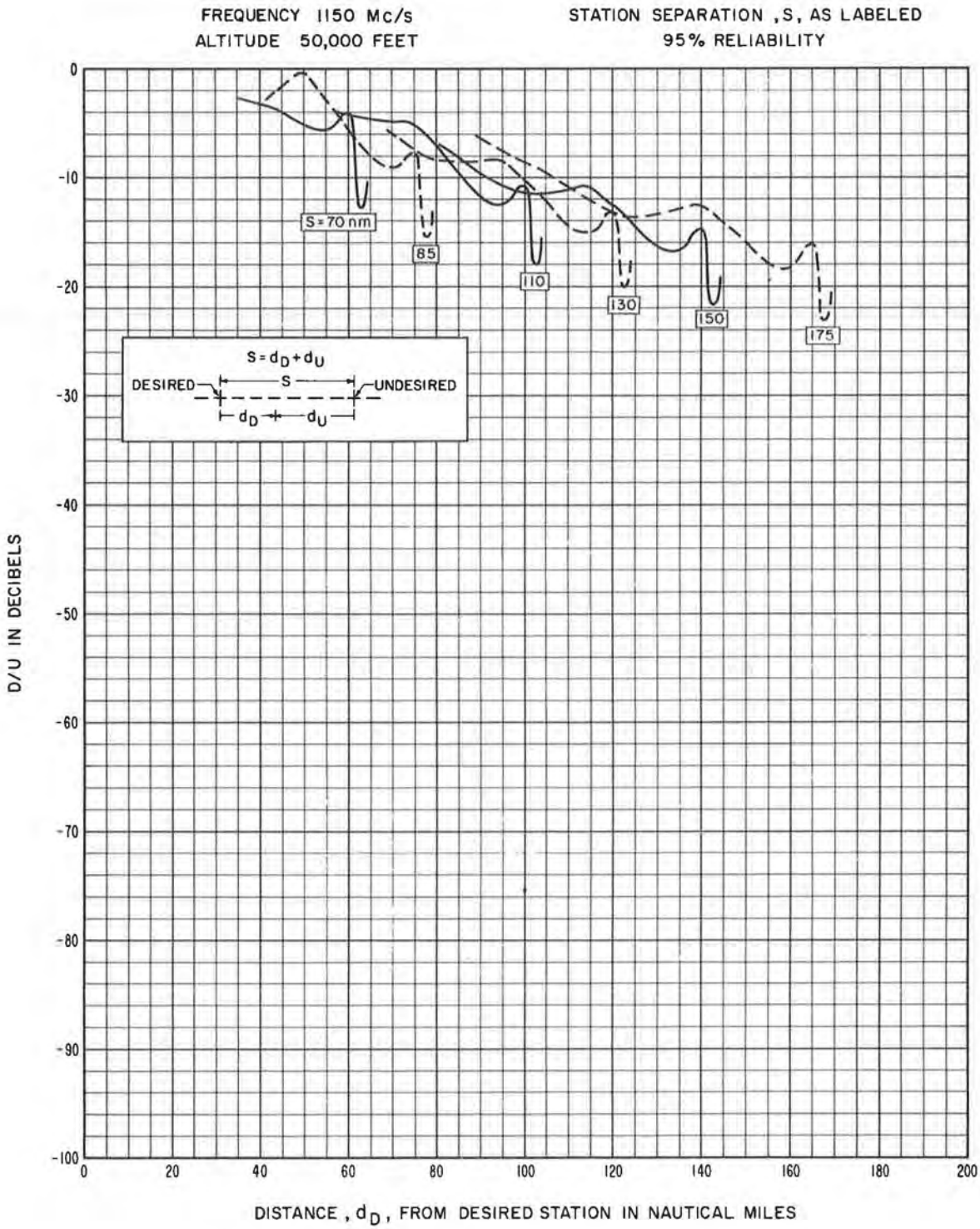

TACAN Signal Ratios; Altitude = 50,000 feet

Figure 58

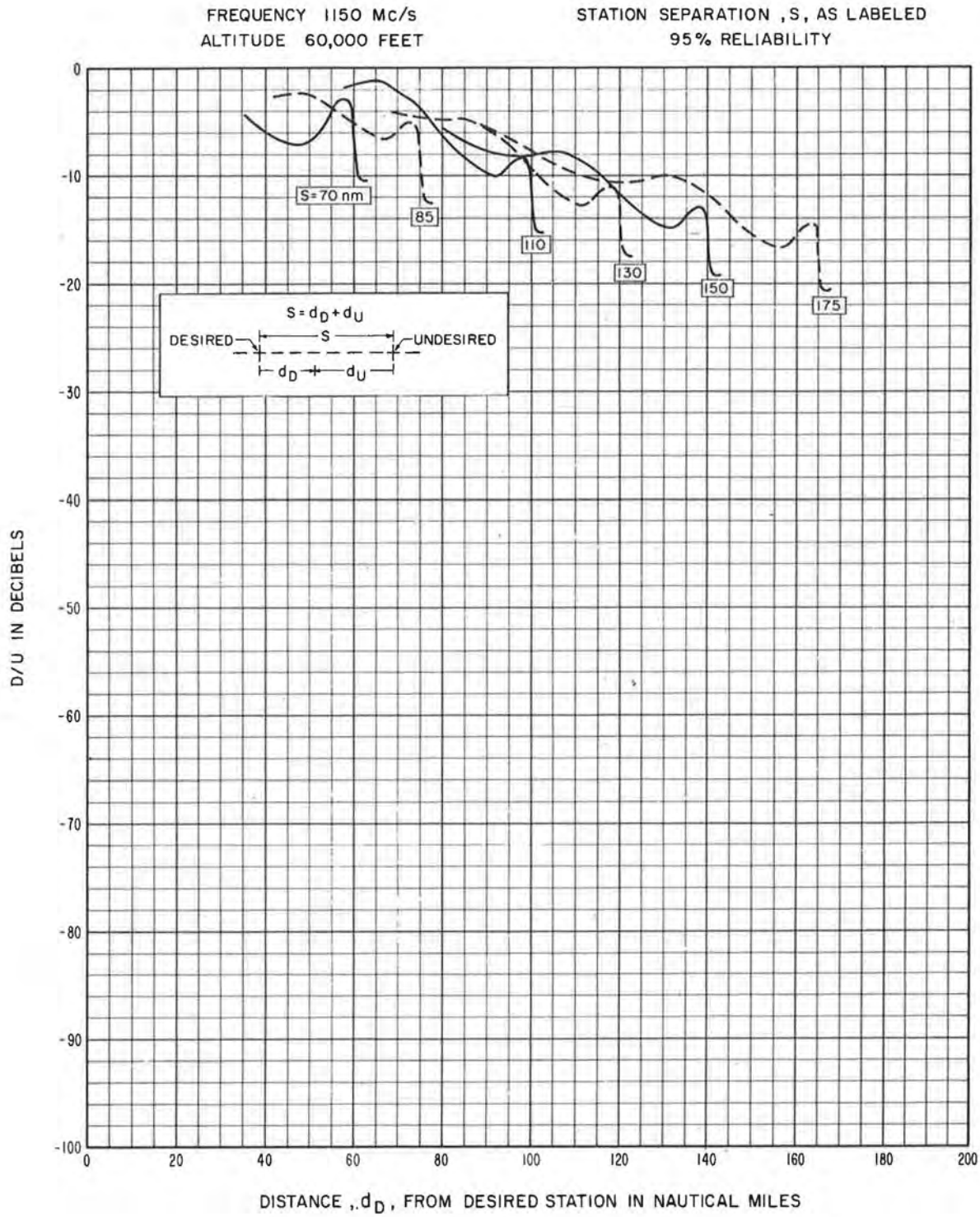

TACAN Signal Ratios; Altitude = 60,000 feet

Figure 59

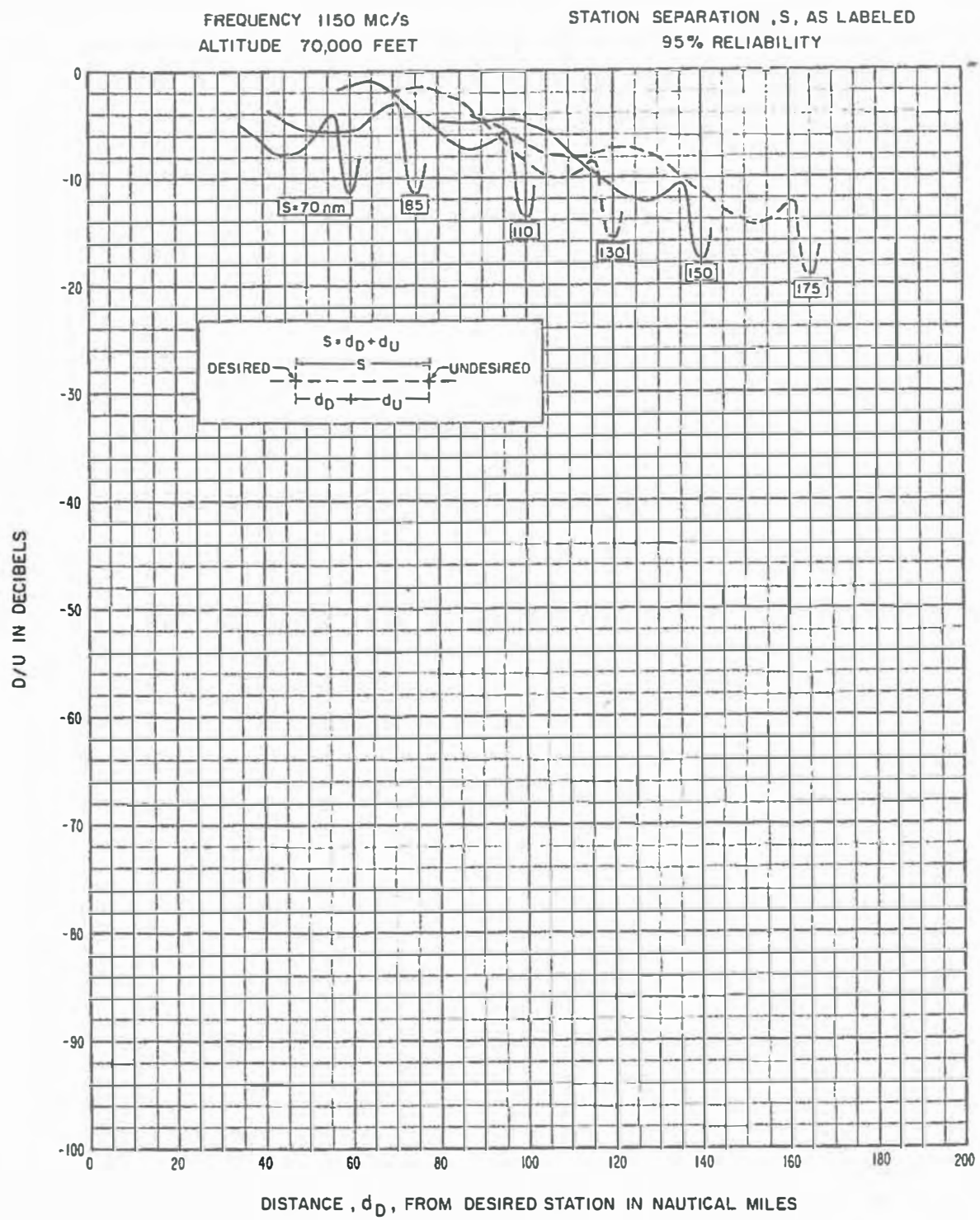

TACAN Signal Ratios; Altitude = 70,000 feet
Figure 60

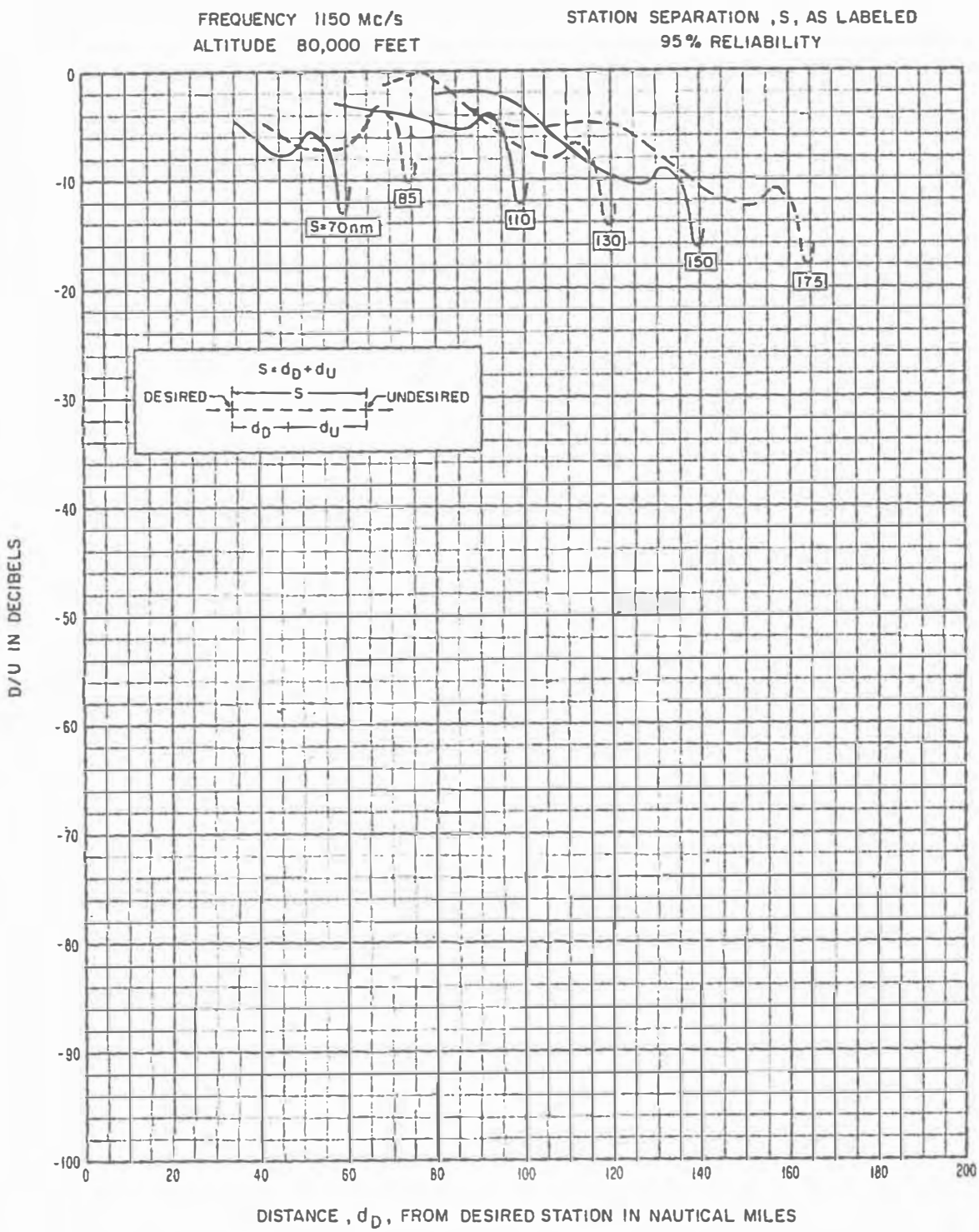

TACAN Signal Ratios; Altitude = 80, 000 feet

Figure 61

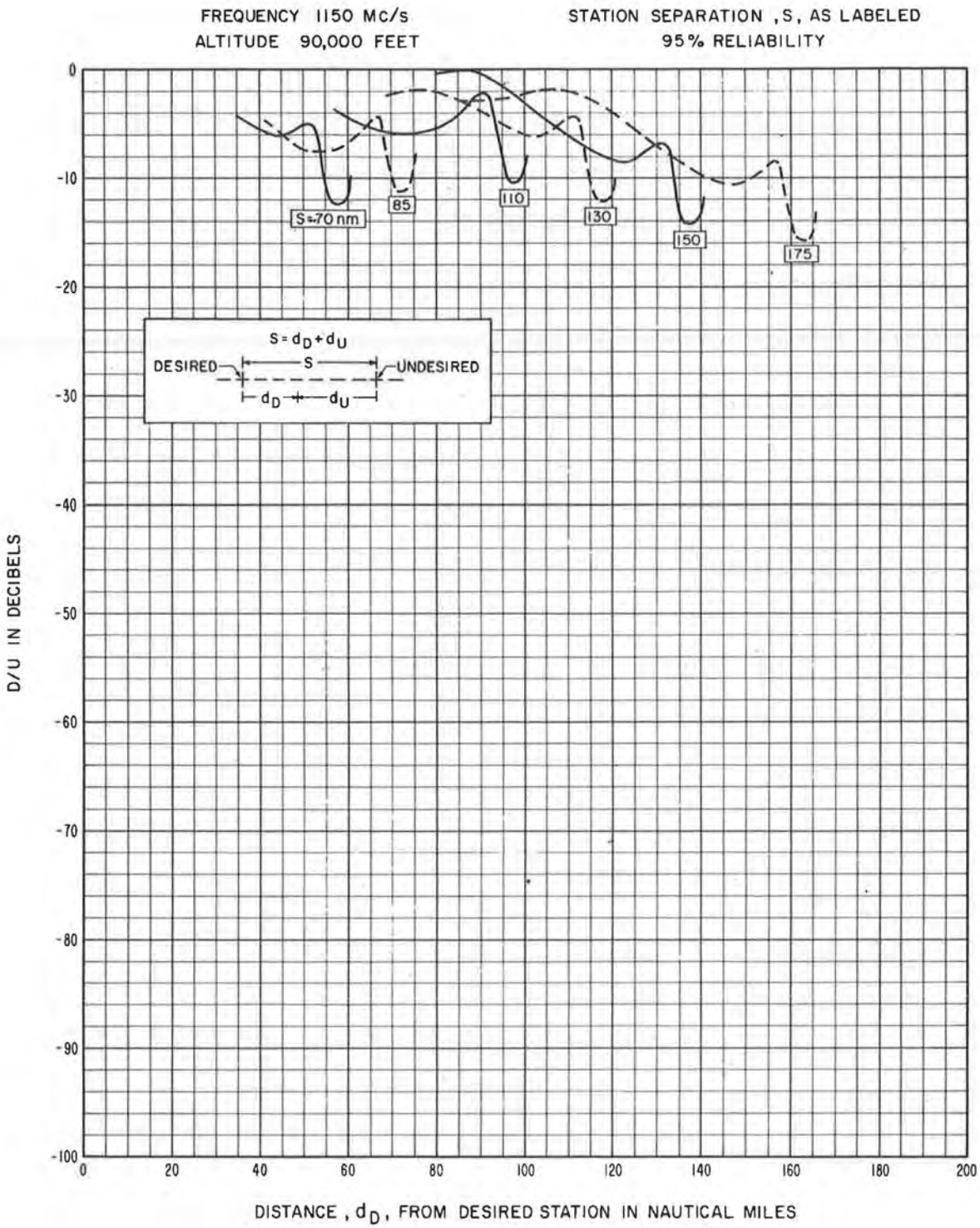

TACAN Signal Ratios; Altitude = 90,000 feet

Figure 62

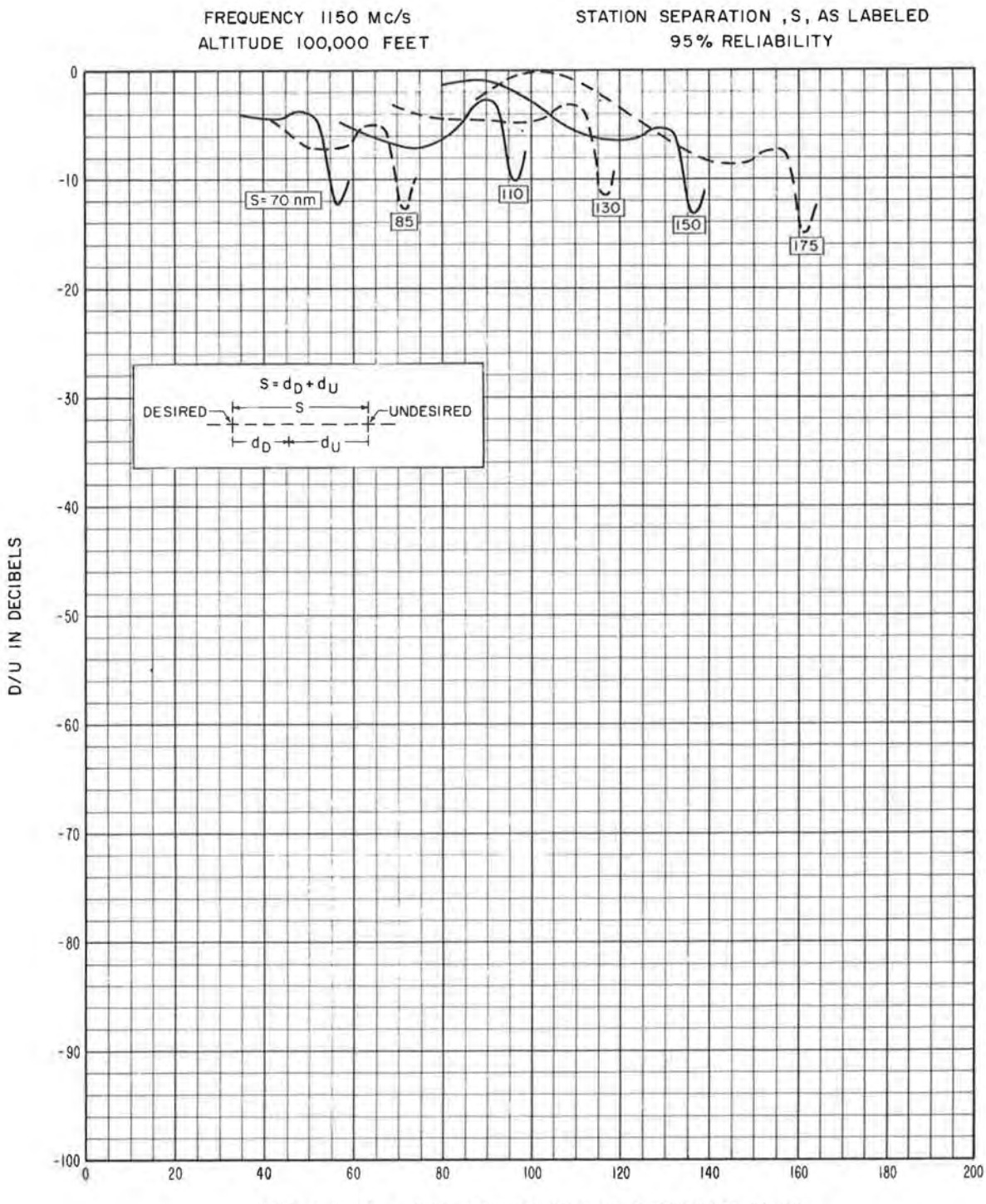

TACAN Signal Ratios; Altitude = 100,000 feet

Figure 63

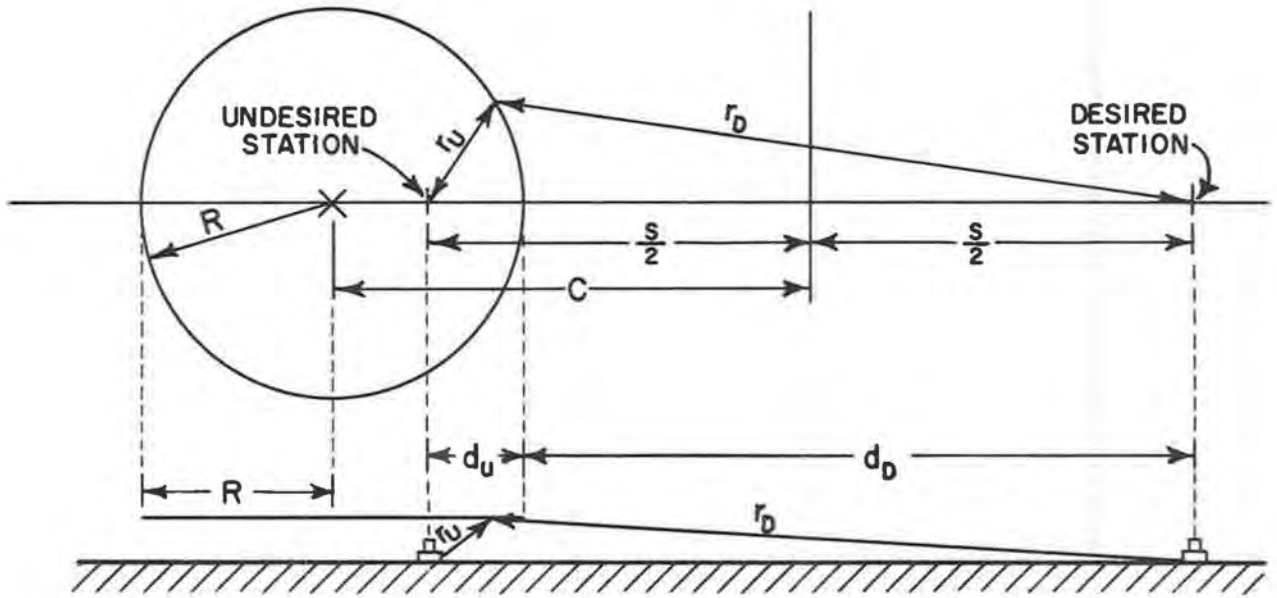

Locus of D/U(95) = Constant

Figure 64

APPENDIX I PROPAGATION MODELS

I.1 Desired Station ILS Localizer Model

A smooth, spherical earth model was used to calculate transmission loss for the desired ILS at 110 Mc/s. A linear-gradient atmosphere was assumed for the initial calculations so that for a first approximation radio rays could be considered to be straight lines above an earth having an effective radius of 4/3 its actual value. Calculation methods are based on material contained in an NBS Technical Note by Rice, et al.[1966].

Only the gain of the transmitting antenna is included in the calculation of a reference transmission loss, with unity gain assumed for the aircraft antenna. In this study, the reference transmission loss, L_m, is defined to include the free-space gain of the ground station antenna as a function of the elevation angle as well as the effect of ground reflections.

Within the radio horizon, values of the reference transmission loss, L_m, were calculated using geometric optics methods, [Kirby, et al., 1952]. These methods take into account the interference between the direct and the ground-reflected ray. Figure 65 shows the geometry for this ray interference problem, and defines many of the symbols used in the analysis. Using this geometry, curves of L_m versus distance were calculated for each assumed aircraft altitude.

The first step was the determination of the grazing angle ψ. For a given value of d the following equations were used:

$$d = d_1 + d_2 \quad , \tag{8}$$

$$h_1' \cong h_1 - d_1^2 / 2a \quad , \tag{9}$$

$$h_2' \cong h_2 - d_2^2 / 2a \quad , \tag{10}$$

$$\tan \psi \cong h_1' / d_1 = h_2' / d_2 \quad . \tag{11}$$

Equations (9), (10), and (11) are approximate relations. To utilize the electronic computer in solving the above expressions for grazing angle, ψ, an iteration method was used, assuming for each d different values of d_1 until the equations were satisfied within the desired limits of accuracy, which was $\pm 10^{-6}$ miles. Final values for ψ for each assumed total distance d were then used in calculating various auxiliary angles and quantities to be used in ray-tracing and in the final calculation of the transmission loss, L_m.

Using the previously calculated value of ψ other geometrical parameters shown in figure 65 were calculated as follows:

$$\sin \phi_1 = (a \cos \psi) / (a + h_1) \quad , \tag{12}$$

$$\sin \phi_2 = (a \cos \psi) / (a + h_2) \quad , \tag{13}$$

$$\theta_1 = \pi/2 - \psi - \phi_1 \quad , \tag{14}$$

$$\theta_2 = \pi/2 - \psi - \phi_2 \,, \tag{15}$$

$$r_1 = (a \sin \theta_1) / (\sin \phi_1) \,, \tag{16}$$

$$r_2 = (a \sin \theta_2) / (\sin \phi_2) \,, \tag{17}$$

$$\theta_0 = \theta_1 + \theta_2 \,, \tag{18}$$

$$r_0 = \sqrt{(h_1 - h_2)^2 + 4(a + h_1)(a + h_2)[\sin(\theta_0/2)]^2} \,, \tag{19}$$

$$\sin \beta = [r_2 \sin(\pi - 2\psi)] / r_0 \,, \tag{20}$$

$$\gamma_{01} = \beta - \psi - \theta_1 \,, \tag{21}$$

$$\gamma_{r1} = -(\psi + \theta_1) \,. \tag{22}$$

The divergence factor D was calculated using

$$D \cong \frac{1}{\sqrt{1 + \dfrac{2d_1 d_2}{a\, d \tan \psi}}} \,. \tag{23}$$

Voltage gains *, g_{01} and g_{r1}, of the ground antenna relative to that of an isotropic radiator were calculated by

$$g_{01} = 1.28 \cos \gamma_{01} \,, \tag{24}$$

* These expressions were used to account for the vertical free-space radiation pattern of the antennas. Allowance for actual antenna gains (sec. 2.1) was made when required.

$$g_{r1} = 1.28 \cos \gamma_{r1} \quad . \tag{25}$$

The phase angle Δ, in radians, between the direct and reflected rays due only to the difference in ray length was calculated using

$$\Delta \cong \frac{67.46 f_{Mc} h_1' h_2'}{d} \quad , \tag{26}$$

where $f_{Mc} = 110$ Mc/s.

Then L_m was calculated from the following formula:

$$L_m = 36.58 + 20 \log_{10} f_{Mc} \tag{27}$$

$$+ 20 \log_{10} r_0 - 10 \log_{10} \left\{ g_{01}^2 + [D|R| g_{r1}]^2 - 2 g_{01} g_{r1} D|R| \cos \Delta \right\}$$

In the above equations, distances and heights are measured in statute miles and angles measured in radians. The distance, d, was converted to nautical miles after L_m was calculated.

Because the linear gradient atmosphere may predict too much bending [Bean and Thayer, 1959] at large distances and low angles a ray leaving the ground station antenna at the same angle, γ_{01}, as the direct ray (calculated using a linear gradient atmosphere) was traced through an exponential atmosphere until it reached the aircraft altitude. The great circle distance below the ray was then used in the final calculations instead of the distance, d, first assumed. The exponential

atmosphere used corresponds to the reference atmosphere given by Rice, et al. [1966] with a surface refractivity of N_s = 301 N-units.

Calculations of transmission loss beyond the radio horizon were made by combining smooth-earth diffraction with tropospheric scatter. The short-cut method of Vogler [1961] was used for diffraction computations. Scatter computations and methods of combining the two mechanisms follow the work by Rice, et al. [1966].

Calculations for the beyond-the-horizon case are based on the same exponential atmosphere used for within-the-horizon computations. The electrical constants of the ground assumed for calculations of the diffracted wave were $\epsilon = 15$ (relative dielectric constant), and $\sigma = 5$ millimhos per meter (conductivity). At the carrier frequency used, however, the effect of ground constants is small.

Finally, from a large number of computations both within and beyond the radio horizon, a set of curves was drawn for discrete aircraft altitudes showing the expected median transmission loss as a function of the great circle distance, d , (assuming the antenna gain of the ground station to correspond to a half-wave dipole). The construction of these curves involved a certain amount of blending in the vicinity of the radio horizon [Kerr, 1964].

Long-term variability, short-term fading, and the effective gain variations of the airborne antenna were treated statistically. Long-term variability was described by the time availability function, $V(p, d)$. Equations and curves given by Rice, et al. [1966] were used to calculate the $V(p, d)^*$ applicable to all hours of the year, for a continental temperate climate.

Short-term fading was described by a cumulative distribution $V_F(p, \theta)$ which includes the summing of a constant vector and a Rayleigh-distributed vector. The angular distance, θ, is defined to be the angle between horizon rays from the transmitter and receiver [Norton, et al., 1955a], and is defined on figure 7. An auxiliary cumulative distribution, $V'_F(p, \theta)$, was developed using (1) fading range data for 100 Mc/s from a paper by Janes [1955] to express fading range as a function of θ, and (2) figure 6 and table 1 from Norton, et al. [1955b] to specify a cumulative distribution, $V'_F(p, \theta)$, for fading range given by a particular value of θ. For this model the fading range values on which $V_F(p, \theta)$ was based were approximated by

$$0 \text{ for } \theta < 0 , \tag{28a}$$

$$1 + 12.4\,\theta \text{ dB for } 0 \le \theta \le 1^\circ , \tag{28b}$$

$$13.4 \text{ dB for } \theta \ge 1^\circ . \tag{28c}$$

* See footnote in section 3.

The cumulative distribution, $V_F(p, \theta)$ and $V'_F(p, \theta)$, are related by

$$V_F(p, \theta) = V'_F(p, \theta) - V'_F(50, \theta) . \quad (29)$$

It was unnecessary to consider a different aircraft antenna gain for the direct and reflected rays because their arrival angles are nearly equal; this would be more apparent if figure 65 were drawn to scale. This made calculations much easier since the effect of aircraft antenna gain on $N\{D/U(95)\}$ could be considered in transmission loss calculations without including the above mentioned gain difference. The method involved is outlined in Appendix II and uses the distribution, $R_A(p)$, shown in figure 3.

Cumulative distributions of transmission loss values were calculated using the following equation:

$$L(p, d) = L_m - [V(p, d) * V_F(p, \theta)] . \quad (30)$$

In this equation all terms except L_m are cumulative distributions, so that the calculation of $L(p, d)$ required the use of a convolution process which is indicated by the operational symbol, $*$, and will be further discussed in Appendix II. As previously implied, in calculating $L(p, d)$ an isotropic aircraft antenna was assumed. When the fading range was zero, the effect of $V_F(p, \theta)$ could be neglected and $V_F(p, \theta)$ was dropped from equation (30).

In the calculations, the ground antenna was assumed to be a single Alford loop 5.5 feet above ground. The total gain of the carrier antenna and the carrier power were not considered in the calculation of $N\{D/U(95)\}$. These can be taken into account by the procedure given in sections 5.1 and 5.2 for converting $D/U(95)$ to $N\{D/U(95)\}$.

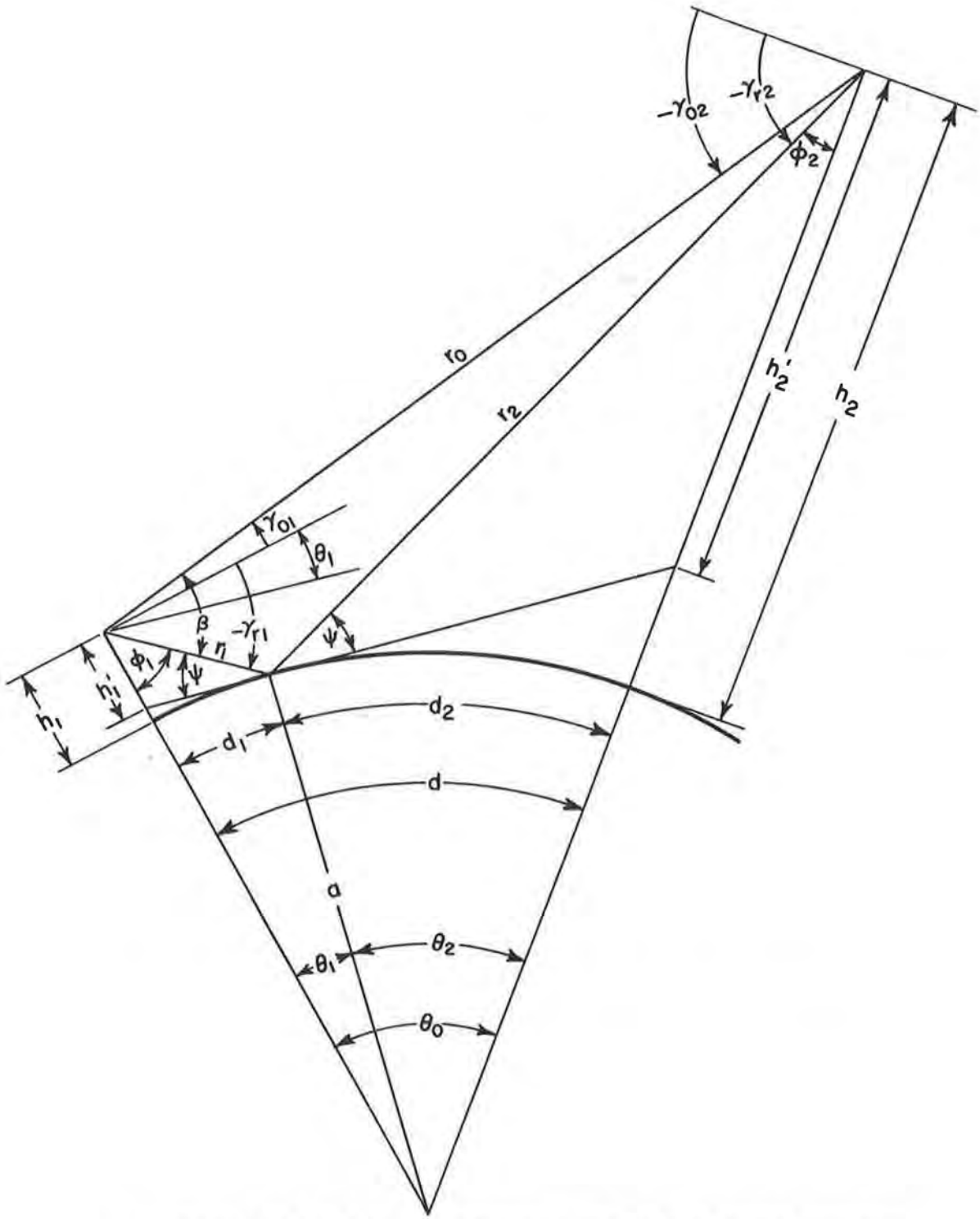

Geometry for Ray Interference within the Radio Horizon

Figure 65

I. 2 Undesired Station ILS Model

The propagation model used for the undesired ILS localizer carrier system was the same as that used for the desired ILS station with respect to assumptions made about the ground antenna and the methods used to calculate L_m beyond the radio horizon. However, a different method was used to calculate L_m within the radio horizon. Also, a different approximation described the fading range.

The within-the-horizon L_m curves for the undesired ILS were developed by utilizing the L_m curve used for the desired ILS along with a similar curve developed by essentially neglecting the ground reflections. Both curves were plotted on the same sheet with loss measured along the ordinate by a scale linear in decibels, and distance from the station measured along the abscissa by a scale linear in nautical miles. The undesired ILS L_m curve was then obtained by interpolating a smooth curve between the curves previously drawn such that the new curve merged with the desired ILS L_m curve in the vicinity of the radio horizon and merged with the "free space" loss curve at about 10 nautical miles from the station. This procedure was used to estimate the effect of terrain roughness around the undesired ILS and to avoid making quantitative assumptions about the effect of terrain roughness on the specular reflection coefficient. The specular reflection coefficient is assumed to be -0.9 at maximum within-the-horizon range (low grazing angle), and as the range is decreased with

fixed altitude (higher grazing angle) the effect of terrain roughness serves to reduce the absolute value of the specular reflection coefficient.

A random reflection coefficient of 0.3 [McGavin and Maloney, 1959] was assumed to be associated with the rough terrain surrounding an undesired ILS. The effect of this reflection was accounted for by the short-term fading function $V_F(p, \theta)$. For this model, the fading range values on which $V_F(p, \theta)$ was based were

$$4.7 \text{ dB for } \theta \leq 0^\circ , \tag{31a}$$

$$1 + 12.4\theta \text{ dB for } 0 \leq \theta \leq 1^\circ , \tag{31b}$$

$$13.4 \text{ dB for } \theta \geq 1^\circ . \tag{31c}$$

I.3 VOR Propagation Model

The propagation model used for the VOR follows the description given for the desired ILS model except in the region where reflection from the counterpoise was considered and in the treatment of aircraft antenna gain. Remarks made concerning antenna assumptions in the discussion of the desired ILS model are applicable to the VOR model except for the specific value of antenna height. A frequency of 110 Mc/s was used in the ILS adjacent channel signal ratio calculations, and 113 Mc/s used otherwise. The fading range values used in the desired ILS model to determine $V_F(p, \theta)$ were also used in the VOR model.

Two L_m -versus-distance curves were calculated for each aircraft altitude within the horizon. One curve was used for reflections from the counterpoise, where applicable, and the other for reflections from the ground. Both curves were blended in the region where the reflection point was close to the edge of the counterpoise. To facilitate this blending, the curves were calculated so that they extended beyond their region of validity.

For reflections from the counterpoise, calculated for elevation angles greater than 5°, the effective earth radius was increased by the height of the counterpoise above ground, so that a sphere through the level of the counterpoise became the reflecting surface with a reflection coefficient of -0.9 and the antenna was assumed to be an Alford loop 4 feet above this surface. The aircraft altitude was also adjusted to compensate for the counterpoise height. In these calculations d_1 was very much smaller than d_2, and the following two approximations were used to simplify the calculations:

$$r_1 \cong h_1 / \sin \psi, \tag{32}$$

$$\theta_1 \cong (r_1 \cos \psi) / a. \tag{33}$$

In calculating the L_m curves to be used in determining VOR service volumes the following equations were used:

$$D = \frac{a(r_1 + r_2)\cos\psi}{(a + h_1)(a + h_2)} \sqrt{\frac{\sin\psi}{\sin\theta_0(\sin\theta_1 \cos\phi_2 + \sin\theta_2 \cos\theta_1)}} , \quad (34)$$

$$\Delta = 33.73\, f_{Mc}\,(r_1 + r_2 - r_0) . \quad (35)$$

Equations 34 and 35 are the "exact" counterparts of equations 23 and 26, respectively. Experience with the "exact" expressions in VOR service volume calculations resulted in a preference for the approximate expressions which were later used in ILS signal-ratio calculations.

The VOR model used for service volume calculations included aircraft gain statistics in distributions of transmission loss values; i.e.,

$$L(p, d) = L_m - [\, V(p, d \text{ or } \theta) * V_F(p, \theta) * V_A(p, \gamma_{02}) \,] , \quad (36)$$

where $V_A(p, \gamma_{02})$ refers to the aircraft antenna gain distributions shown in figure 4, and $V(p, d \text{ or } \theta)$ implies the use of either $V(p, d)$ or $V(p, \theta)$.*

Beyond the region where reflection from the counterpoise was important, L_m was calculated using the methods outlined for the desired ILS model. The antenna was assumed to be an Alford loop located 16 feet above the ground.

---

* See footnote in section 3.

I.4 TACAN Propagation Model

The TACAN propagation model differs from the VOR model discussed above principally by the use of vertical instead of horizontal polarization and by the assumption of a uniformly rough earth model for transmission loss calculations at the 1150 Mc/s center frequency of the TACAN band. The vertical radiation pattern of the ground station was shown in figure 5. It is based on a typical center array [Casabona, 1956], with the antenna located 18 feet above the center of the VOR counterpoise and 30 feet above ground.

Reference transmission loss, L_m, again including the gain of the transmitting antenna, was calculated using geometric optics methods for distances within the radio horizon, but the reflected energy was treated statistically. Thus, L_m becomes mainly a function of the direct ray path distance and the gain of the transmitting antenna in the appropriate directions.

The statistical treatment of reflections from the counterpoise was based on the assumption that the complex lobe structure due to the high frequency and the high antenna can best be described by a cumulative distribution. This is obtained by adding vectorially two voltages, one at random phase relative to the other. The "constant" vector represents

the direct ray, and its magnitude is unity. The vector at random phase represents the reflected ray and has a magnitude r. The value of r is determined by the reflection coefficient, and voltage gains of transmitting and receiving antennas as a function of the angles shown in figure 65. This cumulative distribution can be considered another factor entering the short-term variability, as the movement of the aircraft through space can be assumed to be random with respect to the complex lobe pattern described by the distribution. A distribution of this type is shown in figure 66. The cumulative distribution, $V'_C(p, r)$, due to the vector addition of a unity component and a component, r, at random phase, in decibels, is given by Norton, et al. [1955b]:

$$V'_C(p, r) = -10 \log_{10} [1 + r^2 + 2 r \cos \pi(p/100)] \quad , \tag{37}$$

where p is the percentage of time and the argument, $\pi(p/100)$, is in radians. The median of this distribution is obtained by setting p equal to 50:

$$V'_C(50, r) = -10 \log_{10} (1 + r^2) \, . \tag{38}$$

This median value is added to the median transmission loss, L_m, and takes into account the median power contained in the ray reflected from the counterpoise.

The short-term variability, $V_C(p, r)$, used in the same manner as previously shown for $V_F(p, \theta)$ in the VOR case, is given by

$$V_C(p, r) = V'_C(p, r) - V'_C(50, r) . \qquad (39)$$

The relative magnitude, r , of the random component, assumed to be 0.9 for the illustrative example of figure 66, is given by

$$r = (|R_C| g_{r1}) / g_{01} , \qquad (40)$$

where $|R_C|$ is the magnitude of the reflection coefficient associated with the counterpoise, and g_{01} and g_{r1} are the voltage gain factors of the transmitting antenna relative to an isotropic radiator in the direction of the direct, and of the ground-reflected ray, respectively, similar to the VOR case. The dependence of the voltage gain on the elevation angles, γ_{01} and γ_{r1}, is shown for the TACAN ground antenna in figure 5.

Values for $|R_C|$ were assumed to be functions of the grazing angle, ψ, as follows.

For $\psi \leq 30^\circ$, $|R_C| = 0$ (no reflection from the counterpoise), (41a)

For $30^\circ < \psi \leq 43^\circ$, $|R_C| = 4.19\ \psi - 2.19$, where ψ is in radians, (41b)

For $\psi > 43^\circ$, $|R_C| = 0.95$. (41c)

Reflection from the uniformly rough ground was assumed to occur for grazing angles less than 30^{o}. In this case a cumulative distribution $V'_{F}(p, K)$, represents the energy scattered from the ground, similar to the function, $V'_{C}(p, r)$, used to represent reflections from the counterpoise. The parameter, K, is defined as $20 \log_{10} k$ with k being the ratio of the root-mean-square value of the field due to scattering of the reflected ray and that due to the direct ray. With an assumed effective ground reflection coefficient magnitude, $|R|$, and antenna voltage gain values, g_{ol} and g_{rl}, as before, k is given by

$$k = (|R|\, g_{rl}) / g_{ol} \quad . \tag{42}$$

The distribution function, $V'_{F}(p, K)$, was discussed and tabulated by Norton, et al. [1955b] for various values of K. The effective ground reflection coefficient, $|R|$, was assumed to be a function of the grazing angle, ψ, as follows:

For $\psi \leq 30^{o}$, $R_{G} = 0.3$, (43a)

For $30^{o} < \psi \leq 43^{o}$, $R_{G} = -0.132\, \psi + 0.992$, where ψ is in radians, (43b)

For $\psi > 43^{o}$, $R_{G} = 0$ (no reflection from the ground because of the presence of the VOR counterpoise). (43c)

From the distribution of $V'_F(p, K)$, the median value for $p = 50$ was determined and subtracted from the median transmission loss value, L_m, to take into account the median power reflected by the rough earth. The short-term variability, $V_F(p, K)$, is given by:

$$V_F(p, K) = V'_F(p, K) - V'_F(50, K) , \tag{44}$$

and will be used later on.

The geometric parameters shown on figure 65 apply to the TACAN case. The statistical treatment of reflections from the ground eliminates the need for calculating a divergence factor. For reflection from the counterpoise the divergence factor is assumed to be unity. The carrier frequency used in the calculations was 1150 Mc/s, and the height of the ground antenna is 30 feet above ground and 18 feet above the counterpoise. The maximum gain of the ground antenna is 8.15 dB relative to an isotropic antenna. This value occurs at an elevation angle of approximately 5^o (see fig. 5).

The reference transmission loss, L_m, for the TACAN case, in view of the procedures described above, is now given by

$$L_m = 36.58 + 20 \log_{10} f_{Mc} + 20 \log_{10} r_o - 20 \log_{10} g_{o1}$$
$$-8.15 + V'_C(50, r) - V'_F(50, K) . \tag{45}$$

Corrections for excess ray bending were made in the same way as for the VOR model, using the same exponential atmosphere.

Calculations of median transmission loss beyond the radio horizon were made by combining smooth-earth diffraction with tropospheric scatter in the same way as was done for VOR. However, the method of calculating diffraction as developed by Vogler [1961] could not be used, because it does not apply to vertical polarization. It was replaced by more general methods described by Norton, et al. [1955a] and by Rice, et al. [1966]. Again, for beyond-the-horizon calculations the grazing angles are essentially zero, and the effect of the counterpoise is neglected. The construction of final propagation curves (L_m versus d) for various discrete aircraft altitudes also involved a certain amount of blending from one propagation mechanism to another.

Long-term variability was described statistically for all distances by the function, $V(p, d)$, using the same methods as in the VOR propagation model. For the TACAN model the function $V(p, \theta)$ was not used at all.

Short-term (within-the-hour) fading within the radio horizon was described by cumulative distribution functions, $V_C(p, r)$ and $V_F(p, K)$, that result from the random addition of voltages due to the direct and the counterpoise or ground-reflected ray as described above.

APPENDIX II COMPUTATION TECHNIQUES

Calculations necessary to produce all desired distributions of transmission loss values or power levels as well as the processes involving the combination of various distributions were so numerous and complex that the use of a large electronic computer was necessary.

The calculation of L_m was accomplished by modifying existing programs to include the effect of the transmitting antenna only as a function of distance and aircraft height. For each aircraft altitude resulting propagation curves were reduced to a set of tables that includes L_m information for each of the propagation models discussed in Appendix I. Additional tables for distribution of short-term variability and aircraft antenna power gain ratios were developed. This information was then used in Signal Ratio Prediction Programs to generate tables of signal ratios for various values of time availability as a function of interference type, station separation and aircraft location. Values extracted from these tables were used in plotting the curves shown in sections 5.1 through 5.5.

Signal Ratio Prediction Programs served to systematize the signal ratio calculations for various aircraft altitudes, station separations and distances. Of the three such programs used (ILS, VOR, and TACAN) the ILS program was the simplest. The following discussion

is considered adequate to illustrate the general character of the prediction programs.

II.1 ILS Signal Ratio Prediction Program

The ILS Signal Ratio Prediction Program consists primarily of a series of loops by which the calculations are sequenced and systematic changes of parameters achieved. Figure 67 is a flow diagram of the program showing the series of loops and the computational sequence.

The primary loop considers different aircraft altitudes. At the start of each pass around the loop a set of L_m tables (as explained above) for a particular height is read into the computer. This loop continues until the supply of tables is exhausted. Altitudes of 500, 1,000, 2,000, 3,000, 4,000, 6,250, 12,000, and 18,000 feet were used.

A secondary loop considers the distance along the great circle path on the ground from the undesired station to the aircraft, d_U. An initial value of 5 nautical miles is used, and this is incremented by 5 until 325 nautical miles is reached.

For a given undesired distance, an inner loop is used to calculate the time distributions of transmission loss for the two

number of percentage values between $p = 1\%$ and $p = 99\%$ are selected and punched on cards.

The calculations are primarily handled by three subroutines: FALTG, VPD, and INTERP. This technique enables the program to be more easily changed for other combinations of systems not being considered in this study.

The convolution of distributions is handled by the subroutine FALTG.

The subroutine VPD calculates the predicted long-term variability (or power fading) as a function of the effective distance using the methods developed for a continental temperate climate [Rice, et al., 1966].

With the extensive use of tables, the need to interpolate often arises, and linear interpolation will not always suffice. Therefore, a subroutine INTERP was included in the program; this calculates the n^{th} Lagrangian approximation [Lance, 1960], where $n \leq m - 1$ with m being the number of entries in the table. The special case $n = 1$ results in linear interpolation. As a practical matter, n is usually required to be less than five. This is necessary because Lagrangian interpolation may exhibit large oscillations between tabular entries whenever they do not lie on rather smooth analytic functions.

This is an abbreviated discussion; the calculation procedure was more involved than indicated. In particular, the method used to extend calculations to a station separation of 20 nautical miles was not discussed.

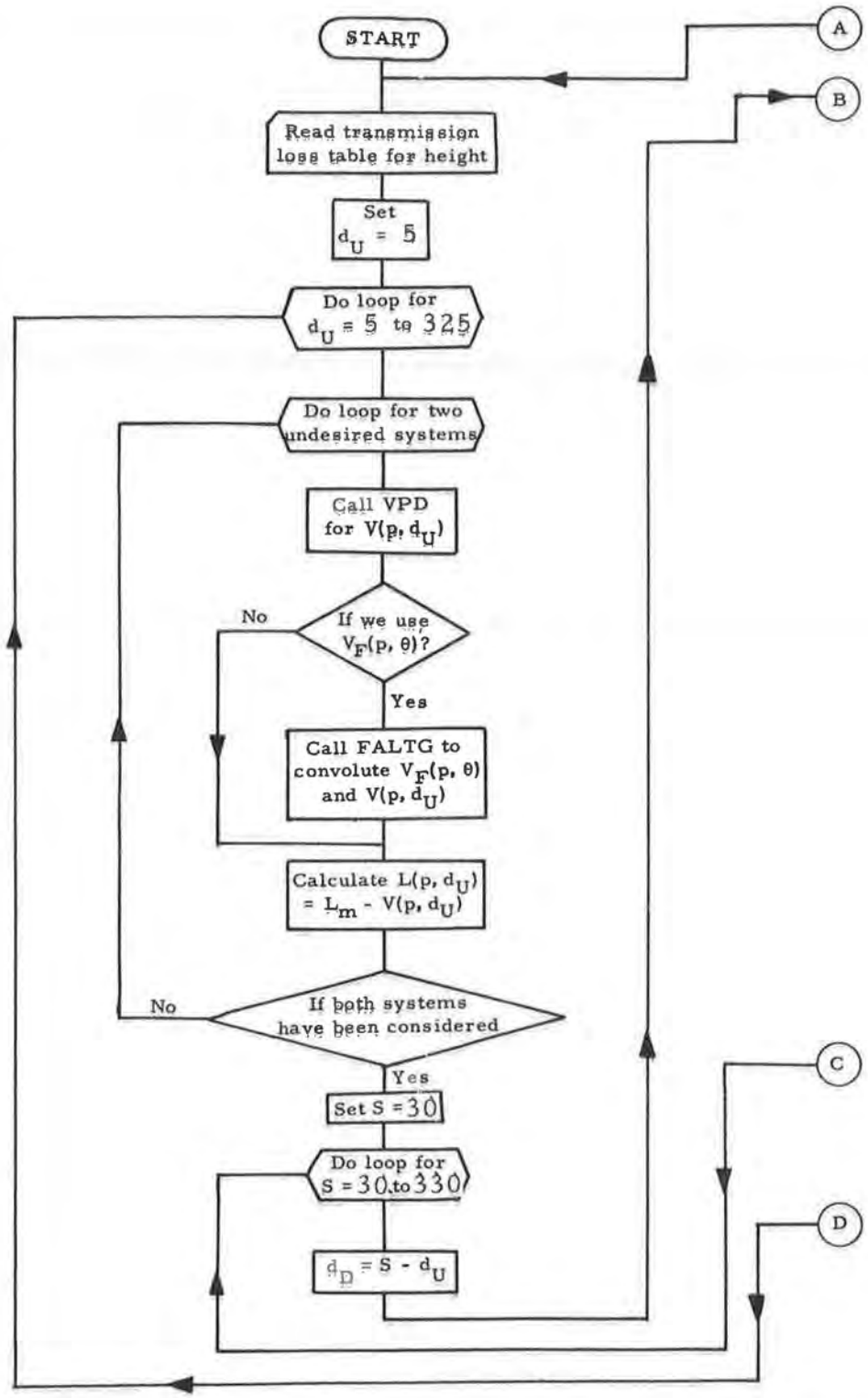

Continued on next page

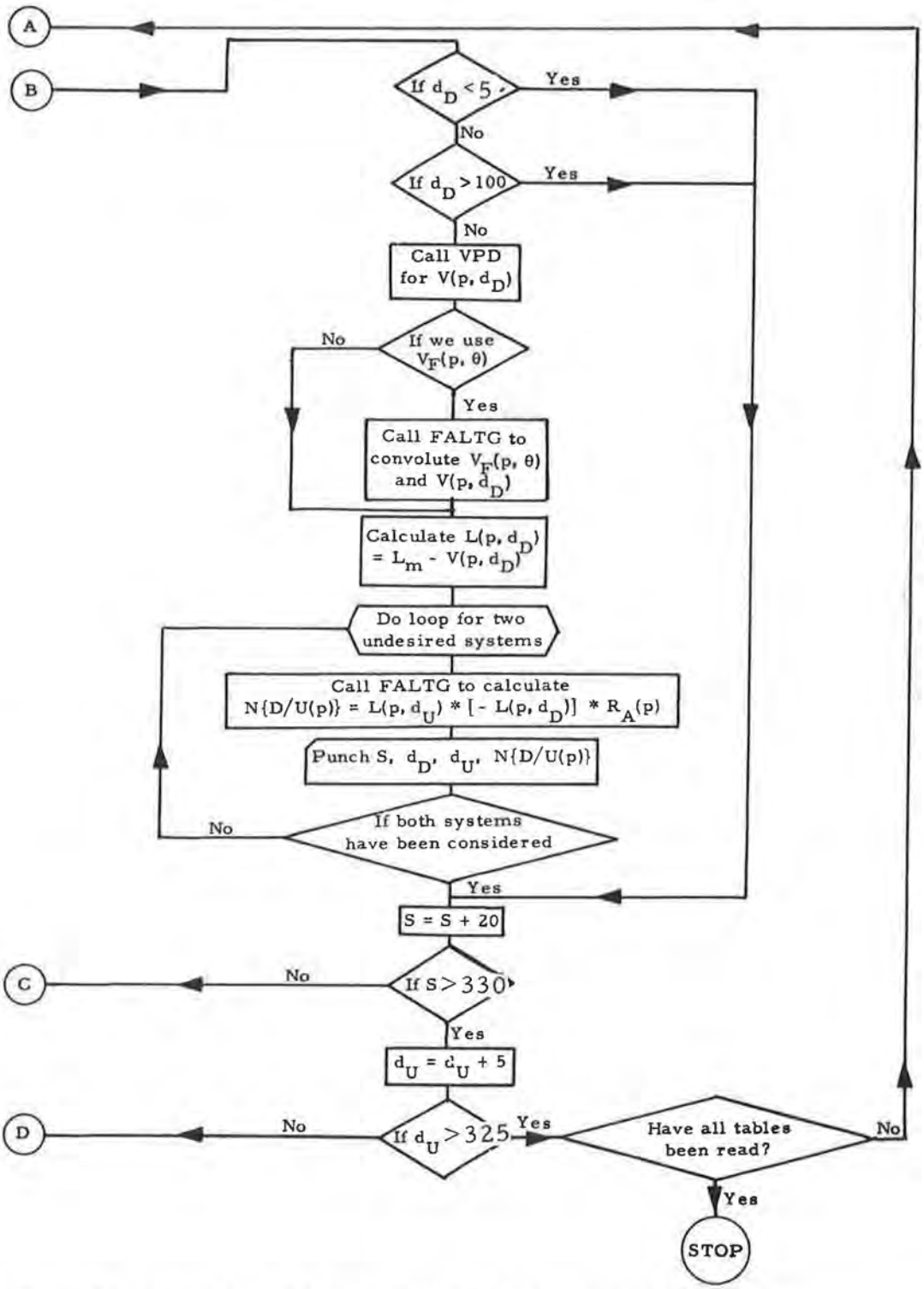

Flow Diagram for ILS Signal Ratio Prediction Program

Figure 67

APPENDIX III. COMPARISON OF THE RESULTS WITH PREVIOUS STUDIES

In 1951, Staras, Rice, and Herbstreit predicted VOR service volumes [Radio Technical Commission for Aeronautics, 1955]. The curves they developed are not in overall agreement with curves presented here; e.g., ranges previously estimated for D/U(95) of 14 and 20 dB vary from ~35 nautical miles less to ~10 nautical miles greater than comparable ranges given in this report when the aircraft is located within the radio horizon of the desired station. Although the antennas, both ground and air, used in the two predictions were not identical, they were so similar that only minor differences between prediction curves would be likely because of different antennas. However, since 1951 more refined methods for calculating transmission loss beyond the radio horizon and for estimating time variability have been developed. Thus, major differences in prediction curves are probably caused by different variability estimates, and different predicted median fields beyond the radio horizon. The power output for VOR used in the earlier study was 3 dB lower than that used here, but only the curves for service without interference would be affected by this difference.

The TACAN curves developed by Decker [1957] also differ from the curves presented here; e.g., ranges previously estimated for d/U(95) of 8 dB vary from ~35 nautical miles less to ~10 nautical miles

greater than comparable ranges given in this report, when the aircraft is located within the radio horizon of the desired station. The same ground station antenna was used in both studies, but in the earlier study it was placed 100 feet above the ground, whereas this study used a height of 30 feet. Although the method used to account for ground reflections was almost identical, the actual numbers involved were different, because of the different ground antenna height and different estimates of the effective ground reflection coefficient. This may account for minor differences in the prediction curves. However, different estimates of long-term variability, $V(p, d)$, were found to be more significant. Decker's probability-of-service curves applicable to interference-limited service also included limitations due to noise (transmitter power and receiver sensitivity). In the present study, interference and noise limitations were treated separately.

REFERENCES

Air Force Technical Order (1961), Ground Telecommunications Performance Standards, Part 5 of 6, Tropospheric Systems, performed by the Central Radio Propagation Laboratory of the National Bureau of Standards under sponsorship of the Ground Electronics Engineering and Installation Agency (Directorage of Engineering, RPZM), United States Air Force, T.O. 31-Z-10-1, published under authority of the Secretary of the Air Force (June 15, 1961).

Barsis, A. P., K. A. Norton, and P. L. Rice (1962), Predicting the performance of tropospheric communication links, singly and in tandem, IRE Trans. on Comm. Systems, CS-10, No. 1, 2-22.

Bean, B. R., and G. D. Thayer (1959), Models of the atmospheric radio refractive index, Proc. IRE 47, No. 5, 740.

Casabona, A. M. (1956), Antenna for the AN/URN-3 TACAN beacon, Electrical Communication, Vol. 33, No. 1, 35-59.

Civil Aeronautics Administration (1957), Description and theory of the Instrument Landing System, Federal Airways Manual of Operation, IV-B-1-4, 4.

Commercial Jetstar Antenna Installation (1959), Report No. ER-3938 (Company Confidential).

Convair 880 Jet-Liner Antennas (1959), Report No. ZN-22-006.

Davenport, W. B., and W. L. Root (1958), An Introduction to The Theory of Random Signals and Noise, Chapter 3, (McGraw-Hill Book Co. Inc., New York.)

Decker, M. T. (1957), TACAN coverage and channel requirements, IRE Transactions on Aeronautical and Navigational Electronics, ANE-4, No. 3, 135-143.

Federal Aviation Agency (1964), Directional V-Ring localizer antenna array, Selection Memorandum No. 19.

Federal Aviation Agency (1965), V-Ring localizer antenna array, Specification No. FAA-E-2186.

Gierhart, G. D., and M. E. Johnson (1965), Interference predictions for the Instrument Landing System, NBS Technical Note 324.

Janes, H. B (1955), An analysis of within-the-hour fading in 100-to 1,000-Mc transmission, J. Res. NBS 54, No. 4, 231-250.

Kerr, D. E. (1964), Propagation of short radio waves, MIT Radiation Laboratory Series 13, 125-130 (Boston Technical Publishers, Inc., Lexington, Mass.).

Kirby, R. S., J. W. Herbstreit, and K. A. Norton (1952), Service range for air-to-ground and air-to-air communications at frequencies above 50 Mc, Proc. IRE 40, No. 5, 525-536.

Lance, G. N. (1960), Numerical Methods for High Speed Computers, 142-144 (Iliffe, London).

McGavin, R. E., and L. J. Maloney (1959), Study of 1,046 megacycles per second of the reflection coefficient of irregular terrain at grazing angles, J. Res. NBS 63D (Radio Prop.), No. 2, 235-248.

Norton, K. A. (1953), Transmission loss in radio propagation, Proc. IRE 41, No. 1, 146-152.

Norton, K. A. (1959), System loss in radio-wave propagation, Proc. IRE 47, No. 9, 1661.

Norton, K. A., P. L. Rice, and L. E. Vogler (1955a), The use of angular distance in estimating transmission loss and fading range for propagation through a turbulent atmosphere over irregular terrain, Proc. IRE 43, No. 10, 1488-1526.

Norton, K. A., L. E. Vogler, W. V. Mansfield, and P. J. Short (1955b), The probability distribution of the amplitude of a constant vector plus a Rayleigh-distributed vector, Proc. IRE 43, No. 10, 1354-1361.

Radio Technical Commission for Aeronautics (1955), ILS/VOR/DME frequency channel utilization, Paper 97-55/DO-66, Appendix A.

Rice, P. L., A. G. Longley, K. A. Norton, and A. P. Barsis (1966), Transmission loss predictions for tropospheric communication circuits, NBS Technical Note 101 (Revised).

Vogler, L. E. (1961), Smooth earth diffraction calculations for horizontal polarization, J. Res. NBS 65D (Radio Prop.), No. 4, 397-399.

GPO 834-335